(12) INTERNATIONAL APPLICATION PUBLISHED UNDER THE PATENT COOPERATION TREATY (PCT)

(19) World Intellectual Property Organization
International Bureau

(43) International Publication Date
8 January 2015 (08.01.2015)

WIPO | PCT

(10) International Publication Number
WO 2015/003149 A2

(51) International Patent Classification:
A61K 47/48 (2006.01)

(21) International Application Number:
PCT/US2014/045444

(22) International Filing Date:
3 July 2014 (03.07.2014)

(25) Filing Language: English

(26) Publication Language: English

(30) Priority Data:

61/843,274	5 July 2013 (05.07.2013)	US
61/930,798	23 January 2014 (23.01.2014)	US
61/931,366	24 January 2014 (24.01.2014)	US
61/978,009	10 April 2014 (10.04.2014)	US

(71) Applicant: **H. LEE MOFFITT CANCER CENTER AND RESEARCH INSTITUTE, INC.** [US/US]; 12902 Magnolia Drive, Tampa, Florida 33612 (US).

(72) Inventors: **LIST, Alan F.**; 15706 Cochester Road, Tampa, Florida 33647 (US). **WEI, Sheng**; 1630 Burniston Drive, Tampa, Florida 33647 (US).

(74) Agents: **GILES, P. Brian** et al.; Meunier Carlin & Curfman, LLC, Suite 500, 817 W. Peachtree Street NW, Atlanta, Georgia 30308 (US).

(81) Designated States *(unless otherwise indicated, for every kind of national protection available)*: AE, AG, AL, AM, AO, AT, AU, AZ, BA, BB, BG, BH, BN, BR, BW, BY, BZ, CA, CH, CL, CN, CO, CR, CU, CZ, DE, DK, DM, DO, DZ, EC, EE, EG, ES, FI, GB, GD, GE, GH, GM, GT, HN, HR, HU, ID, IL, IN, IR, IS, JP, KE, KG, KN, KP, KR, KZ, LA, LC, LK, LR, LS, LT, LU, LY, MA, MD, ME, MG, MK, MN, MW, MX, MY, MZ, NA, NG, NI, NO, NZ, OM, PA, PE, PG, PH, PL, PT, QA, RO, RS, RU, RW, SA, SC, SD, SE, SG, SK, SL, SM, ST, SV, SY, TH, TJ, TM, TN, TR, TT, TZ, UA, UG, US, UZ, VC, VN, ZA, ZM, ZW.

(84) Designated States *(unless otherwise indicated, for every kind of regional protection available)*: ARIPO (BW, GH, GM, KE, LR, LS, MW, MZ, NA, RW, SD, SL, SZ, TZ, UG, ZM, ZW), Eurasian (AM, AZ, BY, KG, KZ, RU, TJ, TM), European (AL, AT, BE, BG, CH, CY, CZ, DE, DK, EE, ES, FI, FR, GB, GR, HR, HU, IE, IS, IT, LT, LU, LV, MC, MK, MT, NL, NO, PL, PT, RO, RS, SE, SI, SK, SM, TR), OAPI (BF, BJ, CF, CG, CI, CM, GA, GN, GQ, GW, KM, ML, MR, NE, SN, TD, TG).

Declarations under Rule 4.17:

— *of inventorship (Rule 4.17(iv))*

Published:

— *without international search report and to be republished upon receipt of that report (Rule 48.2(g))*

— *with sequence listing part of description (Rule 5.2(a))*

(54) Title: SOLUBLE CD33 FOR TREATING MYELODYSPLASTIC SYNDROMES (MDS)

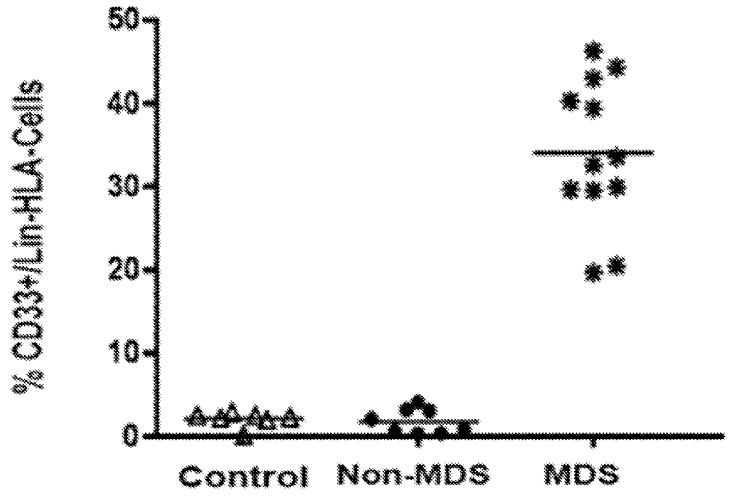

FIGURE 1A

(57) Abstract: Disclosed are compositions and methods for treating disease or condition caused or exacerbated by S100A9 activity, such as myelodysplastic syndromes (MDS) using a composition comprising an effective amount of a CD33/S100A9 inhibitor.

WO 2015/003149 A2

SOLUBLE CD33 FOR TREATING MYELODYSPLASTIC SYNDROMES (MDS)

CROSS-REFERENCE TO RELATED APPLICATIONS

This application claims benefit of U.S. Provisional Application No. 61/843,274, filed July 5, 2013, U.S. Provisional Application No. 61/930,798, filed January 23, 2014, U.S. Provisional Application No. 61/931,366, filed January 24, 2014, and U.S. Provisional Application No. 61/978,009, filed April 10, 2014, which are hereby incorporated herein by reference in their entirety.

STATEMENT REGARDING FEDERALLY SPONSORED RESEARCH OR DEVELOPMENT

This invention was made with Government Support under Grant No. CA131076 and Grant No. AI056213 awarded by the National Institutes of Health. The Government has certain rights in the invention.

BACKGROUND

Myelodysplastic syndromes (MDS) are hematopoietic stem cell malignancies with a rising prevalence owing to the aging of the American population. MDS comprise a group of malignant hematologic disorders associated with impaired erythropoiesis, dysregulated myeloid differentiation and increased risk for acute myeloid leukemia (AML) transformation. The incidence of MDS is increasing with 15,000 to 20,000 new cases each year in the United States and large numbers of patients requiring chronic blood transfusions. Ineffective erythropoiesis remains the principal therapeutic challenge for patients with more indolent subtypes, driven by a complex interplay between genetic abnormalities intrinsic to the MDS clone and senescence dependent inflammatory signals within the bone marrow (BM) microenvironment. Although three agents are approved for the treatment of MDS in the United States (US), lenalidomide (LEN) represents the only targeted therapeutic. Treatment with LEN yields sustained red blood cell transfusion independence accompanied by partial or complete resolution of cytogenetic abnormalities in the majority of patients with a chromosome 5q deletion (del5q), whereas only a minority of patients with non-del5q MDS achieve a meaningful response, infrequently accompanied by cytogenetic improvement. Although responses in patients with del5q MDS are

relatively durable, lasting a median of 2.5 years, resistance emerges over time with resumption of transfusion dependence.

SUMMARY

It is shown herein that $CD33^+$ myeloid-derived suppressor cells (MDSCs) specifically accumulate in the BM of MDS patients and impair hematopoiesis through a mechanism that involves S100A9 as an endogenous ligand for CD33 initiated signaling. Therefore, disclosed are compositions and methods for treating MDS that generally involve administering an effective amount of a CD33/S100A9 antagonist to inhibit activation of MDSCs. For example, the method can involve administering to the subject a therapeutically effective amount of a composition comprising an agent that binds and sequesters S100A9.

In some embodiments, the CD33/S100A9 antagonist binds and sequesters endogenous S100A9 and inhibits its binding to CD33 receptor on MDSCs. Therefore, in some embodiments, the CD33/S100A9 antagonist is a molecule containing a S100A9-binding domain. For example, the CD33/S100A9 antagonist can be a chimeric fusion protein comprising the ectodomain of CD33, Toll like Receptor 4 (TLR4), Receptor for Advanced Glycation End Products (RAGE), or a combination thereof. This ectodomain of CD33, TLR4, and/or RAGE can be any fragment of CD33, TLR4, and/or RAGE capable of binding S100A9. For example, in some cases the CD33 ectodomain contains only the variable region of CD33.

Therefore, disclosed is a recombinant fusion protein comprising an immunoglobulin Fc region; and one, two, three, or more of an extracellular domain of human CD33, extracellular domain of TLR4, extracellular domain of RAGE, or a combination thereof that binds S100A9 protein and is linked by a peptide bond or a peptide linker sequence to the carboxy-terminus of the immunoglobulin Fc region. The fusion protein can further contain a biotin acceptor peptide that can be biotinylated with biotin ligase (BirA) in the presence of biotin and ATP.

In some embodiments, the fusion protein comprises a formula selected from the group consisting of:

eCD33 – eTLR4 – Fc,

eCD33 – eRAGE – Fc,

eTLR4 – eRAGE – Fc,

eRAGE – eTLR4 – Fc,

eCD33 – eTLR4 – eRAGE – Fc,

eCD33 – eRAGE – eTLR4 – Fc,

eTLR4 – eCD33 – eRAGE – Fc,

eRAGE – eCD33 – eTLR4 – Fc,

eTLR4 – eRAGE – eCD33 – Fc, and

eRAGE – eTLR4 – eCD33 – Fc,

wherein "eCD33" is the extracellular domain of human CD33,

wherein "eTLR4" is the extracellular domain of TLR4,

wherein "eRAGE" is the extracellular domain of RAGE,

wherein "Fc" is the immunoglobulin Fc region, and

wherein "–" is a peptide linker or a peptide bond.

In some embodiments, the fusion protein comprises a formula selected from the group consisting of:

eCD33 – Fc – Avi,

eTLR4 – Fc – Avi,

eRAGE – Fc – Avi,

eCD33 – eTLR4 – Fc – Avi,

eCD33 – eRAGE – Fc – Avi,

eTLR4 – eRAGE – Fc – Avi,

eRAGE – eTLR4 – Fc – Avi,

eCD33 – eTLR4 – eRAGE – Fc – Avi,

eCD33 – eRAGE – eTLR4 – Fc – Avi,

eTLR4 – eCD33 – eRAGE – Fc – Avi,

eRAGE – eCD33 – eTLR4 – Fc – Avi,

eTLR4 – eRAGE – eCD33 – Fc – Avi, and

eRAGE – eTLR4 – eCD33 – Fc – Avi

wherein "eCD33" is the extracellular domain of human CD33,

wherein "eTLR4" is the extracellular domain of TLR4,

wherein "eRAGE" is the extracellular domain of RAGE,

wherein "Fc" is the immunoglobulin Fc region,

wherein "Avi" is an optional biotin acceptor peptide that can be biotinylated with biotin ligase (BirA) in the presence of biotin and ATP, and

wherein "–" is a peptide linker or a peptide bond.

The S100A9 protein can be present as a monomer or dimer. For example, the S100A9 protein can be in association with S100A8 protein as heterodimer. In these cases, the CD33/S100A9 antagonist binds and sequesters the S100A8/A9 heterodimer complex.

In some cases, the CD33/S100A9 antagonist is multivalent, e.g., it contains at least 2, 3, or more S100A9-binding domains. For example, the CD33/S100A9 antagonist can be a chimeric fusion protein comprising a combination of one or more CD33 ectodomains, one or more TLR4 ectodomains, and/or one or more RAGE ectodomains. The fusion protein can further comprise an immunoglobulin heavy chain constant region (Fc), e.g., from IgG4, IgG2 or IgG1.

Multiple copies of the fusion protein can also be combined to form a multivalent complex. Therefore, in some embodiments, two, three, four, five, or more fusion proteins can be linked to a core molecule or particle. For example, the Fc portion can be biotinylated. The biotinylated fusion protein can then be conjugated to a multimeric (e.g., tetrameric) streptavidin. In other embodiments, two or more fusion proteins are conjugated to the surface of a liposome or other microparticle. The multivalent complex can be homogeneous, i.e., containing multiple copies of one type of one fusion protein, or it can be heterogeneous. For example, the multivalent complex can contain combinations of CD33, TLR4, and RAGE fusion proteins. In addition, the multivalent complex can contain multivalent fusion proteins, i.e., at least two fusion protein containing two or more S100A9-binding domains.

In other embodiments, the CD33/S100A9 inhibitor binds and inhibits endogenous CD33 receptor on MDSCs. Therefore, in some embodiments, the CD33/S100A9 antagonist is a molecule containing a CD33 binding domain. For example, the CD33/S100A9 inhibitor can be a recombinant protein that binds CD33 without activating MDSCs and competes for binding of endogenous S100A9. For example, the CD33/S100A9 inhibitor can be a mutant or truncated variant of S100A9, i.e., dominant negative S100A9.

In some embodiments, the CD33/S100A9 inhibitor is an antibody or aptamer that specifically binds CD33 or S100A9 thereby inhibiting endogenous CD33/S100A9 activation.

Also disclosed are methods for treating a disease or condition in a subject that is caused or exacerbated by S100A9 activity, comprising administering to the subject a composition comprising a CD33/S100A9 antagonist disclosed herein.

Also disclosed are methods for identifying an agent for treating MDS. In some embodiments, the methods involve screening candidate agents for the ability to prevent S100A9 binding to CD33. In other embodiments, the methods involve screening candidate agents for the ability to prevent activation of CD33 by S100A9.

The details of one or more embodiments of the invention are set forth in the accompanying drawings and the description below. Other features, objects, and advantages of the invention will be apparent from the description and drawings, and from the claims.

DESCRIPTION OF DRAWINGS

Figures 1A to 1N show increased accumulation and function of MDSC in BM cells from MDS patients. Figure 1A shows percent of MDSCs in the BM-MNCs of MDS (n=12), age-matched healthy (n=8) and non-MDS cancer specimens (n=8, 4 breast 4 lymphoma, $P<0.0001$). Figure 1B shows chromosome 7 FISH of sorted MDSC or non-MDSC from MDS BM-MNC (n=5, CEP7 and 7q31). Figures 1C and 1D show ^{3}H-thymidine incorporation (Fig. 1C) and IFN-γ ELISA (Fig. 1D) of stimulated autologous T cells co-cultured with sorted MDS-MDSCs at 1:0.25 and 1:0.5 ratios (T cells:MDSC). Error bars denote standard deviation of three separate patient samples tested in triplicate. Figure 1E shows BrDu incorporation of stimulated T cells after admixing with autologous unsorted, MDSCs depleted (-MDSC) or remixed (+MDSC) BM-MNCs. Figures 1F to 1I show sorted MDSCs from MDS or healthy donor BM tested for IL-10 (Fig. 1F), TGFβ (Fig. 1G), arginase (Fig. 1H) and NO (Fig. 1I) production by ELISA after 24 hours of culture. Figure 1J shows MDSC:erythroid precursor contact zone of admixed sorted MDS-MDSC and autologous erythroid precursors at a ratio of 1:3 (MDSC:erythroid precursor) by microscopy at 0 and 30 minutes. Cells were stained for CD71, glycophorin A, CD33 and granzyme B. Figure 1K shows sorted MDSCs from MDS or healthy donors labeled with CD33 and granzyme B co-incubated with purified autologous erythroid precursors (0 or 30 min) and monitored by microscopy. (L) Counts of MDSC-HPC conjugate mobilized granules. Figure 1M shows Annexin V exposure on erythroid precursors ($CD71^{+}CD235a^{+}$) incubated with or without sorted autologous MDS-BM MDSC. Figure 1N shows colony forming ability of unsorted, -MDSC or remixed (+MDSC) MDS BM-MNCs (ratio of 1:3, *, $P<0.005$, **, $P<0.001$).

Figures 2A to 2G show CD33 signals to enhance MDSC suppressive functions. Figure 2A shows BM-MNCs from MDS patients (n=12), age matched healthy donors (n=8) and non-MDS cancers (n=8) analyzed for CD33's Mean fluorescence intensity (MFI), * = $P<0.0005$. Figure 2B shows concentration of IL-10, TGF-β, and VEGF from the supernatant of CD33 (or isotype) cross-linked U937 cells. Bars represent mean ±SEM of three wells on three separate experiments. Figure 2C shows BM-MNCs isolated from healthy donors and infected with an adenoviral vector containing either GFP (Ad-GFP) or CD33 (Ad-CD33) for 72 hours before flow cytometric analysis of the mature myeloid markers, CD11c, CD80, and CCR7, with non-

infected cells as a control. Figure 2D shows results of colony formation assay where after sorting out MDSCs from the BM of MDS patients, the remaining MDSC negative cells were cultured with MDSCs that have been mock infected or infected with lentiviral vector (LV) containing non-targeted shRNA or CD33 shRNA (shCD33) for 14 days. The MDSCs were also cultured for 72 hours after infection with LV containing constructs described above before culturing with MDSC negative BM cells. *, $P<0.001$, **, $P<0.0001$, versus cells treated with control shRNA. Figure 2E to 2G shows IL-10 (Fig. 2E) and TGF-β (Fig. 2F) in the supernatants assayed by ELISA. *, $P<0.05$, versus cells treated with control shRNA. Figure 2G shows arginase activity in the shCD33 treated cells. *$P<0.05$, versus cells treated with control shRNA.

Figures 3A to 3O show identification of S100A9 as a native ligand for CD33. Figure 3A shows Coomasie blue staining of BM lysates precipitated with either control IgG or CD33-fusion. Figure 3B shows transfected SJCRH30 cells (S100A8 on top left and S100A9 lower left) stained with CD33-fusion (APC). Figure 3C shows S100A9 capture ELISA of lysates from un-transfected (negative) or S100A9 transfected cells. Secondary antibody was either anti-S100A9 (positive control) or CD33-fusion. Figure 3D shows serial dilution of both AD293 and SJCRH30 cell lysates, either un-transfected or transfected with vector or S100A9, onto a PVDF membrane and blotted with CD33-fusion. Coomasie blue staining serves as loading control. Figure 3E shows S100A9 immunoprecipitation of SJCRH30 CD33/S100A9 co-transfected cell lysate blotted against CD33. Figure 3F shows PBMC and BM-MNCs from healthy and MDS samples immunoprecipitated with CD33-fusion and blotted for S100A9. Figure 3G shows immunofluorescence staining of recombinant human S100A9-DDK incubated with either CD33-transfected (top panel) or vector-transfected (lower panel) SJCRH30 cells at indicated time points. DAPI= nuclei, APC-DDK= rhS100A9. Figures 3H to 3I show treatment of SJCRH30-CD33 cells with rhS100A9 induced IL-10 (Fig. 3H) and TGF-β expression (Fig. 3I). Figures 3J to 3K show treatment of U937 cells (high CD33 expression myeloid cell line) with rhS100A9 also induces IL-10 (Fig. 3J) and TGFβ expression (Fig. 3K). Figure 3L shows S100A9 protein concentration in the plasma of MDS patients (n=6) measured by ELISA. Figures 3M to 3N show MDS-MDCS treated with 1 μg of rhS100A9 stained for CD33-FITC and anti-DDK-APC (Fig. 3M) and immunoprecipitated with anti-CD33 antibody followed by blotting with anti-SHP-1 (Fig. 3N). Figure 3O shows BM plasma from either healthy donors (n=3) or MDS-patients (n=3) used to assay SHP-1 recruitment. In all experiments, error bars represent the SEM of three separate experiments.

Figures 4A to 4N show S100A9 signaling through CD33 in MDS BM is associated with MDSC activation and suppressive function. Figures 4A to 4H show healthy BM cells infected with adenovirus containing GFP or CD33 expression vectors assessed by Q-PCR for the expression of IL-10 (Fig. 4A), TGF-β (Fig. 4C), ARG2 (Fig. 4E) or NOS2 (Fig. 4F), or by ELISA for IL-10 (Fig. 4B) and TGF-β (Fig. 4D). Q-PCR (Fig. 4G) and flow cytometry of GFP expression (Fig. 4H) determined transfection efficiency. Figures 4I and 4J show healthy BM cells' RAGE, TLR4, CD33 or their combination blocked prior to culturing cells by themselves or with 1ug of S100A9 for 48 hours to determine IL-10 gene and protein expression (Q-PCR and ELISA, (Fig. 4I)) or TGF-β gene and protein expression (Fig. 4J). Figure 4K shows silencing S100A8 and S100A9 expression in primary MDS-BM cells using specific shRNA (demonstrated by western blot). Figures 4L to 4N show that silencing inhibits the expression of IL-10 (Fig. 4L) and TGF-β (Fig. 4M). *, $P<0.01$, **, $P<0.001$, versus cells treated with control shRNA. Figure 4N shows blocking S100A8 and S100A9 expression by specific shRNA promotes colony formation in BM cells isolated from patients with MDS, *, $P<0.05$, versus cells treated with control shRNA. In all experiments, error bars represent the SEM of triplicate determination with three separate primary specimens.

Figures 5A to 5P show S100A9Tg mice have increased accumulation and activation of MDSC and display dysplastic features that recapitulate human MDS pathology. Figure 5A shows $Gr1^+CD11b^+$ MDSC accumulation in BM-MNCs isolated from S100A9Tg mice at 6, 18 or 24 weeks, S100A9KO or WT mice at both 6 and 24 weeks. Figure 5B shows percent of MDSC from BM, spleen and PBMC of S100A9Tg mice at 6, 18 and 24 weeks of age by flow cytometry. Figures 5C to 5D show spleen cells assayed against the maturation markers $F4/80^+Gr1^-$ (Fig. 5C) and $I\text{-}Ad^+$ (Fig. 5D). Figure 5E shows FACS sorted $Gr\text{-}1^+CD11b^+$ cells (+MDSC) from the BM of mice described in Figure 5A remixed back with autologous 1 x 10^5 MDSC-negative population (containing HSPC, -MDSC) at 1:1 ratio for 14 days before evaluating colony formation. An MDSC- negative population was used as the control. Figure 5F shows MDSCs from WT, S100A9Tg and S100A9 KO mice FACS sorted and incubated in a 96-well plate for 24 hrs after which IL-10 and TGF-β production were measured by ELISA. Figures 5G to 5N show comparison of the hematopathological analysis of WT (Figs. 5G-5J) and S100A9Tg mice (Figs. 5K-5N). MDS-BM primary specimens were tested for the location of S100A9 in CD33 positive cells (Fig. 5O) and CD34 positive cells (Fig. 5P). Flow figures representative of triplicate experiments.

Figures 6A to 6I show mix transplant of S100A9 enriched HSC and WT HSC continues effects on hematopoiesis. Figure 6A shows proportion of MDSC in mice lethally irradiated mice (900Gy) transplanted with enriched HSCs from either WT, S100A9Tg or a 1:1 mixture of the two at 8 weeks (post-engraftment). Figure representative of 5 transplant experiments. Figure 6B shows GFP expression of MDSCs in Figure 6A. Figure 6C shows percent of LSK HSC, defined as $Lineage^{-}cKit^{+}Sca\text{-}1^{+}$, in lethally irradiated mice after transplant with WT, S100A9Tg or 1:1 mix of enriched HSCs. Figures 6D to 6F show proportion and concentration of white blood cells (WBC) (Fig. 6D), hemoglobin (HGB) (Fig. 6E) and RBCs (Fig. 6F) measured weekly by CBC post-transplant. Error bars are the SEM of n=5. Figure 6G shows percentage of CD34 positive cells in MDSC-depleted MDS-BM specimens treated with or without S100A9 for 48 hours. Figure 6H shows same experiment as in Figure 6G, assessing surface expression of Annexin V and PI after treatment with S100A9. Figure 6I shows healthy human CD34 cells (Lonza Wakersfield) were treated as in Figure 6H and cultured for 48 hours followed by AnnexinV/PI flow cytometric analysis.

Figures 7A to 7I show targeting MDSC activation and signaling can improve suppressive BM microenvironment. Figures 7A to 7B show ATRA decreases MDSCs in the BM of S100A9Tg mice (Fig. 7A) and promotes the expression of myeloid maturation markers (Fig. 7B). Figure 7C shows BFU colony formation of WT and S100A9Tg mice BM cells treated with ATRA. All of the cultures were duplicates. *, $P<0.05$, between ATRA treated and vehicle treated S100A9Tg mice. Figure 7D shows the number of RBC, WBC and platelets from CBC analysis of ATRA treated and untreated mice. *, $P<0.05$, between ATRA treated and vehicle treated S100A9Tg mice. Figure 7E shows relative expression levels of DAP12 from isolated MDSC from either healthy or MDS specimens by qPCR (n=5). Figure 7F shows AD293 cells transfected with either vector, WT-DAP12, dominant negative DAP12 (DN) or active DAP12 (P23) for 48 hours and analyzed by western blot for the expression of phosphorylated or total Syk and ERK. This is representative of three independent experiments. MDSC were isolated from the BM of MDS patients and infected with adenoviral vector containing either WT or active DAP12 (P23) for 48 or 72 hours. Figures 7G and 7H show surface expression of CD14 or CD15 (Fig. 7G) or the maturation markers CD80, CCR7 and CD11c (Fig. 7H) analyzed by flow cytometry. Figure 7I shows MDSCs purified from BM-MNCs of MDS patients by FACS sorting and cells infected with LV-WT DAP12 or LV-P23. Colony formation assays were performed in methylcellulose for 14 days. Results are shown as mean ± SEM of 7 patients. *, $P<0.01$, **, $P<0.001$, versus cells infected with LV-WT.

Figure 8shows percent engraftment in transplanted mice. Wild type female FVB/NJ mice were transplanted with enriched HSC from either WT, S100A9Tg or a 1:1 ratio of WT:Tg male cells. The percent of engraftment was assessed by measuring the expression of the SRY gene by qPCR normalized against un-transplanted male mice BM cells. GAPDH serves as the internal control.

Figure 9 is a model of CD33/Siglec 3-mediated signaling either through ITIM or ITAM motifs. CD33 has two cytosolic ITIM motifs. Src kinases phosphorylate tyrosine residues present in the ITIMS after CD33 cross-linking or upon interaction with its ligand(s). Phosphorylated ITIMs recruit and activate phosphatases (SHP1, SHP2, or SHIP-1), resulting in down regulation of MAPK and ultimately, cellular inhibition and the production of inhibitory cytokines. Activation of CD33 also induces S100A8 and S100A9 expression, which are secreted and act as heterodimers for CD33 or TLR4, and as such, mediates inflammation and MDSC activation. Siglecs that lack ITIMs possess charged amino acids in their trans-membrane domain, which allow association with DAP12, an ITAM-bearing activating adaptor. As is the case with ITIMs, Src kinases also phosphorylate tyrosine residues in the ITAM of DAP12. Syk kinase and ZAP70 are then recruited and perpetuate downstream cellular activation, differentiation, and/or maturation.

Figure 10 shows t effect of active DAP12 on immature DC maturation. Primary DCs were prepared from healthy donors and infected with adenoviral vectors containing GFP alone, WT-DAP12, dnDAP12 and active DAP12 (Ad-P23) as indicated. The cells were cultured for 72 hrs before flow cytometric analysis using mature DC surface marker as indicated. Mock infected DC and Isotype IgG included in control group. Each experimental construct was compared to the empty-vector control (filled histograms), and infected cells were gated on GFP prior to analysis.

Figure 11 illustrates exemplary embodiments of a CD33/S100A9 antagonist. Figures 11A to 11G show a fusion protein contain the Fc portion of IgG, and a biotin acceptor peptide (e.g., AviTag™ sequence) for biotinylation by BirA or antibody recognition. The fusion protein in Figures 11A, 11C, and 11G contain the ectodomain of CD33. The fusion protein of 11B and 11D contains only the variable region of the ectodomain of CD33 ("vCD33"). The vCD33 region in Figures 11C and 11D contains single nucleotide polymorphisms ("SNPs") compared to the vCD33 in Figures 11A and 11B. The fusion protein depected in Figures 11E, 11F, and 11G contain the ectodomain of Toll like receptor 4 (TLR4). The fusion proteins in Figures 11F and 11G also contain the ectodomain of CD33 (Fig. 11G) or only the vCD33 region (Fig. 11F).

Figure 11H shows a multimeric complex formed by the biotinylation of the AviTag™ sequence and the conjugation of these fusion proteins to a tetrameric streptavidin ("SA"). Figure 11I shows a multimeric complex formed by the incorporation of antibodies that specifically bind AviTag™ into a liposome.

Figures 12A and 12B show fold change of active caspase-1 and IL-1β generation normalized to plasma treated control in four cell populations . Active caspase-1 and IL-1β generation were assessed in four populations by flow cytometry after treatment with CD33-IgG: stem cells (CD34+CD38-), progenitors (CD34+CD38+), erythroids (CD71+), and myeloid cells (CD33+). Fold change of active caspase-1 MFI (Fig. 12A) and IL-1β generation (Fig. 12B).

Figures 13A and 13B show fold change of active caspase-1 and IL-1β generation normalized to plasma treated control in four cell populations . Active caspase-1 and IL-1β generation were assessed in four populations by flow cytometry after treatment with a related pathway inhibitor: stem cells (CD34+CD38-), progenitors (CD34+CD38+), erythroids (CD71+), and myeloid cells (CD33+). Fold change of active caspase-1 MFI (Fig. 13A) and IL-1β generation (Fig. 13B).

Figures 14A to 14C show neutralization of plasma S100A9 by CD33 Chimera trap enhances colony forming capacity in MDS patient specimens. Figures 14A to 14C show erythroid burst-forming units (BFU-E) (Fig. 14B), multipotential colony forming units (CFU-GEMM) (Fig. 14A), and granulocyte/macrophage colony forming units (CFU-GM) (Fig. 14C) in MDS patient specimens treated with IgG, Plasma, or 0.1, 0.5, or 1.0μg of CD33-IgG chimeric trap.

Figures 15A to 15C show change in colony forming capacity in four LR-MDS specimens treated with CD33 chimera. BM-MNC from each patient were incubated with autologous BM plasma and increasing concentrations of CD33-IgG, and were plated in four replicates per treatment condition in methylcellulose. Colonies were counted fourteen days after plating, and were averaged for each patient. The increase in CFC is represented as the fold change normalized to plasma-incubated control for GEMM (Fig. 15A), erythroid (Fig. 15B), and GM (Fig. 15C) colonies, respectively.

Figures 16A to 16E show CD33-chimera trap suppresses pyroptosis-related gene expression in MDS BM-MNC. BM-MNC were isolated from five low risk MDS patients and incubated with autologous BM plasma and increasing concentrations of the CD33 chimera. BM-MNC isolated from five normal donors were used for comparison. RNA was isolated and qPCR was carried out on pyroptosis-related genes Capsapse-1 (Fig. 16A), IL-1β (Fig. 16B), NLRP1

(Fig. 16C), NLRP3 (Fig 16D), and IL-18 (Fig. 16E). Gene expression is represented as the fold change normalized to the normal donors.

DETAILED DESCRIPTION

Immature myeloid-derived suppressor cells (MDSC), known to accumulate in tumor bearing mice and cancer patients, are site-specific inflammatory and T cell immunosuppressive effector cells that contribute to cancer progression (Gabrilovich, D.I., et al. 2009. Nat Rev Immunol 9:162-174; Kusmartsev, S., et al. 2006. Cancer Immunol Immunother 55:237-245). Their suppressive activity is in part driven by inflammation-associated signaling molecules, such as the danger-associated molecular pattern (DAMP) heterodimer S100A8/S100A9 (also known as myeloid-related protein (MRP)-8 and MRP-14, respectively), through ligation of TLR4 (Ehrchen, J.M., et al. 2009. J Leukoc Biol 86:557-566; Vogl, T., et al. 2007. Nat Med 13:1042-1049). Murine $CD11b^{+}Gr1^{+}$ MDSCs form the basis of the vast majority of the mechanistic studies, however, much less has been reported on their human counterparts. Human MDSCs lack most markers of mature immune cells (LIN^{-}, $HLA\text{-}DR^{-}$) but possess CD33, the prototypical member of Sialic acid-binding immunoglobulin-like (Ig) super-family of lectins (Siglec) (Gabrilovich, D.I., et al. 2009. Nat Rev Immunol 9:162-174; Talmadge, J.E. 2007. Clin Cancer Res 13:5243-5248; Talmadge, J.E., et al. 2007. Cancer Metastasis Rev 26:373-400; Crocker, P.R., et al. 2007. Nat Rev Immunol 7:255-266). Importantly, while its precise action is unknown, CD33 possesses an immunoreceptor tyrosine-based inhibitory motif (ITIM) that is associated with immune suppression (Crocker, P.R., et al. 2007. Nat Rev Immunol 7:255-266).

It is shown herein that $LIN^{-}HLA\text{-}DR^{-}CD33^{+}$ MDSCs specifically accumulate in the BM of MDS patients (herein referred to as MDS-MDSC) and impair hematopoiesis through a mechanism that involves S100A9 as an endogenous ligand for CD33 initiated signaling. Importantly, using S100A9 transgenic (S100A9Tg) mice, it is shown that sustained activation of this inflammatory pathway leads to the development of MDS, and that this hematologic phenotype is rescued by strategies that suppress CD33 ITIM-signaling. The disclosed finding that S100A9 ligates CD33 to induce MDSC expansion indicates that targeting this pathway can provide a therapeutic approach for the treatment of MDS. Finally, the discovery of this signaling pathway verifies the role of S100A9 as an important initiator of immune-suppression. S100A9Tg mice may therefore serve as a useful model for the study of MDS pathogenesis, treatment and the overall role of MDSC in cancer.

Therefore, disclosed are compositions and methods for treating MDS that involve the use of a CD33/S100A9 inhibitor to inhibit activation of myeloid-derived suppressor cells (MDSCs).

CD33/S100A9 Inhibitor

In some embodiments, the CD33/S100A9 inhibitor binds and sequesters endogenous S100A9 and inhibits its binding to CD33 receptor on MDSCs. Therefore, in some embodiments, the CD33/S100A9 antagonist is a molecule containing a S100A9 binding domain. In other embodiments, the CD33/S100A9 inhibitor binds and inhibits endogenous CD33 receptor on MDSCs. Therefore, in some embodiments, the CD33/S100A9 antagonist is a molecule containing a CD33 binding domain.

Soluble Receptors

For example, the CD33/S100A9 inhibitor can be a soluble CD33 receptor. A "soluble receptor" is a receptor polypeptide that is not bound to a cell membrane. Soluble receptors are most commonly ligand-binding receptor polypeptides that lack transmembrane and cytoplasmic domains. Soluble receptors can comprise additional amino acid residues, such as affinity tags that provide for purification of the polypeptide or provide sites for attachment of the polypeptide to a substrate, or immunoglobulin constant region sequences. Many cell-surface receptors have naturally occurring, soluble counterparts that are produced by proteolysis. Soluble receptor polypeptides are said to be substantially free of transmembrane and intracellular polypeptide segments when they lack sufficient portions of these segments to provide membrane anchoring or signal transduction, respectively.

For example, the CD33/S100A9 antagonist can be a chimeric fusion protein comprising the ectodomain of CD33, Toll like Receptor 4 (TLR4), Receptor for Advanced Glycation End Products (RAGE), or a combination thereof. This ectodomain of CD33, TLR4, and/or RAGE can be any fragment of CD33, TLR4, and/or RAGE capable of binding S100A9.

Fusion proteins, also known as chimeric proteins, are proteins created through the joining of two or more genes which originally coded for separate proteins. Translation of this fusion gene results in a single polypeptide with function properties derived from each of the original proteins. Recombinant fusion proteins can be created artificially by recombinant DNA technology for use in biological research or therapeutics. Chimeric mutant proteins occur naturally when a large-scale mutation, typically a chromosomal translocation, creates a novel coding sequence containing parts of the coding sequences from two different genes.

The functionality of fusion proteins is made possible by the fact that many protein functional domains are modular. In other words, the linear portion of a polypeptide which

corresponds to a given domain, such as a tyrosine kinase domain, may be removed from the rest of the protein without destroying its intrinsic enzymatic capability. Thus, any of the herein disclosed functional domains can be used to design a fusion protein.

A recombinant fusion protein is a protein created through genetic engineering of a fusion gene. This typically involves removing the stop codon from a cDNA sequence coding for the first protein, then appending the cDNA sequence of the second protein in frame through ligation or overlap extension PCR. That DNA sequence will then be expressed by a cell as a single protein. The protein can be engineered to include the full sequence of both original proteins, or only a portion of either.

If the two entities are proteins, often linker (or "spacer") peptides are also added which make it more likely that the proteins fold independently and behave as expected. Especially in the case where the linkers enable protein purification, linkers in protein or peptide fusions are sometimes engineered with cleavage sites for proteases or chemical agents which enable the liberation of the two separate proteins. This technique is often used for identification and purification of proteins, by fusing a GST protein, FLAG peptide, or a hexa-his peptide (aka: a 6xhis-tag) which can be isolated using nickel or cobalt resins (affinity chromatography).

Amino acid sequences for suitable CD33, TLR4, and RAGE ectodomains are known and adaptable for use in the disclosed compositions and methods. For example, the ectodomain of *Homo sapiens* Myeloid cell surface antigen CD33 (Uniprot P20138 [aa. 18-259] can have the following amino acid sequence:

18-DPN FWLQVQESVT VQEGLCVLVP CTFFHPIPYY DKNSPVHGYW FREGAIISRD SPVATNKLDQ EVQEETQGRF RLLGDPSRNN CSLSIVDARR RDNGSYFFRM ERGSTKYSYK SPQLSVHVTD LTHRPKILIP GTLEPGHSKN LTCSVSWACE QGTPPIFSWL SAAPTSLGPR TTHSSVLIIT PRPQDHGTNL TCQVKFAGAG VTTERTIQLN VTYVPQNPTT GIFPGDGSGK QETRAGVVH-259 (SEQ ID NO:1), or a fragment or variant thereof, e.g., having an amino acid sequence having at least 65%, 70%, 71%, 72%, 73%, 74%, 75%, 76%, 77%, 78%, 79%, 80%, 81%, 82%, 83%, 84%, 85%, 86%, 87%, 88%, 89%, 90%, 91%, 92%, 93%, 94%, 95%, 96%, 97%, 98%, 99% sequence identity to SEQ ID NO:1, wherein the fragment or variant is capable of binding S100A9.

There are at least three known single nucleotide polymorphisms ("SNPs") in the ectodomain of CD33 (i.e., W22R, R69G, S128N). Therefore, the extracellular domain of Homo sapiens CD33 can have the amino acid sequence of SEQ ID NO:1 with any one or more of these

SNPs. For example, the extracellular domain of Homo sapiens CD33 can also have the following amino acid sequence:

18-DPN FX_1LQVQESVT VQEGLCVLVP CTFFHPIPYY DKNSPVHGYW FREGAIISX$_2$D SPVATNKLDQ EVQEETQGRF RLLGDPSRNN CSLSIVDARR RDNGSYFFRM ERGSTKYX$_3$YK SPQLSVHVTD LTHRPKILIP GTLEPGHSKN LTCSVSWACE QGTPPIFSWL SAAPTSLGPR TTHSSVLIIT PRPQDHGTNL TCQVKFAGAG VTTERTIQLN VTYVPQNPTT GIFPGDGSGK QETRAGVVH-259, where X_1 is W or R; wherein X_2 is R or G; and wherein X_3 is S or N (SEQ ID NO:2).

In some cases, the CD33 ectodomain contains only the variable region of CD33 ("vCD33"). For example, in some embodiments, the vCD33 portion has the following amino acid sequence:

19-PN FWLQVQESVT VQEGLCVLVP CTFFHPIPYY DKNSPVHGYW FREGAIISRD SPVATNKLDQ EVQEETQGRF RLLGDPSRNN CSLSIVDARR RDNGSYFFRM ERGSTKYSYK SPQLSVHVTD -135 (SEQ ID NO:3), or a fragment or variant thereof, e.g., having an amino acid sequence having at least 65%, 70%, 71%, 72%, 73%, 74%, 75%, 76%, 77%, 78%, 79%, 80%, 81%, 82%, 83%, 84%, 85%, 86%, 87%, 88%, 89%, 90%, 91%, 92%, 93%, 94%, 95%, 96%, 97%, 98%, 99% sequence identity to SEQ ID NO:3, wherein the fragment or variant is capable of binding S100A9. The vCD33 can also have any one or more of the disclosed SNPs (i.e., W22R, R69G, S128N). Therefore, in some embodiments, the vCD33 portion has the following amino acid sequence:

19-PN FX_1LQVQESVT VQEGLCVLVP CTFFHPIPYY DKNSPVHGYW FREGAIISX$_2$D SPVATNKLDQ EVQEETQGRF RLLGDPSRNN CSLSIVDARR RDNGSYFFRM ERGSTKYX$_3$YK SPQLSVHVTD-135, where X_1 is W or R; wherein X_2 is R or G; and wherein X_3 is S or N (SEQ ID NO:4).

The variable domain of CD33 can be further mutated to create more glycosylation sites in order to enhance binding to S100A9. These mutations can be screened *in silico* and/or tested *in vitro* to evaluate S100A9 binding.

N-linked carbohydrates are linked through N-Acetylglucosamine and asparagines. The N-linked consensus sequence is Asn-X_1- X_2, wherein X_1 is any amino acid other than Pro, and X_2 is Ser or Thr. Most O-linked carbohydrate covalent attachments involve a linkage between the monosaccharide N- Acetylgalactosamine and the amino acids serine or threonine.

Non-limiting examples of mutant sites will be but not limited at CD33 residues that can be mutated to create more glycosylation sites include Q26N, P40N, L78T, and E84N. Other

residues can be identified and tested using routine methods. For example, protein-protein reactions can be assayed using a binding affinity assay, such as an assay that uses surface plasmon resonance (SPR) to detect unlabeled interactants in real time, e.g., using a Biacore™ Sensor Chip (GE Healtchare).

The extracellular domain of *Homo sapiens* Toll-like receptor 4 (TLR4) (Uniprot O00206 [aa. 24-631]) can have the following amino acid sequence:
24-ESWEPCV EVVPNITYQC MELNFYKIPD NLPFSTKNLD LSFNPLRHLG SYSFFSFPEL QVLDLSRCEI QTIEDGAYQS LSHLSTLILT GNPIQSLALG AFSGLSSLQK LVAVETNLAS LENFPIGHLK TLKELNVAHN LIQSFKLPEY FSNLTNLEHL DLSSNKIQSI YCTDLRVLHQ MPLLNLSLDL SLNPMNFIQP GAFKEIRLHK LTLRNNFDSL NVMKTCIQGL AGLEVHRLVL GEFRNEGNLE KFDKSALEGL CNLTIEEFRL AYLDYYLDDI IDLFNCLTNV SSFSLVSVTI ERVKDFSYNF GWQHLELVNC KFGQFPTLKL KSLKRLTFTS NKGGNAFSEV DLPSLEFLDL SRNGLSFKGC CSQSDFGTTS LKYLDLSFNG VITMSSNFLG LEQLEHLDFQ HSNLKQMSEF SVFLSLRNLI YLDISHTHTR VAFNGIFNGL SSLEVLKMAG NSFQENFLPD IFTELRNLTF LDLSQCQLEQ LSPTAFNSLS SLQVLNMSHN NFFSLDTFPY KCLNSLQVLD YSLNHIMTSK KQELQHFPSS LAFLNLTQND FACTCEHQSF LQWIKDQRQL LVEVERMECA TPSDKQGMPV LSLNITCQMN K-631 (SEQ ID NO:5), or a fragment or variant thereof, e.g., having an amino acid sequence having at least 65%, 70%, 71%, 72%, 73%, 74%, 75%, 76%, 77%, 78%, 79%, 80%, 81%, 82%, 83%, 84%, 85%, 86%, 87%, 88%, 89%, 90%, 91%, 92%, 93%, 94%, 95%, 96%, 97%, 98%, 99% sequence identity to SEQ ID NO:5, wherein the fragment or variant is capable of binding S100A9. .

The ectodomain of TLR4 has previously been used in a fusion protein with myeloid differentiation factor 2 (MD-2) to function as a lipopolysaccharide (LPS) trap. MD-2 is necessary for TLR4 to bind LPS. However, it is not necessary for TLR4 to bind and trap S100A9. Therefore, in some embodiments, the fusion protein containing TLR4 does not also contain MD-2. In other embodiments, the fusion protein contains both TLR4 and CD33 ectodomains.

The extracellular domain of *Homo sapiens* Receptor for Advanced Glycation End Products (RAGE) (Accession No. NP_001127 [aa. 23-342]) can have the following amino acid sequence:

23- AQNITARI GEPLVLKCKG APKKPPQRLE WKLNTGRTEA WKVLSPQGGG PWDSVARVLP NGSLFLPAVG IQDEGIFRCQ AMNRNGKETK SNYRVRVYQI PGKPEIVDSA SELTAGVPNK VGTCVSEGSY PAGTLSWHLD GKPLVPNEKG VSVKEQTRRH PETGLFTLQS ELMVTPARGG DPRPTFSCSF SPGLPRHRAL RTAPIQPRVW EPVPLEEVQL VVEPEGGAVA PGGTVTLTCE VPAQPSPQIH WMKDGVPLPL PPSPVLILPE IGPQDQGTYS CVATHSSHGP QESRAVSISI IEPGEEGPTA GSVGGSGLGT LA-342 (SEQ ID NO:6), or a fragment or variant thereof, e.g., having an amino acid sequence having at least 65%, 70%, 71%, 72%, 73%, 74%, 75%, 76%, 77%, 78%, 79%, 80%, 81%, 82%, 83%, 84%, 85%, 86%, 87%, 88%, 89%, 90%, 91%, 92%, 93%, 94%, 95%, 96%, 97%, 98%, 99% sequence identity to SEQ ID NO:6, wherein the fragment or variant is capable of binding S100A9.

A receptor extracellular domain of CD33, TLR4, and/or RAGE can be expressed as a fusion with immunoglobulin heavy chain constant regions, typically an Fc fragment, which contains two constant region domains and lacks the variable region. Such fusions can be secreted as multimeric molecules wherein the Fc portions are disulfide bonded to each other and two receptor polypeptides are arrayed in close proximity to each other. This chimeric molecule can be produced as fusion protein, which can be formed by the chemical coupling of the constituent polypeptides or it can be expressed as a single polypeptide from nucleic acid sequence encoding the single contiguous fusion protein. A single chain fusion protein is a fusion protein having a single contiguous polypeptide backbone. Fusion proteins can be prepared using conventional techniques in molecular biology to join the two genes in frame into a single nucleic acid, and then expressing the nucleic acid in an appropriate host cell under conditions in which the fusion protein is produced. In particular, the CD33/S100A9 inhibitor can be a chimeric fusion protein comprising the ectodomain of CD33, TLR4, and/or RAGE and an immunoglobulin heavy chain constant region (Fc), e.g., from IgG1.

In some cases, the CD33/S100A9 antagonist is multivalent, e.g., it contains at least 2, 3, or more S100A9-binding domains. In some cases, the antagonist contains at least one CD33 ectodomain and a S100A9-binding domain selected from the group consisting of a TLR4 ectodomain and a RAGE ectodomain.

Multiple copies of the fusion protein can also be combined to form a multivalent complex. Therefore, in some embodiments, two or more fusion proteins can be linked to a core molecule or particle. In its simplest form, a multivalent complex comprises a multimer of two or three or four or more of the disclosed fusion proteins associated (e.g. covalently or otherwise

linked) with one another preferably via a linker molecule. Suitable linker molecules include multivalent attachment molecules such as avidin, streptavidin and extravidin, each of which can have four binding sites for biotin.

In some embodiments, the fusion protein can be biotinylated. Once biotinylated, the biotinylated fusion protein can then be conjugated to a tetrameric streptavidin. Proteins can be biotinylated chemically or enzymatically. Chemical biotinylation utilises various conjugation chemistries to yield nonspecific biotinylation of amines, carboxylates, sulfhydryls and carbohydrates. Enzymatic biotinylation results in biotinylation of a specific lysine within a certain sequence by a bacterial biotin ligase. Most chemical biotinylation reagents consist of a reactive group attached via a linker to the valeric acid side chain of biotin. This linker can also mediate the solubility of biotinylation reagents; linkers that incorporate poly(ethylene) glycol (PEG) can make water-insoluble reagents soluble or increase the solubility of biotinylation reagents that are already soluble to some extent.

Enzymatic biotinylation is most often carried out by genetically linking the protein of interest at its N-terminus, C-terminus or at an internal loop to a 15 amino acid biotin acceptor peptide, also termed AviTag™ or Acceptor Peptide (AP). The tagged protein is then incubated with biotin ligase (BirA) in the presence of biotin and ATP. Enzymatic biotinylation can be carried out in vitro but BirA also reacts specifically with its target peptide inside mammalian and bacterial cells and at the cell surface, while other cellular proteins are not modified. Therefore, the fusion protein can further contain a biotin acceptor peptide that can be biotinylated with BirA in the presence of biotin and ATP. For example, the Fc portion can be enzymatically biotinylated using the AviTag™ system (Avidity, LLC, Aurora, Colorado), which involves incorporating a 15 amino acid peptide sequence into the chimeric fusion protein that can be biotinylated by the BirA enzyme of *E. coli*. In some embodiments, this biotin acceptor peptide has the amino acid sequence GLNDIFEAQKIEWHE (SEQ ID NO:7).

Oligonucleotides are readily biotinylated in the course of oligonucleotide synthesis by the phosphoramidite method using biotin phosphoramidite. Upon the standard deprotection, the conjugates obtained can be purified using reverse-phase or anion-exchange HPLC.

In other embodiments, two or more fusion proteins are conjugated to the surface of a liposome or other microparticle to form the multivalent complex. A number of reports describe the attachment of antibodies to liposomes. For example, US 5,620,689 discloses so-called "immunoliposomes" in which antibody or antibody fragments effective to bind to a chosen antigen on a B lymphocyte or a T lymphocyte, are attached to the distal ends of the membrane

lipids in liposomes having a surface coating of polyethylene glycol chains. In some embodiments, the disclosed multivalent complexes comprising immunoliposomes containing antibodies that specifically bind the disclosed fusion proteins. For example, the antibodies can bind the Fc portion of the fusion protein, or tag on the protein, such as the biotin acceptor peptide.

The multivalent complex can be homogeneous, i.e., containing multiple copies of one type of one fusion protein, or it can be heterogeneous. For example, the multivalent complex can contain combinations of CD33 and TLR4 fusion proteins. In addition, the multivalent complex can contain multivalent fusion proteins, i.e., at least two fusion protein containing two or more S100A9-binding domains.

The disclosed chimeric fusion proteins can also contain a peptide linker sequences connecting the one or more CD33 and/or TLR4 ectodomains to each other, to the Fc portion, or any combination thereof. For example, the peptide linker can have the amino acid sequence DIEGRMD (SEQ ID NO:8).

In other embodiments, the CD33/S100A9 inhibitor binds and inhibits endogenous CD33 receptor on MDSCs. For example, the CD33/S100A9 inhibitor can be a recombinant protein that binds CD33 without activating MDSCs and competes for binding of endogenous S100A9 (e.g., a mutant or truncated variant of S100A9).

Antibodies

Antibodies that can be used in the disclosed compositions and methods include whole immunoglobulin (i.e., an intact antibody) of any class, fragments thereof, and synthetic proteins containing at least the antigen binding variable domain of an antibody. The variable domains differ in sequence among antibodies and are used in the binding and specificity of each particular antibody for its particular antigen. However, the variability is not usually evenly distributed through the variable domains of antibodies. It is typically concentrated in three segments called complementarity determining regions (CDRs) or hypervariable regions both in the light chain and the heavy chain variable domains. The more highly conserved portions of the variable domains are called the framework (FR). The variable domains of native heavy and light chains each comprise four FR regions, largely adopting a beta-sheet configuration, connected by three CDRs, which form loops connecting, and in some cases forming part of, the beta-sheet structure. The CDRs in each chain are held together in close proximity by the FR regions and, with the CDRs from the other chain, contribute to the formation of the antigen binding site of antibodies.

Also disclosed are fragments of antibodies which have bioactivity. The fragments, whether attached to other sequences or not, include insertions, deletions, substitutions, or other selected modifications of particular regions or specific amino acids residues, provided the activity of the fragment is not significantly altered or impaired compared to the nonmodified antibody or antibody fragment.

Techniques can also be adapted for the production of single-chain antibodies specific to an antigenic protein of the present disclosure. Methods for the production of single-chain antibodies are well known to those of skill in the art. A single chain antibody can be created by fusing together the variable domains of the heavy and light chains using a short peptide linker, thereby reconstituting an antigen binding site on a single molecule. Single-chain antibody variable fragments (scFvs) in which the C-terminus of one variable domain is tethered to the N-terminus of the other variable domain via a 15 to 25 amino acid peptide or linker have been developed without significantly disrupting antigen binding or specificity of the binding. The linker is chosen to permit the heavy chain and light chain to bind together in their proper conformational orientation.

Divalent single-chain variable fragments (di-scFvs) can be engineered by linking two scFvs. This can be done by producing a single peptide chain with two VH and two VL regions, yielding tandem scFvs. ScFvs can also be designed with linker peptides that are too short for the two variable regions to fold together (about five amino acids), forcing scFvs to dimerize. This type is known as diabodies. Diabodies have been shown to have dissociation constants up to 40-fold lower than corresponding scFvs, meaning that they have a much higher affinity to their target. Still shorter linkers (one or two amino acids) lead to the formation of trimers (triabodies or tribodies). Tetrabodies have also been produced. They exhibit an even higher affinity to their targets than diabodies.

Aptamers

The term "aptamer" refers to oligonucleic acid or peptide molecules that bind to a specific target molecule. These molecules are generally selected from a random sequence pool. The selected aptamers are capable of adapting unique tertiary structures and recognizing target molecules with high affinity and specificity. A "nucleic acid aptamer" is a DNA or RNA oligonucleic acid that binds to a target molecule via its conformation, and thereby inhibits or suppresses functions of such molecule. A nucleic acid aptamer may be constituted by DNA, RNA, or a combination thereof. A "peptide aptamer" is a combinatorial protein molecule with a variable peptide sequence inserted within a constant scaffold protein. Identification of peptide

aptamers is typically performed under stringent yeast dihybrid conditions, which enhances the probability for the selected peptide aptamers to be stably expressed and correctly folded in an intracellular context.

Nucleic acid aptamers are typically oligonucleotides ranging from 15-50 bases in length that fold into defined secondary and tertiary structures, such as stem-loops or G-quartets. Nucleic acid aptamers preferably bind the target molecule with a K_d less than 10^{-6}, 10^{-8}, 10^{-10}, or 10^{-12}. Nucleic acid aptamers can also bind the target molecule with a very high degree of specificity. It is preferred that the nucleic acid aptamers have a K_d with the target molecule at least 10, 100, 1000, 10,000, or 100,000 fold lower than the K_d of other non-targeted molecules.

Nucleic acid aptamers are typically isolated from complex libraries of synthetic oligonucleotides by an iterative process of adsorption, recovery and reamplification. For example, nucleic acid aptamers may be prepared using the SELEX (Systematic Evolution of Ligands by Exponential Enrichment) method. The SELEX method involves selecting an RNA molecule bound to a target molecule from an RNA pool composed of RNA molecules each having random sequence regions and primer-binding regions at both ends thereof, amplifying the recovered RNA molecule via RT-PCR, performing transcription using the obtained cDNA molecule as a template, and using the resultant as an RNA pool for the subsequent procedure. Such procedure is repeated several times to several tens of times to select RNA with a stronger ability to bind to a target molecule. The base sequence lengths of the random sequence region and the primer binding region are not particularly limited. In general, the random sequence region contains about 20 to 80 bases and the primer binding region contains about 15 to 40 bases. Specificity to a target molecule may be enhanced by prospectively mixing molecules similar to the target molecule with RNA pools and using a pool containing RNA molecules that did not bind to the molecule of interest. An RNA molecule that was obtained as a final product by such technique is used as an RNA aptamer. An aptamer database containing comprehensive sequence information on aptamers and unnatural ribozymes that have been generated by *in vitro* selection methods is available at aptamer.icmb.utexas.edu.

A nucleic acid aptamer generally has higher specificity and affinity to a target molecule than an antibody. Accordingly, a nucleic acid aptamer can specifically, directly, and firmly bind to a target molecule. Since the number of target amino acid residues necessary for binding may be smaller than that of an antibody, for example, a nucleic acid aptamer is superior to an antibody, when selective suppression of functions of a given protein among highly homologous proteins is intended.

Non-modified nucleic acid aptamers are cleared rapidly from the bloodstream, with a half-life of minutes to hours, mainly due to nuclease degradation and clearance from the body by the kidneys, a result of the aptamer's inherently low molecular weight. This rapid clearance can be an advantage in applications such as *in vivo* diagnostic imaging. However, several modifications, such as 2'-fluorine-substituted pyrimidines, polyethylene glycol (PEG) linkage, etc. are available to increase the serum half-life of aptamers to the day or even week time scale.

Another approach to increase the nuclease resistance of aptamers is to use a Spiegelmer. Spiegelmers are ribonucleic acid (RNA)-like molecules built from the unnatural L-ribonucleotides. Spiegelmers are therefore the stereochemical mirror images (enantiomers) of natural oligonucleotides. Like other aptamers, Spiegelmers are able to bind target molecules such as proteins. The affinity of Spiegelmers to their target molecules often lies in the pico-to nanomolar range and is thus comparable to antibodies. In contrast to other aptamers, Spiegelmers have high stability in blood serum since they are less susceptible to be cleaved hydrolytically by enzymes. Nonetheless, they are excreted by the kidneys in a short time due to their low molar mass. Unlike other aptamers, Spiegelmers may not be directly produced by the SELEX method. This is because L-nucleic acids are not amenable to enzymatic methods, such as polymerase chain reaction. Instead, the sequence of a natural aptamer identified by the SELEX method is determined and then used in the artificial synthesis of the mirror image of the natural aptamer.

Peptide aptamers are proteins that are designed to interfere with other protein interactions inside cells. They consist of a variable peptide loop attached at both ends to a scaffold. This double structural constraint greatly increases the binding affinity of the peptide aptamer to levels comparable to an antibody.

The variable loop length is typically composed of about ten to twenty amino acids, and the scaffold may be any protein which has good solubility. Currently, the bacterial protein Thioredoxin-A is the most used scaffold protein, the variable loop being inserted within the reducing active site, the two Cysteines lateral chains being able to form a disulfide bridge.

Peptide aptamer selection can be made using different systems, but the most used is currently the yeast two-hybrid system. Peptide aptamer can also be selected from combinatorial peptide libraries constructed by phage display and other surface display technologies such as mRNA display, ribosome display, bacterial display and yeast display. These experimental procedures are also known as biopannings. Among peptides obtained from biopannings,

mimotopes can be considered as a kind of peptide aptamers. All the peptides panned from combinatorial peptide libraries have been stored in a special database with the name MimoDB.

Pharmaceutical Composition

The disclosed compositions can be used therapeutically in combination with a pharmaceutically acceptable carrier. By "pharmaceutically acceptable" is meant a material that is not biologically or otherwise undesirable, i.e., the material may be administered to a subject, along with the nucleic acid or vector, without causing any undesirable biological effects or interacting in a deleterious manner with any of the other components of the pharmaceutical composition in which it is contained. The carrier would naturally be selected to minimize any degradation of the active ingredient and to minimize any adverse side effects in the subject, as would be well known to one of skill in the art.

Suitable carriers and their formulations are described in Remington: The Science and Practice of Pharmacy (19th ed.) ed. A.R. Gennaro, Mack Publishing Company, Easton, PA 1995. Typically, an appropriate amount of a pharmaceutically-acceptable salt is used in the formulation to render the formulation isotonic. Examples of the pharmaceutically-acceptable carrier include, but are not limited to, saline, Ringer's solution and dextrose solution. The pH of the solution is preferably from about 5 to about 8, and more preferably from about 7 to about 7.5. Further carriers include sustained release preparations such as semipermeable matrices of solid hydrophobic polymers containing the antibody, which matrices are in the form of shaped articles, e.g., films, liposomes or microparticles. It will be apparent to those persons skilled in the art that certain carriers may be more preferable depending upon, for instance, the route of administration and concentration of composition being administered.

Pharmaceutical carriers are known to those skilled in the art. These most typically would be standard carriers for administration of drugs to humans, including solutions such as sterile water, saline, and buffered solutions at physiological pH. The compositions can be administered intramuscularly or subcutaneously. Other compounds will be administered according to standard procedures used by those skilled in the art.

Pharmaceutical compositions may include carriers, thickeners, diluents, buffers, preservatives, surface active agents and the like in addition to the molecule of choice. Pharmaceutical compositions may also include one or more active ingredients such as antimicrobial agents, antiinflammatory agents, anesthetics, and the like.

Preparations for parenteral administration include sterile aqueous or non-aqueous solutions, suspensions, and emulsions. Examples of non-aqueous solvents are propylene glycol,

polyethylene glycol, vegetable oils such as olive oil, and injectable organic esters such as ethyl oleate. Aqueous carriers include water, alcoholic/aqueous solutions, emulsions or suspensions, including saline and buffered media. Parenteral vehicles include sodium chloride solution, Ringer's dextrose, dextrose and sodium chloride, lactated Ringer's, or fixed oils. Intravenous vehicles include fluid and nutrient replenishers, electrolyte replenishers (such as those based on Ringer's dextrose), and the like. Preservatives and other additives may also be present such as, for example, antimicrobials, anti-oxidants, chelating agents, and inert gases and the like.

Compositions for oral administration include powders or granules, suspensions or solutions in water or non-aqueous media, capsules, sachets, or tablets. Thickeners, flavorings, diluents, emulsifiers, dispersing aids or binders may be desirable.

Some of the compositions may potentially be administered as a pharmaceutically acceptable acid- or base- addition salt, formed by reaction with inorganic acids such as hydrochloric acid, hydrobromic acid, perchloric acid, nitric acid, thiocyanic acid, sulfuric acid, and phosphoric acid, and organic acids such as formic acid, acetic acid, propionic acid, glycolic acid, lactic acid, pyruvic acid, oxalic acid, malonic acid, succinic acid, maleic acid, and fumaric acid, or by reaction with an inorganic base such as sodium hydroxide, ammonium hydroxide, potassium hydroxide, and organic bases such as mono-, di-, trialkyl and aryl amines and substituted ethanolamines.

Methods of Treatment

Also disclosed are methods for treating a disease in a subject that is caused or exacerbated by S100A9 activity, comprising administering to the subject a composition comprising a CD33/S100A9 antagonist disclosed herein.

The innate immune system is crucial for initiation and amplification of inflammatory responses. During this process, phagocytes are activated by PAMPs that are recognized by PRRs. Phagocytes are also activated by endogenous danger signals called alarmins or DAMPs via partly specific, partly common PRRs. Two members of the S100 protein family, S100A8 and S100A9, have been identified recently as important endogenous DAMPs. The complex of S100A8 and S100A9 (also called calprotectin) is actively secreted during the stress response of phagocytes. These molecules have been identified as endogenous activators of TLR4 and have been shown to promote lethal, endotoxin-induced shock. Importantly, S100A8/S100A9 is not only involved in promoting the inflammatory response in infections but was also identified as a potent amplifier of inflammation in autoimmunity as well as in cancer development and tumor spread. This proinflammatory action of S100A8/S100A9 involves autocrine and paracrine

mechanisms in phagocytes, endothelium, and other cells. As a net result, extravasation of leukocytes into inflamed tissues and their subsequent activation are increased. Thus, S100A8/S100A9 plays a pivotal role during amplification of inflammation.

Diseases that are associated with S100A8/S100A9 activity include, but are not limited to, rheumatoid arthritis, juvenile idiopathic arthritis, psoriatic arthritis, sepsis, atherosclerosis, acute coronary syndrome/myocardial infarction, diabetes, psoriasis/inflammatory skin disease, inflammatory bowel disease, vasculitis, transplant rejection, SLE/glomerulonephritis, pancreatitis, cancer, dermatomyositis/polymyositis, and hyperzincemia/systemic inflammation. In addition, disease characterized by recurrent infections, hepato-splenomegaly, anemia, vasculopathie, concomitant cutaneous ulcers, and systemic inflammation are defined by extraordinarily high levels of S100A8/S100A9 in extracellular fluids.

In some embodiments, the method involves treating infection and/or preventing sepsis in a patient in need thereof. Sepsis is caused by the immune system's response to a serious infection, most commonly bacteria, but also fungi, viruses, and parasites in the blood, urinary tract, lungs, skin, or other tissues. There are number of microbial factors which can cause the typical septic inflammatory cascade. An invading pathogen is recognised by its pathogen-associated molecular pattern (PAMP). Examples of PAMPs are lipopolysaccharides (LPS) in Gram-negative bacteria, flagellin in Gram-negative bacteria, muramyl dipeptide in the peptidoglycan cell wall of a Gram-positive bacteria and CpG bacterial DNA. These PAMPs are recognized by the innate immune system's pattern recognition receptors (PRR). There are four families of PRRs: the toll-like receptors, the C-type lectin receptors, the nucleotide oligemerization domain-like receptors and the RigI-helicases. S100A8/S100A9 acts as an endogenous TLR4 ligand involved in amplification of LPS effects on phagocytes upstream of TNF-α. Although TNF-α is critical for LPS toxicity, blockade of TNF-α had a harmful rather than protective effect in human sepsis. Moreover, in a small study, S100A8/S100A9 levels were demonstrated to decrease in surviving patients during recovery from sepsis, and nonsurvivors were characterized by high S100A8/S100A9 serum levels. Sepsis is usually treated with intravenous fluids and antibiotics. The disclosed CD33/S100A9 antagonist can be used instead of, or in addition to, intravenous antibiotics.

In some embodiments, the method involves treating an inflammatory and/or autoimmune disease in a patient in need thereof. S100A8/S100A9 contributes to the pathogenesis of different types of arthritis. Macrophage-derived S100A8/S100A9 amplifies the inflammatory response in antigen-induced arthritis and also acts as endogenous DAMP in the absence of infection or

pathogenic agents. Autoimmunity is the failure of an organism in recognizing its own constituent parts as self, thus leading to an immune response against its own cells and tissues. Any disease that results from such an aberrant immune response is termed an autoimmune or autoinflammatory disease. Autoimmune and autoinflammatory diseases share common characteristics in that both groups of disorders result from the immune system attacking the body's own tissues, and also result in increased inflammation. Prominent examples include Celiac disease, diabetes mellitus type 1 (IDDM), Sarcoidosis, systemic lupus erythematosus (SLE), Sjögren's syndrome, Churg-Strauss Syndrome, Hashimoto's thyroiditis, Graves' disease, idiopathic thrombocytopenic purpura, Addison's Disease, rheumatoid arthritis (RA), gouty arthritis, Polymyositis (PM), Dermatomyositis (DM), graft-versus-host disease, pernicious anemia, Addison disease, scleroderma, Goodpasture's syndrome, inflammatory bowel diseases such as Crohn's disease, colitis, atypical colitis, chemical colitis; collagenous colitis, distal colitis, diversion colitis: fulminant colitis, indeterminate colitis, infectious colitis, ischemic colitis, lymphocytic colitis, microscopic colitis, gastroenteritis, Hirschsprung's disease, inflammatory digestive diseases, Morbus Crohn, non-chronic or chronic digestive diseases, non-chronic or chronic inflammatory digestive diseases; regional enteritis and ulcerative colitis, autoimmune hemolytic anemia, sterility, myasthenia gravis, multiple sclerosis, Basedow's disease, thrombopenia purpura, insulin-dependent diabetes mellitus, allergy; asthma, atopic disease; arteriosclerosis; myocarditis; cardiomyopathy; glomerular nephritis; hypoplastic anemia; rejection after organ transplantation and numerous malignancies of lung, prostate, liver, ovary, colon, cervix, lymphatic and breast tissues, psoriasis, acne vulgaris, asthma, autoimmune diseases, celiac disease, chronic prostatits, glomerulonephritis, inflammatory bowel diseases, pelvic inflammatory disease, reperfusion injury sarcoidosis, vasculitis, interstitial cystitis, type 1 hypersensitivities, systemic sclerosis, dermatomyositis, polymyositis, and inclusion body myositis, and allergies. Treatments for autoimmune disease have traditionally been immunosuppressive, anti-inflammatory (steroids), or palliative. Non-immunological therapies, such as hormone replacement in Hashimoto's thyroiditis or Type 1 diabetes mellitus treat outcomes of the autoaggressive response, thus these are palliative treatments. Dietary manipulation limits the severity of celiac disease. Steroidal or NSAID treatment limits inflammatory symptoms of many diseases. IVIG is used for CIDP and GBS. Specific immunomodulatory therapies, such as the TNFα antagonists (e.g. etanercept), the B cell depleting agent rituximab, the anti-IL-6 receptor tocilizumab and the costimulation blocker abatacept have been shown to be useful in treating RA. Some of these immunotherapies may be

associated with increased risk of adverse effects, such as susceptibility to infection. The disclosed CD33/S100A9 antagonist can be used instead of, or in addition to, these existing treatments.

In some embodiments, the method involves treating a neurodegenerative disease or disorder in a patient in need thereof. As used herein, "neurodegenerative disease" includes neurodegenerative disease associated with protein aggregation, also referred to as "protein aggregation disorders", "protein conformation disorders", or "proteinopathies". Neurodegenerative disease associated with protein aggregation include diseases or disorders characterized by the formation of detrimental intracellular protein aggregates (e.g., inclusions in the cytosol or nucleus) or extracellular protein aggregates (e.g., plaques). "Detrimental protein aggregation" is the undesirable and harmful accumulation, oligomerization, fibrillization or aggregation, of two or more, hetero- or homomeric, proteins or peptides. A detrimental protein aggregate may be deposited in bodies, inclusions or plaques, the characteristics of which are often indicative of disease and contain disease- specific proteins. For example, superoxide dismutase-1 aggregates are associated with ALS, poly-Q aggregates are associated with Huntington's disease, and α-synuclein-containing Lewy bodies are associated with Parkinson's disease.

Neurological diseases are also associated with immune failure related to increasing levels of disease-causing factors that exceed the ability of the immune system to contain, or a situation in which immune function deteriorates or is suppressed concomitantly with disease progression, due to factors indirectly or directly related to the disease-causing entity. MDSCs can cause T-cell deficiency by suppressing effector T cell activity, thus promoting neurodegenerative disease associated with immune failure.

Representative examples of Protein Aggregation Disorders or Proteopathies include Protein Conformational Disorders, Alpha-Synucleinopathies, Polyglutamine Diseases, Serpinopathies, Tauopathies or other related disorders. Other examples of neurological diseases or include, but are not limited to, Amyotrophic Lateral Sclerosis (ALS), Huntington's Disease (HD), Parkinson's Disease (PD), Spinal Muscular Atrophy (SMA), Alzheimer's Disease (AD), diffuse Lewy body dementia (DLBD), multiple system atrophy (MSA), dystrophia myotonica, dentatorubro-pallidoluysian atrophy (DRPLA), Friedreich's ataxia, fragile X syndrome, fragile XE mental retardation, Machado-Joseph Disease (MJD or SCA3), spinobulbar muscular atrophy (also known as Kennedy's Disease), spinocerebellar ataxia type 1 (SCAl) gene, spinocerebellar ataxia type 2 (SCA2), spinocerebellar ataxia type 6 (SCA6), spinocerebellar ataxia type 7

(SCA7), spinocerebellar ataxia type 17 (SCA17), chronic liver diseases, familial encephalopathy with neuroserpin inclusion bodies (FENIB), Pick's disease, corticobasal degeneration (CBD), progressive supranuclear palsy (PSP), amyotrophic lateral sclerosis/parkinsonism dementia complex, Cataract, serpinopathies, haemolytic anemia, cystic fibrosis, Wilson's Disease, neurofibromatosis type 2, demyelinating peripheral neuropathies, retinitis pigmentosa, Marfan syndrome, emphysema, idiopathic pulmonary fibrosis, Argyophilic grain dementia, corticobasal degeneration, diffuse neurofibrillary tangles with calcification, frontotemporal dementia/parkinsonism linked to chromosome 17, Hallervorden-Spatz disease, Nieman-Pick disease type C, subacute sclerosing panencephalitis, cognitive disorders including dementia (associated with Alzheimer's disease, ischemia, trauma, vascular problems or stroke, HIV disease, Parkinson's disease, Huntington's disease, Pick's disease, Creutzfeldt-Jacob disease, perinatal hypoxia, other general medical conditions or substance abuse); delirium, amnestic disorders or age related cognitive decline; anxiety disorders including acute stress disorder, agoraphobia, generalized anxiety disorder, obsessive-compulsive disorder, panic attack, panic disorder, post-traumatic stress disorder, separation anxiety disorder, social phobia, specific phobia, substance-induced anxiety disorder and anxiety due to a general medical condition; schizophrenia or psychosis including schizophrenia (paranoid, disorganized, catatonic or undifferentiated), schizophreniform disorder, schizoaffective disorder, delusional disorder, brief psychotic disorder, shared psychotic disorder, psychotic disorder due to a general medical condition and substance-induced psychotic disorder; substance-related disorders and addictive behaviors (including substance-induced delirium, persisting dementia, persisting amnestic disorder, psychotic disorder or anxiety disorder; tolerance, dependence or withdrawal from substances including alcohol, amphetamines, cannabis, cocaine, hallucinogens, inhalants, nicotine, opioids, phencyclidine, sedatives, hypnotics or anxiolytics); movement disorders, including akinesias and akinetic-rigid syndromes (including Parkinson's disease, drug-induced parkinsonism, postencephalitic parkinsonism, progressive supranuclear palsy, corticobasal degeneration, parkinsonism-ALS dementia complex and basal ganglia calcification), medication-induced parkinsonism (such as neuroleptic-induced parkinsonism, neuroleptic malignant syndrome, neuroleptic-induced acute dystonia, neuroleptic-induced acute akathisia, neuroleptic-induced tardive dyskinesia and medication-induced postural tremor), Gilles de la Tourette's syndrome, epilepsy, and dyskinesias including tremor (such as rest tremor, postural tremor and intention tremor), chorea (such as Sydenham's chorea, Huntington's disease, benign hereditary chorea, neuroacanthocytosis, symptomatic chorea, drug-induced chorea and hemiballism),

myoclonus (including generalized myoclonus and focal myoclonus), tics (including simple tics, complex tics and symptomatic tics), and dystonia (including generalized dystonia such as iodiopathic dystonia, drug-induced dystonia, symptomatic dystonia and paroxysmal dystonia, and focal dystonia such as blepharospasm, oromandibular dystonia, spasmodic dysphonia, spasmodic torticollis, axial dystonia, dystonic writer's cramp and hemiplegic dystonia)]; obesity, bulimia nervosa and compulsive eating disorders; pain including bone and joint pain (osteoarthritis), repetitive motion pain, dental pain, cancer pain, myofacial pain (muscular injury, fibromyalgia), perioperative pain (general surgery, gynecological), chronic pain, neuropathic pain, post-traumatic pain, trigeminal neuralgia, migraine and migraine headache; obesity or eating disorders associated with excessive food intake and complications associated therewith; attention-deficit/hyperactivity disorder; conduct disorder; mood disorders including depressive disorders, bipolar disorders, mood disorders due to a general medical condition, and substance-induced mood disorders; muscular spasms and disorders associated with muscular spasticity or weakness including tremors; urinary incontinence; amyotrophic lateral sclerosis; neuronal damage including ocular damage, retinopathy or macular degeneration of the eye, hearing loss or tinnitus; emesis, brain edema and sleep disorders including narcolepsy, and apoptosis of motor neuron cells. Illustrative examples of the neuropathic pain include diabetic polyneuropathy, entrapment neuropathy, phantom pain, thalamic pain after stroke, post-herpetic neuralgia, atypical facial neuralgia pain after tooth extraction and the like, spinal cord injury, trigeminal neuralgia and cancer pain resistant to narcotic analgesics such as morphine. The neuropathic pain includes the pain caused by either central or peripheral nerve damage. And it includes the pain caused by either mononeuropathy or polyneuropathy.

In some cases, the method involves enhancing tumor immune response in a patient in need thereof. S100A8/S100A9 expression is increased in patients with various tumors. Soluble factors secreted from tumor cells are believed to induce overexpression of S100A8/S100A9, resulting in increased generation of MDSCs. These MDSCs can inhibit anti-tumor responses by CD8+ T cells and thus promote tumor growth. The cancer of the disclosed methods can be any cell in a subject undergoing unregulated growth, invasion, or metastasis. In some aspects, the cancer can be any neoplasm or tumor for which radiotherapy is currently used. In some aspects, the cancer can be any tumor that is resistant to standard of care therapy. Thus, Also provided are methods of sensitizing tumors to standard care therapy, comprising administering to the subject an effective amount of a compound or composition as disclosed herein. For example, the cancer can be a neoplasm or tumor that is not sufficiently sensitive to radiotherapy using

standard methods. Thus, the cancer can be a sarcoma, lymphoma, leukemia, carcinoma, blastoma, or germ cell tumor. A representative but non-limiting list of cancers that the disclosed compositions can be used to treat include lymphoma, B cell lymphoma, T cell lymphoma, mycosis fungoides, Hodgkin's Disease, myeloid leukemia, bladder cancer, brain cancer, nervous system cancer, head and neck cancer, squamous cell carcinoma of head and neck, kidney cancer, lung cancers such as small cell lung cancer and non-small cell lung cancer, neuroblastoma/glioblastoma, ovarian cancer, pancreatic cancer, prostate cancer, skin cancer, liver cancer, melanoma, squamous cell carcinomas of the mouth, throat, larynx, and lung, colon cancer, cervical cancer, cervical carcinoma, breast cancer, epithelial cancer, renal cancer, genitourinary cancer, pulmonary cancer, esophageal carcinoma, head and neck carcinoma, large bowel cancer, hematopoietic cancers; testicular cancer; colon and rectal cancers, prostatic cancer, and pancreatic cancer. The disclosed CD33/S100A9 antagonist can be used instead of, or in addition to, existing antineoplastic drugs and/or radiation treatments.

As disclosed herein, $LIN^-HLA\text{-}DR^-CD33^+$ MDSCs specifically accumulate in the BM of myelodysplastic syndromes (MDS) patients and impair hematopoiesis through a mechanism that involves S100A9 as an endogenous ligand for CD33 initiated signaling. Therefore, the disclosed method can involve treating MDS in a patient in need thereof. The myelodysplastic syndromes (MDS) are hematological (blood-related) medical conditions with ineffective production (or dysplasia) of the myeloid class of blood cells. In some cases, the MDS patient has a chromosome 5q deletion (del(5q)). However, in other cases, the patient has non-del5q MDS. Although three agents are approved for the treatment of MDS in the United States (US), lenalidomide (LEN) represents the only targeted therapeutic. Therefore, the disclosed CD33/S100A9 antagonist can be used instead of, or in addition to, lenalidomide.

In some embodiments, the method involves treating anemia of chronic disease (including cancer-related anemia) in a patient, comprising administering to the subject an effective amount of a composition as disclosed herein.

Administration

The disclosed CD33/S100A9 inhibitors may be administered in a therapeutically effective amount to a subject to treat a disease caused or exacerbated by S100A9 activity. The disclosed compositions, including pharmaceutical composition, may be administered in a number of ways depending on whether local or systemic treatment is desired, and on the area to be treated. For example, the disclosed compositions can be administered intravenously, intraperitoneally, intramuscularly, subcutaneously, intracavity, or transdermally. The

compositions may be administered orally, parenterally (e.g., intravenously), by intramuscular injection, by intraperitoneal injection, transdermally, extracorporeally, ophthalmically, vaginally, rectally, intranasally, topically or the like, including topical intranasal administration or administration by inhalant.

Parenteral administration of the composition, if used, is generally characterized by injection. Injectables can be prepared in conventional forms, either as liquid solutions or suspensions, solid forms suitable for solution of suspension in liquid prior to injection, or as emulsions. A revised approach for parenteral administration involves use of a slow release or sustained release system such that a constant dosage is maintained. See, e.g., U.S. Patent No. 3,610,795, which is incorporated by reference herein.

The compositions disclosed herein may be administered prophylactically to patients or subjects who are at risk for MDS. Thus, the method can further comprise identifying a subject at risk for MDS prior to administration of the herein disclosed compositions.

The exact amount of the compositions required will vary from subject to subject, depending on the species, age, weight and general condition of the subject, the severity of the allergic disorder being treated, the particular nucleic acid or vector used, its mode of administration and the like. Thus, it is not possible to specify an exact amount for every composition. However, an appropriate amount can be determined by one of ordinary skill in the art using only routine experimentation given the teachings herein. For example, effective dosages and schedules for administering the compositions may be determined empirically, and making such determinations is within the skill in the art. The dosage ranges for the administration of the compositions are those large enough to produce the desired effect in which the symptoms disorder are effected. The dosage should not be so large as to cause adverse side effects, such as unwanted cross-reactions, anaphylactic reactions, and the like. Generally, the dosage will vary with the age, condition, sex and extent of the disease in the patient, route of administration, or whether other drugs are included in the regimen, and can be determined by one of skill in the art. The dosage can be adjusted by the individual physician in the event of any counterindications. Dosage can vary, and can be administered in one or more dose administrations daily, for one or several days. Guidance can be found in the literature for appropriate dosages for given classes of pharmaceutical products. For example, guidance in selecting appropriate doses for antibodies can be found in the literature on therapeutic uses of antibodies, e.g., Handbook of Monoclonal Antibodies, Ferrone et al., eds., Noges Publications, Park Ridge, N.J., (1985) ch. 22 and pp. 303-357; Smith et al., Antibodies in Human Diagnosis

and Therapy, Haber et al., eds., Raven Press, New York (1977) pp. 365-389. A typical daily dosage of the antibody used alone might range from about 1 μg/kg to up to 100 mg/kg of body weight or more per day, depending on the factors mentioned above.

Screening Methods

Also provided herein is a method of identifying an agent that can be used to treat MDS in a subject. The method can comprise providing a sample comprising CD33 and S100A9 under conditions that allow CD33 and S100A9 to bind, contacting the sample with a candidate agent, detecting the level of CD33/S100A9 binding, and comparing the binding level to a control, wherein a decrease in CD33/S100A9 binding compared to the control identifies an agent that can be used to treat an inflammatory disease.

The binding of S100A9 to CD33 can be detected using routine methods, such as immunodetection methods, that do not disturb protein binding. The methods can be cell-based or cell-free assays. The steps of various useful immunodetection methods have been described in the scientific literature, such as, e.g., Maggio et al., Enzyme-Immunoassay, (1987) and Nakamura, et al., Enzyme Immunoassays: Heterogeneous and Homogeneous Systems, Handbook of Experimental Immunology, Vol. 1: Immunochemistry, 27.1-27.20 (1986), each of which is incorporated herein by reference in its entirety and specifically for its teaching regarding immunodetection methods. Immunoassays, in their most simple and direct sense, are binding assays involving binding between antibodies and antigen. Many types and formats of immunoassays are known and all are suitable for detecting the disclosed biomarkers. Examples of immunoassays are enzyme linked immunosorbent assays (ELISAs), radioimmunoassays (RIA), radioimmune precipitation assays (RIPA), immunobead capture assays, Western blotting, dot blotting, gel-shift assays, Flow cytometry, protein arrays, multiplexed bead arrays, magnetic capture, in vivo imaging, fluorescence resonance energy transfer (FRET), and fluorescence recovery/localization after photobleaching (FRAP/ FLAP).

In general, candidate agents can be identified from large libraries of natural products or synthetic (or semi-synthetic) extracts or chemical libraries according to methods known in the art. Those skilled in the field of drug discovery and development will understand that the precise source of test extracts or compounds is not critical to the screening procedure(s) used.

Accordingly, virtually any number of chemical extracts or compounds can be screened using the exemplary methods described herein. Examples of such extracts or compounds include, but are not limited to, plant-, fungal-, prokaryotic- or animal-based extracts, fermentation broths, and synthetic compounds, as well as modification of existing compounds. Numerous methods

are also available for generating random or directed synthesis (e.g., semi-synthesis or total synthesis) of any number of chemical compounds, including, but not limited to, saccharide-, lipid-, peptide-, and nucleic acid-based compounds. Synthetic compound libraries are commercially available, e.g., from purveyors of chemical libraries including but not limited to ChemBridge Corporation (16981 Via Tazon, Suite G, San Diego, CA, 92127, USA, www.chembridge.com); ChemDiv (6605 Nancy Ridge Drive, San Diego, CA 92121, USA); Life Chemicals (1103 Orange Center Road, Orange, CT 06477); Maybridge (Trevillett, Tintagel, Cornwall PL34 0HW, UK)

Alternatively, libraries of natural compounds in the form of bacterial, fungal, plant, and animal extracts are commercially available from a number of sources, including O2H, (Cambridge, UK), MerLion Pharmaceuticals Pte Ltd (Singapore Science Park II, Singapore 117528) and Galapagos NV (Generaal De Wittelaan L11 A3, B-2800 Mechelen, Belgium).

In addition, natural and synthetically produced libraries are produced, if desired, according to methods known in the art, e.g., by standard extraction and fractionation methods or by standard synthetic methods in combination with solid phase organic synthesis, micro-wave synthesis and other rapid throughput methods known in the art to be amenable to making large numbers of compounds for screening purposes. Furthermore, if desired, any library or compound, including sample format and dissolution is readily modified and adjusted using standard chemical, physical, or biochemical methods. In addition, those skilled in the art of drug discovery and development readily understand that methods for dereplication (e.g., taxonomic dereplication, biological dereplication, and chemical dereplication, or any combination thereof) or the elimination of replicates or repeats of materials already known for their effect on MDS should be employed whenever possible.

Candidate agents encompass numerous chemical classes, but are most often organic molecules, e.g., small organic compounds having a molecular weight of more than 100 and less than about 2,500 Daltons. Candidate agents can include functional groups necessary for structural interaction with proteins, particularly hydrogen bonding, and typically include at least an amine, carbonyl, hydroxyl or carboxyl group, for example, at least two of the functional chemical groups. The candidate agents often contain cyclical carbon or heterocyclic structures and/or aromatic or polyaromatic structures substituted with one or more of the above functional groups.

In some embodiments, the candidate agents are proteins. In some aspects, the candidate agents are naturally occurring proteins or fragments of naturally occurring proteins. Thus, for

example, cellular extracts containing proteins, or random or directed digests of proteinaceous cellular extracts, can be used. In this way libraries of procaryotic and eucaryotic proteins can be made for screening using the methods herein. The libraries can be bacterial, fungal, viral, and vertebrate proteins, and human proteins.

Definitions

The term "antibody" refers to natural or synthetic antibodies that selectively bind a target antigen. The term includes polyclonal and monoclonal antibodies. In addition to intact immunoglobulin molecules, also included in the term "antibodies" are fragments or polymers of those immunoglobulin molecules, and human or humanized versions of immunoglobulin molecules that selectively bind the target antigen.

A "chimeric molecule" is a single molecule created by joining two or more molecules that exist separately in their native state. The single, chimeric molecule has the desired functionality of all of its constituent molecules.

A "fusion protein" refers to a polypeptide formed by the joining of two or more polypeptides through a peptide bond formed between the amino terminus of one polypeptide and the carboxyl terminus of another polypeptide. The fusion protein can be formed by the chemical coupling of the constituent polypeptides or it can be expressed as a single polypeptide from nucleic acid sequence encoding the single contiguous fusion protein. A single chain fusion protein is a fusion protein having a single contiguous polypeptide backbone. Fusion proteins can be prepared using conventional techniques in molecular biology to join the two genes in frame into a single nucleic acid, and then expressing the nucleic acid in an appropriate host cell under conditions in which the fusion protein is produced.

The term "inhibit" refers to a decrease in an activity, response, condition, disease, or other biological parameter. This can include but is not limited to the complete ablation of the activity, response, condition, or disease. This may also include, for example, a 10% reduction in the activity, response, condition, or disease as compared to the native or control level. Thus, the reduction can be a 10, 20, 30, 40, 50, 60, 70, 80, 90, 100%, or any amount of reduction in between as compared to native or control levels.

A "liposome" is a small vesicle composed of various types of lipids, phospholipids and/or surfactant which is useful for delivery of a drug (such as the antagonists disclosed herein and, optionally, a chemotherapeutic agent) to a mammal. The components of the liposome are commonly arranged in a bilayer formation, similar to the lipid arrangement of biological membranes.

The terms "peptide," "protein," and "polypeptide" are used interchangeably to refer to a natural or synthetic molecule comprising two or more amino acids linked by the carboxyl group of one amino acid to the alpha amino group of another.

The term "percent (%) sequence identity" or "homology" is defined as the percentage of nucleotides or amino acids in a candidate sequence that are identical with the nucleotides or amino acids in a reference nucleic acid sequence, after aligning the sequences and introducing gaps, if necessary, to achieve the maximum percent sequence identity. Alignment for purposes of determining percent sequence identity can be achieved in various ways that are within the skill in the art, for instance, using publicly available computer software such as BLAST, BLAST-2, ALIGN, ALIGN-2 or Megalign (DNASTAR) software. Appropriate parameters for measuring alignment, including any algorithms needed to achieve maximal alignment over the full-length of the sequences being compared can be determined by known methods.

The term "pharmaceutically acceptable" refers to those compounds, materials, compositions, and/or dosage forms which are, within the scope of sound medical judgment, suitable for use in contact with the tissues of human beings and animals without excessive toxicity, irritation, allergic response, or other problems or complications commensurate with a reasonable benefit/risk ratio.

The term "specifically binds", as used herein, when referring to a polypeptide (including antibodies) or receptor, refers to a binding reaction which is determinative of the presence of the protein or polypeptide or receptor in a heterogeneous population of proteins and other biologics. Thus, under designated conditions (e.g. immunoassay conditions in the case of an antibody), a specified ligand or antibody "specifically binds" to its particular "target" (e.g. an antibody specifically binds to an endothelial antigen) when it does not bind in a significant amount to other proteins present in the sample or to other proteins to which the ligand or antibody may come in contact in an organism. Generally, a first molecule that "specifically binds" a second molecule has an affinity constant (Ka) greater than about 10^5 M^{-1} (e.g., 10^6 M^{-1}, 10^7 M^{-1}, 10^8 M^{-1}, 10^9 M^{-1}, 10^{10} M^{-1}, 10^{11} M^{-1}, and 10^{12} M^{-1} or more) with that second molecule.

The term "subject" refers to any individual who is the target of administration or treatment. The subject can be a vertebrate, for example, a mammal. Thus, the subject can be a human or veterinary patient. The term "patient" refers to a subject under the treatment of a clinician, e.g., physician.

The term "therapeutically effective" refers to the amount of the composition used is of sufficient quantity to ameliorate one or more causes or symptoms of a disease or disorder. Such amelioration only requires a reduction or alteration, not necessarily elimination.

The term "treatment" refers to the medical management of a patient with the intent to cure, ameliorate, stabilize, or prevent a disease, pathological condition, or disorder. This term includes active treatment, that is, treatment directed specifically toward the improvement of a disease, pathological condition, or disorder, and also includes causal treatment, that is, treatment directed toward removal of the cause of the associated disease, pathological condition, or disorder. In addition, this term includes palliative treatment, that is, treatment designed for the relief of symptoms rather than the curing of the disease, pathological condition, or disorder; preventative treatment, that is, treatment directed to minimizing or partially or completely inhibiting the development of the associated disease, pathological condition, or disorder; and supportive treatment, that is, treatment employed to supplement another specific therapy directed toward the improvement of the associated disease, pathological condition, or disorder.

A number of embodiments of the invention have been described. Nevertheless, it will be understood that various modifications may be made without departing from the spirit and scope of the invention. Accordingly, other embodiments are within the scope of the following claims.

EXAMPLES

Example 1: Microenvironment Induced Myelodysplasia mediated by Myeloid-Derived Suppressor Cells.

Methods

MDS patients. The majority of patients with MDS were low risk unless otherwise specified. All patients were confirmed by central review and classified in accordance with either the World Health Organization criteria or International Prognostic Scoring System (IPSS). Patients were recruited from the Malignant Hematology clinic at the H. Lee Moffitt Cancer Center & Research Institute and the Radboud University Nijmegen Medical Centre, Department of Hematology in the Netherlands. Bone marrow mononuclear cells (BM-MNC) were isolated from heparinized BM aspirates by Ficoll-Hypaque gradient centrifugation, as previously described (Wei, S., et al. 2009. Proc Natl Acad Sci U S A 106:12974-12979). MDSCs were defined and purified by fluorescence activated cell sorting (FACS) of $CD33^{+}$ cells lacking expression of lineage (Lin^{-}) markers (CD3, CD14, CD16, CD19, CD20, CD56) and HLA-DR.

Mice. All mouse work was approved by the Institutional Animal Care and Use Committee at the University of South Florida. Wild type (WT) FVB/NJ mice were purchased from Jackson Laboratories, and S100A9 knockout mice (KO) and S100A9 transgenic mice (Tg) were generated and used as previously described (Cheng, P., et al. 2008. J Exp Med 205:2235-2249; Manitz, M.P., et al. 2003. Mol Cell Biol 23:1034-1043). S100A9Tg mice were generated from FVB/NJ homozygous mice and bred for more than 15 generations. For the competitive transplant experiment, 18 week old FVB/NJ wild type female mice were irradiated once in a rotating gamma irradiator for a total dose of 900Gy. Concurrently, BM cells were isolated from the tibias and femurs of age-matched male WT or S100A9Tg mice from which HSCs were then enriched by magnetic cell sorting (MACS, Millitenyi Biotech) following the manufacturer's protocol. Six hours post-irradiation $1x10^7$ enriched HSCs were given by tail vein injection into recipient mice. Mice were then monitored every other day with weight measurements under a sterile hood. Peripheral blood for CBC was collected from the antero-orbital vein by Vivarium staff at the center weekly. By 8 weeks (after which the WT recipients were engrafted, WBC > $3x10^3$ cells/ml of blood) mice were euthanized by CO_2 aspiration at which point peripheral blood was collected by heart puncture followed by dissection of tibias and femurs (as before) and spleen for assessment.

Fluorescence in situ hybridization (FISH). FISH was done at the Cytogenetics Laboratory of Moffitt Cancer Center, and detailed methods have been previously described (Wei, S., et al. 2009. Proc Natl Acad Sci U S A 106:12974-12979). Target DNA from MDSC positive (MDS-MDSC) cells and MDSC negative cells was purified from the same patients who were previously confirmed to have del5q or del7q using a commercially available test (Abbott laboratory).

Immunostaining. BM-MNCs were purified from MDS patients, diluted to a concentration of $3x10^5$ cells/ml, cytospinned onto microscope slides and fixed with methanol/acetone (3:1 ratio at -20 °C for 30 min). Washes were done with triton X-100 buffer for 5 min and 50 mM Tris Buffer (pH 7.4) for 10 min prior to blocking for non-specific binding with serum. 5he slides were stained with the primary antibodies: rabbit anti-CD33 antibody (1:100 dilution, Santa Cruz), mouse anti-granzyme B (1:100 dilution, Fitzgerald Industries) and mouse anti-human CD71 (1:100 dilution, BD Biosciences) followed by their respective secondary antibodies, AlexaFluor-594 goat anti-rabbit IgG (Invitrogen), FITC goat anti-mouse (Sigma) and Alexa-350 goat anti-mouse IgG (Molecular Probes). Rat anti-human glycophorin A was pre-conjugated to Alexa-647 using a kit from Molecular Probes) before addition to the sample (1:50 dilution, AbD

Serotec) followed by mounting the slides with aqueous medium (Molecular Probes, USA). Immunofluorescence was detected using a Zeiss automated upright fluorescence microscope and images captured by a Nikon camera with the Capture Program AxioVision. Detailed methods for immuno-staining on S100A9 transfected SJCRH30 cells have been published previously (Chen, X., et al. 2008. Blood 113(14):3226-34). Specifically, SJCRH30 cells, which lack detectable expression levels of both CD33 and S100A9, were transfected with either S100A9 or S100A8 (negative control) for 48-72 hours. After incubation with CD33-fusion for 30 min (2μg/ml), 1 x 10^4 cells were cytospinned onto slides and then stained with a secondary anti-human IgG1-APC before analysis by immunofluorescence microscopy. Similarly, SJCRH30 cells, stable-transfected with CD33, were incubated with rhS100A9 tagged with DDK for various time points and stained by the same methodology before analysis.

Suppression assays. To determine whether MDSCs are capable of mediating T cell suppression, $CD45^+$ $CD33^+$ $CD11b^+$ Lin^- cells were sorted from full bone marrow of MDS patients by FACS. The following antibodies were used: CD45-PECy7, CD33-PECy5, CD11b-FITC, CD3-PE, CD14-PE, CD20-PE (all Beckman Coulter, Fullerton, CA, USA), CD16-PE, CD19-PE (DAKO, Glostrup, Denmark) and CD56-PE (BD Biosciences, San Diego, CA, USA). T cells were isolated by Magnetic Activated Cell Sorting (MACS) using CD3 microbeads (Miltenyi Biotec, Aubern, CA, USA) from autologous peripheral blood. 20,000 T cells were seeded in a 96 wells round bottom plate in triplicate in Iscove's modified Dulbecco medium (IMDM; Invitrogen, Carlsbad, CA) supplemented with 10% human serum PAA (PAA Laboratories, Pasching, Austria). Cultures were stimulated with 30 U/ml IL-2 (Chiron, Emeryville, CA, USA), and anti-CD3/anti-CD28 coated beads (Invitrogen, Carlsbad, CA, USA) at a 1:2 ratio of T cells to beads. MDSCs were admixed with T cell cultures at ratios of 1:2 and 1:4 and supplemented with 10 ng/ml GM-CSF to support MDSC viability. After 3 days of co-culture, culture supernatants were harvested to measure IFN-γ concentration by ELISA (Pierce Endogen, Rockford, IL, USA). Subsequently, 0.5 μCi ^{3}H-thymidine (Perkin Elmer, Groningen, the Netherlands) was added to each well and, after overnight incubation, ^{3}H -thymidine incorporation was measured using a 1205 Wallac Betaplate counter (PerkinElmer). To determine whether differences in proliferation and IFN- γ production were statistically significant, one-way Anova with Bonferroni post-hoc test was used. Statistical significance was accepted for p values < 0.05.

Colony-forming Assay. Cells isolated from either human BM, or from S100A9Tg, S100A9KO or WT tibias and femurs were subjected to ACK for 5 min at room temperature

(Sigma) to lyse the red blood cells. Remaining BM cells were then seeded into complete methylcellulose media (MethoCult complete medium with necessary cytokines and growth factors (StemCell Technologies) and the mixture was placed in duplicate gridded 35-mm culture dishes (2×10^5 cells/dish) and incubated at 37°C in 5% CO_2 for 7-14 days. After incubation, colonies of BFU-E and CFU-GM were identified manually and counted using an inverted light microscope. For the colony formation assays performed using ATRA treated mice, we administered ATRA at 250 μg (200 μl) or vehicle (Olive oil) orally for five consecutive days before resting two days.

mRNA expression by Real-time Quantitative. RT-PCR and quantitative RT-PCR (qRT-PCR) reactions were performed by means of iQ SYBR Green Supermix (Bio-Rad). The reaction mixture (25 μl total) contained 12.5 μl iQ SYBR green supermix, 0.25 μl forward primer (s GAPDH) (20μM), 11μl RNase-free water, and 1.0μl cDNA. The following cycles were performed 1 x 3 min at 95°C, 40 amplification cycles (15 s 95 °C, 60 s 56 °C), 1 x 1 min 95 °C, 1 x 1 negative control without cDNA template was run with every assay. The optimal melting point of dsDNA I and min 55 °C and a melting curve (80 x 10 s 55 °C with an increase of 0.5 °C per 10 seconds). The efficiency of the reaction was optimized beforehand. Transcript copy number per individual was calculated by normalization to GAPDH expression. The relative level of gene expression for each patient was calculated by normalization to the average expression level observed in five controls. CD33 transfected and un-transfected SJCRH 30 cells were treated with 1 μg of rhS100A9 for 20 min and the expression measured by Q-PCR for the presence of IL10 and TGFβ from total RNA and calculated by the ΔΔCt method where rhS100A9 untreated cells were the experimental control and the housekeeping gene GAPDH was the internal control. Error bars represent the SEM of three separate experiments.

Preparation of the CD33/Siglec 3 chimeric fusion protein. Recombinant soluble fusion of CD33/Siglec 3 ectodomain were constructed as described previously (Cannon, J.P., et al. 2012. Immunogenetics 64:39-47; Cannon, J.P., et al. 2011. Methods Mol Biol 748:51-67; Cannon, J.P., et al. 2008. Immunity 29:228-237). Specifically, cDNA fragments encoding CD33/Siglec 3 ectodomain were amplified by PCR and inserted into a vector that encodes the human Fcγ followed by a c-terminal recognition site for E. coli biotin ligase. This vector has been engineered to facilitate the fusion of gene segments encoding extracellular Ig-type domains to the Fc region of human IgG1. The recombinant proteins were expressed in 293T cells post-transfection, using Lipofectamine (Invitrogen), with three successive harvests of 25 ml OPTI-MEM I serum-free medium. The harvests were pooled, centrifuged at 500*g* for 10 min to remove

debris and stored at 4 °C in 0.02% sodium azide. Concentrations of CD33-fusions in culture supernatants were determined by Bradford assay (Biorad, Carlsbad, CA).

Mass spectrometry. Following in-gel tryptic digestion, peptides were extracted and concentrated under vacuum centrifugation. A nanoflow liquid chromatograph (Easy-nLC, Proxeon, Odense, Denmark) coupled to an electrospray ion trap mass spectrometer (LTQ, Thermo, San Jose, CA) was used for tandem mass spectrometry peptide sequencing experiments. The sample was first loaded onto a trap column (BioSphere C18 reversed-phase resin, 5 μm, 120 Å, 100 μm ID, NanoSeparations, Nieuwkoop, Netherlands) and washed for 3 minutes at 8 ml/minute. The trapped peptides were eluted onto the analytical column, (BioSphere C18 reversed-phase resin, 150 mm, 5 μm, 120 Å, 100 μm ID, NanoSeparations, Nieuwkoop, Netherlands). Peptides were eluted in a 60 minute gradient from 5% B to 45% B (solvent A: 2% acetonitrile + 0.1% formic acid; solvent B: 90% acetonitrile + 0.1% formic acid) with a flow rate of 300 nl/min. Five tandem mass spectra were collected in a data-dependent manner following each survey scan. Sequences were assigned using Mascot (www.matrixscience.com) searches against human IPI entries. Carbamidomethylation of cysteine, methionine oxidation, and deamidation of asparagine and glutamine were selected as variable modifications, and as many as 2 missed tryptic cleavages were allowed. Precursor mass tolerance is set to 2.5 and fragment ion tolerance to 0.8. Results from Mascot were compiled in Scaffold, which was used for manual inspection of peptide assignments and protein identifications.

Identifications of specific binding of S100A9 to CD33/Siglec 3. ELISA assay *for CD33-fusion binding cell lysate of S100A9 transfected SJCRH 30 cells.* Ninety-six well flat-bottom ELISA plates were coated overnight with 1ug/ml of monoclonal anti-S100A9, as per the manufacturer's suggestions. After washing with 1 X PBS-T, 50 μl of lysates from un-transfected cells (negative) or S100A9 transfected cells was added to the wells. Secondary antibody was either a S100A9 polyclonal antibody (positive control) or CD33-fusion as indicated followed by ELISA HRP reaction analysis at 440 nm.

Preparation of adenoviral vector expressing CD33. CD33 plasmid (GeneCopeia) was subcloned into a pShuttle-IRES-hrGFP-1 vector (containing the CMV promoter and hrGFP). The PmeI-digested shuttle vectors were then co-transformed into electro-competent BJ5183 bacteria with pAdEasy-1 (containing the viral backbone) and selected on Kanamycin LB plates. The plasmid in the bacteria was amplified and purified using a plasmid maxiprep system (Qiagen). The complete adenoviral vector was linearized by PacI digestion and then transfected

into AD293 cells using Lipofectamine (Invitrogen). All recombinant adenoviruses were amplified in AD293 cells. Viral stocks were obtained by amplification of the AD293 cells followed by standard two-step CsCl gradient ultracentrifugation, dialysis, and storage in a glycerol stock (10% volume/volume) at -80°C. The titer of each viral stock was routinely tested to be 10^{11}-10^{12} pfu by plaque forming assay using AD293 cells.

Preparation of shRNA lentiviral vectors. SureSilencing™ shRNA Plasmid for Human S100A8, S100A9 and CD33 and negative control (non-target) were purchased from SABiosciences. 293T cells were transfected using transfection reagent (SABiosciences,) according to manufacturer's instructions. Following 6 hours of incubation, the transfection reagent was removed and replaced with fresh DMEM supplemented with 10% fetal bovine serum. Virus containing medium was collected 24–48hr later. Plasmids, pcDNA3 wild-type DAP12 and P23-DAP12 were cut with HindIII and XhoI (Promega), and DNA Polymerase I Large (KlenowI) (New England Biolabs Inc.) was used to fill in recessed 3' ends of DNA fragments. pWPI, which contains a GFP expression cassette (Addgene Organization), was digested using PMEI (New England Biolabs Inc.). After cutting DNA and vector, pWPI were purified by Strata Prep PCR purification kit (Qiagen), DNAs were ligated (Takara DNA ligation kit, Fisher) into vector pWPI and STBL2 competent cells were transformed (Invitrogen). 293T cells were transfected with pWPI lentivirus vector, the packaging plasmid, psPAX2, and the envelope plasmid, pMD2.G (Addgene Organization) using the Lipofectemine-2000 (Invitrogen) at a ratio of 4:3:1 according to standard protocols. Following 6 hours of incubation, the transfection reagent was removed and replaced with fresh DMEM supplemented with 10% fetal bovine serum. Virus containing medium was collected 24–48hr later. Cell infection was performed as described above. Four days after the first infection, transduced cells were isolated by FACS sorting GFP^+ cells with >99% purity.

Infection of MDSC from MDS patients. MDSCs isolated from MDS patients were infected three times using virus-containing infection medium at 24 hr intervals in the presence of 8μg/ml polyberene. For each infection, cells were plated in 12-well dishes at 1 x 10^6 cells/well. Four days after the first infection, cells were harvested and used for real time PCR, Western blot analysis, flow cytometry, or colony formation assays.

Flow cytometry. BM-MNCs were stained with appropriate specific conjugated antibodies in PBS with 2% BSA buffer. For MDSC sorting, FITC anti-CD3 and FITC anti-HLA-DR were used as positive controls and isotype IgG were used for negative control and to detect non-specific staining. Cells were gently mixed and incubated for 30 min at 4 °C in the dark. Samples

were washed with PBS and centrifuged at 500 *g* for 5 min. For cells used in phenotypic analysis only, 0.5 ml of 1% paraformaldehyde in PBS was added prior to analysis.

Cells were washed in PBS and then stained with PE-conjugated mAbs specific to CD40, CD80, CD83, CD86, CCR7, CD11c, CD14, HLA-DR, TLR2, or TLR4 and relevant isotype controls (eBioscience) for 30 min in the dark, on ice. The cells were then washed with PBS containing 0.5% BSA. Live cells were gated based on negative staining for 7-AAD. Samples were acquired on a FACSCalibur flow cytometer and the analysis was performed using Flowjo 6.3.4 software.

Arginase activity. Arginase activity was measured in cell lysates as previously described (Youn, J.I., et al. 2008. J Immunol 181:5791-5802). In brief, cells were lysed for 30 min with 100 µl of 0.1% Triton X-100. Subsequently, 100 µl of 25 mM Tris-HCl and 10 µl of 10 mM $MnCl_2$ were added, and the enzyme was activated by heating for 10 min at 56°C. Arginine hydrolysis was conducted by incubating the lysate with 100 µl of 0.5 M L-arginine (pH 9.7) at 37 °C for 120 min. The reaction was stopped with 900 µl of H_2SO_4 (96%)/H_3PO_4 (85%)/H_2O (1/3/7, v/v/v). Urea concentration was measured at 540 nm after addition of 40 µl of α-isonitrosopropiophenone (dissolved in 100% ethanol), followed by heating at 95 °C for 30 min.

NO production. Equal volumes of culture supernatants (100 µl) were mixed with Greiss reagent solution (1% sulfanilamide in 5%phosphoric acid and 0.1%N-1-naphthylethylenediamine dihydrochloride) in double-distilled water and incubated for 10 min at room temperature. Absorbance of the mixture was measured at 550nm using a microplate plate reader (Bio-Rad). Nitrite concentrations were determined by comparing the absorbance values for the test samples to a standard curve generated by serial dilution of 0.25 mM sodium nitrite.

Western Blot analysis. Cell lysates were prepared by resuspending cell pellet in 1% NP-40, 10 mM Tris, 140 mM NaCl, 0.1 mM PMSF, 10 mM iodoacetamide, 50 mM NaF, 1 mM EDTA, 0.4 mM sodium orthovanadate, 10µg/ml leupeptin, 10 µg/ml pepsatin, and 10µg/ml aprotinin and lysing on ice for 30 min. Cell lysates were centrifuged at 12,000 *g* for 15 min to remove nuclei and cell debris. The protein concentration of the soluble extracts was determined by using the Bio-Rad (Bradford) protein assay. 50 µg of protein (per lane) was separated on a 10% SDS-polyacrylamide gel by electrophoresis then transferred to a PVDF membrane. Membranes were probed for indicated antibody: anti-S100A8 or anti-S100A9 (MRP8 or calgranulin A and anti-MRP14 or calgranulin B respectively, Santa Cruz); anti-S100A8/A9 (Santa Cruz); anti-phospho Erk, anti- total Erk, anti-phospho Syk, and anti- total Syk (Cell Signaling). Proteins were detected with the enhanced chemiluminescence detection system

(ECL, Amersham). Lysate from S100A9 un-transfected, empty vector and S100A9 transfect SJCRH30 or AD293 cells was serially-diluted (as indicated in the figure) with the first lysate, starting at 50 μg, followed by loading onto a nitrocellulose membrane and blocked overnight at 4°C in 5% milk. Following incubation with CD33-fusion for 2 hours at room temperature, and staining with an anti-human IgG HRP-conjugated secondary, the membrane was washed and used for radiograph analysis to demonstrated specific S100A9 binding to CD33. The membrane was afterwards used for Coomassie blue staining to show the relative equal loading of proteins on each dot in the nitrocellulose membrane.

Complete peripheral blood cell counts (CBC). CBC was performed by animal core laboratory pathological personnel in the vivarium at the Moffitt Cancer Center. The mouse blood parameters were determined as described in Table 1 with a Heska Hematrue Hematology Analyzer.

Pathological examination of spleen and BM biopsy from wt and S100A9Tg mice. Bone marrow cells were obtained from bilateral tibiae and femura from 6 month old S100A9Tg and wt control mice as previously described (Xu, S., et al. 2010. J Biomed Biotechnol 2010:105940). Touch prints of murine splenocytes were prepared as described (Ioachim, H.L., et al. 2008. Iochim's lymph node pathology. Chapter 3. cytopathology. Wolters Kluwer/Lippincott Williams &Wilkins. :p 21-22). Bone marrow aspirates and touch-imprints were stained using Wright-Giemsa stain. Sections of bone marrow and spleen were fixed in 10% phosphate-buffered neutral formalin, decalcified (only applied to bone marrow) and embedded in paraffin by routine procedures. Sections were cut at 4 μm and stained with hematoxylin and eosin (H&E) and periodic acid Schiff (PAS). The presence of myelodysplastic features characteristic of MDS was evaluated by experienced hematopathologist. BM core biopsy shows 50% cellularity with maturing trilineage hematopoiesis (H&E, 200x). Figure 5E shows a high power view of the BM biopsy that demonstrates normal appearing megakaryocytes with normal lobation. Mixed myeloid and erythroid precursors are normally distributed with estimated M:E ratio of 2:1 (H&E, 600x). Wright-Giemsa stained BM aspirate exhibits full maturation in all three lineages without dysplastic features (Wright-Giemsa, 1000x). Inlet shows a normal lobated megakaryocyte (Figure 5F). Touch imprint of mouse spleen displays predominance of small and mature appearing lymphocytes intermingled with occasional erythropoietic precursors (Wright-Giemsa, 1000 x) (Figure 5G). BM core biopsy reveals hypercellularity, approximately 95% with increased megakaryocytes, especially in small forms (H&E, 200x) (Figure 5H). High power magnification highlights dysplastic megakaryocytes with single or hypolobated, or disjointed

nuclei and markedly increased in number (H&E, 600x) (insert) (Figure 5I). Inlet includes two markedly dysplastic micromegakaryocytes with hypolobation. BM aspirates exhibits mildly increased blasts admixed with myeloid and erythroid precursors. The latter demonstrates slightly irregular nuclear contour and minimal megaloblastoid changes (Wright-Giemsa, 1000x) (Figure 5J). Inlet contains two blasts showing delicate or fine chromatin, prominent nucleoli, high N:C ratio, and scant basophilic cytoplasm. Touch preparation of transgenic mouse spleen show increased erythroid precursors; some of them displaying enlarged size with abnormal nuclearity and occasional nuclear bridge (Wright-Giemsa, 1000x) (Figure 5K).

Statistics. All data was presented as means ± SEM. Statistical calculations were performed with Microsoft Excel or GraphPad Prism analysis tools. Differences between individual groups were analyzed by paired t-test. P values of <0.05 were considered to be statistically significant.

Results

$Lin^-HLA\text{-}DR^-CD33^+$ MDSC are expanded in MDS primary BM specimens and direct suppression of autologous erythroid precursors. Bone marrow mononuclear cells (BM-MNC) were isolated from MDS BM aspirates (n=12), age-matched healthy BM (n=8), or non-MDS cancer patients (4 breast and 4 lymphoma) and analyzed for the presence of $LIN^-HLA\text{-}DR^-CD33^+$ MDSCs by flow cytometry. MDS patients exhibited markedly higher numbers of MDSCs (median 35.5%, $P<0.0001$) compared to healthy donors or non-MDS cancer patients (less than 5%, Figure 1A). To determine if MDS-MDSCs are derived from the malignant MDS clone, $LIN^-HLA\text{-}DR^-CD33^+$ MDSCs were sorted from MDS specimens with chromosome 5q [del(5q)] or 7q [del(7q)] deletion and analyzed by fluorescence *in situ* hybridization (FISH) with specific probes.

Cytogenetically abnormal cells harboring del(5q) or del(7q) were restricted to the non-MDSC population, whereas $LIN^-HLA\text{-}DR^-CD33^+$ MDSCs displayed a corresponding normal chromosome complement (Figure 1B). Exome sequencing studies have shown that clonal somatic gene mutations are demonstrable in the vast majority of MDS specimens lacking chromosome abnormalities by metaphase karyotyping. To further evaluate the relationship between MDSC and the MDS clone, a QPCR array of the most common gene mutations in MDS (Qiagen) was performed in purified MDSC and non-MDSC populations from primary bone marrow MDS specimens. Mutations involving *CBL, EZH2, IDH1/2, N-RAS, SRSF2, U2A535* and *RUNX1* genes were detected in the MDS specimens, however, all mutations were restricted

to the MDSC-depleted fraction (Table 1), indicating that $LIN^-HLA\text{-}DR^-CD33^+$ MDSC are distinct from the malignant clone.

Table 1: qBiomarker™ Somatic Mutation PCR Array Human Myelodysplastic Syndromes (n=6)

Gene	COSMIC ID	nt change	AA change	NON-MDSC						MDSC N=6
				Pt 1	Pt 2	Pt 3	Pt 4	Pt 5	Pt 6	
ASXL1	36166	c.1772_1773insA	p.Y591fs*1	-	-	-	-	-	-	-
ASXL1	41716	c.1888_1909del22	p.H630fs*66	-	-	-	-	-	-	-
ASXL1	41717	c.2302C>T	p.Q768*	-	-	-	-	-	-	-
ASXL1	52930	c.2324T>G	p.L775*	-	-	-	-	-	-	-
ASXL1	41715	c.3202C>T	p.R1068*	-	-	-	-	-	-	-
CBL	34052	c.1111T>C	p.Y371H	-	-	-	-	-	-	-
CBL	34055	c.1139T>C	p.L380P	-	+	+	+	+	+	-
CBL	34057	c.1150T>C	p.C384R	-	+	+	+	-	+	-
CBL	34077	c.1259G>A	p.R420Q	-	-	-	-	+	-	-
DNMT3A	53042	c.2644C>T	p.R882C	-	-	-	-	-	-	-
DNMT3A	87007	c.2711C>T	p.P904L	-	-	-	-	-	-	-
EZH2	37031	c.1936T>A	p.Y646N	-	+	+	+	-	+	-
EZH2	37029	c.1937A>C	p.Y646S	-	+	+	+	-	+	-
EZH2	37028	c.1937A>T	p.Y646F	-	+	+	+	+	+	-
IDH1	28748	c.394C>A	p.R132S	-	-	-	-	-	-	-
IDH1	28749	c.394C>G	p.R132G	-	+	+	+	+	+	-
IDH1	28747	c.394C>T	p.R132C	-	+	-	-	+	+	-
IDH1	28746	c.395G>A	p.R132H	-	+	+	+	-	-	-
IDH1	28750	c.395G>T	p.R132L	-	+	+	+	+	+	-
IDH2	41877	c.418C>T	p.R140W	-	+	+	+	-	-	-
IDH2	41590	c.419G>A	p.R140Q	+	-	-	-	+	+	-
IDH2	41875	c.419G>T	p.R140L	-	+	+	+	+	+	-
IDH2	34039	c.514A>T	p.R172W	+	+	+	+	+	+	-
IDH2	33733	c.515G>A	p.R172K	-	+	+	+	+	+	-
IDH2	33732	c.515G>T	p.R172M	-	+	+	+	-	+	-
IDH2	34090	c.516G>T	p.R172S	-	-	+	-	-	-	-
NRAS	580	c.181C>A	p.Q61K	-	+	+	+	+	+	-
NRAS	584	c.182A>G	p.Q61R	-	+	+	+	-	+	-
NRAS	583	c.182A>T	p.Q61L	-	-	-	-	-	-	-
NRAS	586	c.183A>C	p.Q61H	-	+	+	+	+	+	-
NRAS	585	c.183A>T	p.Q61H	-	-	-	-	+	-	-
NRAS	563	c.34G>A	p.G12S	-	+	-	-	-	+	-
NRAS	562	c.34G>T	p.G12C	-	+	+	+	+	-	-
NRAS	564	c.35G>A	p.G12D	-	-	+	-	+	+	-
NRAS	565	c.35G>C	p.G12A	-	+	-	+	+	+	-
NRAS	566	c.35G>T	p.G12V	-	+	+	+	+	+	-
NRAS	569	c.37G>C	p.G13R	-	+	+	+	+	+	-
NRAS	570	c.37G>T	p.G13C	-	+	+	+	+	+	-
NRAS	573	c.38G>A	p.G13D	-	-	-	-	-	-	-
NRAS	574	c.38G>T	p.G13V	-	+	-	+	+	+	-
RUNX1	24756	c.167T>C	p.L56S	-	+	+	-	-	+	-
RUNX1	24736	c.319C>T	p.R107C	-	+	+	+	-	+	-

RUNX1	24769	c.496C>T	p.R166*	-	-	-	-	-	-	-
RUNX1	24721	c.592G>A	p.D198N	-	-	-	-	-	-	-
RUNX1	24799	c.593A>G	p.D198G	-	-	-	-	+	-	-
RUNX1	24805	c.602G>A	p.R201Q	-	+	-	+	-	-	-
RUNX1	24731	c.611G>A	p.R204Q	-	-	-	+	+	-	-
SF3B1	110693	c.1866G>T	p.E622D	-	-	-	-	-	-	-
SF3B1	110695	c.1874G>T	p.R625L	-	-	-	-	-	-	-
SF3B1	131560	c.1984C>G	p.H662D	-	-	-	-	-	-	-
SF3B1	130416	c.1986C>A	p.H662Q	-	-	-	-	-	-	-
SF3B1	110692	c.1986C>G	p.H662Q	-	-	-	-	-	-	-
SF3B1	110694	c.1996A>G	p.K666E	-	-	-	-	-	-	-
SRSF2	98000028	c.284C>A	P95H	-	+	+	+	+	+	-
SRSF2	98000029	c.284C>T	P95L	-	+	+	+	+	-	-
SRSF2	98000030	c.284C>G	P95R	-	+	+	+	+	+	-
TET2	41644	c.1648C>T	p.R550*	-	+	+	-	-	-	-
TET2	43417	c.2746C>T	p.Q916*	-	-	-	-	-	-	-
TP53	10648	c.524G>A	p.R175H	-	-	-	-	-	-	-
TP53	10662	c.743G>A	p.R248Q	-	+	+	+	-	-	-
TP53	10660	c.818G>A	p.R273H	-	-	-	-	+	-	-
TP53	10656	c.742C>T	p.R248W	-	-	-	-	-	-	-
TP53	10659	c.817C>T	p.R273C	-	-	-	-	+	-	-
TP53	10704	c.844C>T	p.R282W	-	-	-	-	-	-	-
TP53	10817	c.747G>T	p.R249S	-	+	+	+	+	+	-
TP53	6932	c.733G>A	p.G245S	-	-	-	-	+	-	-
TP53	10758	c.659A>G	p.Y220C	-	+	+	-	+	-	-
TP53	10654	c.637C>T	p.R213*	-	-	-	-	-	-	-
TP53	10670	c.469G>T	p.V157F	-	-	-	+	-	-	-
TP53	10705	c.586C>T	p.R196*	-	-	-	+	-	+	-
TP53	10645	c.527G>T	p.C176F	-	-	+	+	-	+	-
TP53	10889	c.536A>G	p.H179R	-	+	+	+	-	+	-
TP53	10808	c.488A>G	p.Y163C	-	+	+	+	-	-	-
TP53	10722	c.853G>A	p.E285K	-	+	-	-	-	+	-
TP53	43606	c.734G>A	p.G245D	-	+	+	+	+	-	-
TP53	10779	c.818G>T	p.R273L	-	+	+	+	+	+	-
TP53	10725	c.701A>G	p.Y234C	+	+	+	+	-	+	-
U2AF35	98000031	c.470A>C	Q157P	+	+	+	+	-	+	-
U2AF35	98000032	c.470A>G	Q157R	-	+	+	+	-	+	-
U2AF35	98000033	c.101C>T	S34F	-	-	-	-	-	-	-
U2AF35	98000034	c.101C>A	S34Y	+	+	+	+	-	+	-
DNMT3A	99000100	copy_number	copy_number	-	-	-	-	-	-	-

Sample was fresh and sorted prior to genomic DNA isolation. According to the manufacturer's analysis description: the raw CT for a given mutation assay in a test sample is compared with a predefined CT cutoff. Based on the difference, the mutation can be considered as "Present" (+), "Borderline" (-/+), or "Absent" (-).

Recognized functional properties of MDSC include suppression of antigen stimulated or CD3 stimulated T cell proliferation and interferon-gamma (IFN-γ) production (Gabrilovich, D.I.,

et al. 2009. Nat Rev Immunol 9:162-174; Ostrand-Rosenberg, S., et al. 2009. J Immunol 182:4499-4506). T cells purified from the BM of MDS patients showed reduced T cell proliferation (Figure 1C) and IFN-γ production (Figure 1D) after co-culture with autologous MDS-MDSC, demonstrating the expected suppressive activity of these cells. To further validate these findings, MDSCs were depleted from MDS BM specimens prior to anti-CD3/anti-CD28 stimulation and then the MDSC were added back to the control group. MDSC-depletion significantly improved T cell responses compared to the MDSC-supplemented group (Figure 1E), thereby linking the observed impaired T cell responsiveness to the actions of BM-derived MDSCs. In addition, suppressive MDS-MDSC overproduced suppressive cytokines such as IL-10 and TGF-β (Figure 1F & G), as well as nitric oxide (NO) and arginase compared to MDSCs isolated from healthy donors (Figure 1H & I). Collectively, these data demonstrate that LIN^- $HLA\text{-}DR^-CD33^+$ MDSC are a unique and functional cellular subset supporting a pro-inflammatory microenvironment and immune tolerance in the BM of MDS patients.

MDSC-mediated suppressive and cytotoxic effector functions require direct contact with target cells. One mechanism utilized by cytotoxic effectors is the mobilization of pore-forming granules and the release of caspase-activating effector proteases, such as granzyme B, to the site of effector:target contact thereby inducing apoptosis of the target cell (Chen, X., et al. 2008. Blood 113(14):3226-34). Since MDSC reside in close proximity with hematopoietic progenitor cells (HPCs) that in MDS display an increased apoptotic rate, MDSC-mediated cytostatic activity may contribute to HPC death. To address this, MDS-MDSC granule mobilization and release of granzyme B were examined using four-color immunofluorescence staining. MDS-MDSCs exhibited strong granzyme B polarization at the site of cell contact with $CD235a^+$ (glycophorin A)/$CD71^+$ autologous erythroid precursors (Figure 1J). After 30 minutes incubation, the frequency of such effector-target conjugates in MDS patient specimens was significantly higher (34%) than in samples from healthy donors (5% $P<0.001$, Figure 1K & L). These cellular interactions resulted in apoptosis of targeted erythroid precursors (Figure 1M) demonstrating that in addition to known MDSC-mediated immune suppressive functions, there is an unrecognized MDSC-mediated hematopoietic suppressive capacity. To corroborate this finding, the effects of MDSC on the proliferative capacity of HPCs were examined in MDS-MDSC-depleted, HSPC enriched, BM patient specimens in a methylcellulose colony formation assay. Burst-forming unit-erythroid (BFU-E) and colony forming unit-granulocyte/macrophage (CFU-GM) colony formation was significantly higher in MDSC-depleted specimens compared

to both MDSC-supplemented and unsorted samples (Figure 1N), demonstrating that MDSC have a direct suppressive role on erythroid and myeloid progenitor cell development.

Increased CD33 expression and signaling contribute to MDSC suppressive functions and hematopoietic impairment. MDSCs in humans characteristically express the surface transmembrane glycoprotein CD33, a Siglec 3 receptor that along with other members of this family, have prominent roles in inflammation (Crocker, P.R., et al. 2007. Nat Rev Immunol 7:255-266; Blasius, A.L., et al. 2006. Blood 107:2474-2476; Blasius, A.L., et al. 2006. Trends Immunol 27:255-260; Lajaunias, F., et al. 2005. Eur J Immunol 35:243-251; Nutku, E., et al. 2003. Blood 101:5014-5020; von Gunten, S., et al. 2008. Ann N Y Acad Sci 1143:61-82; Paul, S.P., et al. 2000. Blood 96:483-490; Ulyanova, T., et al. 2001. J Biol Chem 276:14451-14458; Avril, T., et al. 2004. J Immunol 173:6841-6849; Ikehara, Y., et al. 2004. J Biol Chem 279:43117-43125). However, the involvement of CD33 in myelopoiesis remains unexplored. Hence, the relationship between CD33 membrane expression density on MDS-MDSC and their activation and maintenance in MDS BM was investigated. These cells were found to robustly express CD33 at levels higher than $LIN^-HLA\text{-}DR^-CD33^+$ cells isolated from non-MDS-associated cancer patients and healthy donor BM cells (Figure 2A). To explore the functional consequences of CD33 engagement, CD33 was cross-linked in U937 cells (a human monocytic cell line with high CD33 expression), which triggered IL-10, TGF-β and VEGF secretion (Figure 2B). To examine whether CD33 can promote MDSC accumulation and/or activation, CD33 was overexpressed with an adenovirus vector in BM-MNC from healthy donors, which significantly suppressed myeloid cell development as evidenced by reduced expression of the maturation markers CD11c, CD80, and CCR7 (Figure 2C). To further establish the role of CD33 in MDSC-mediated BM suppression, CD33 was knocked down in MDS-MDSC using a lentiviral vector (LV) containing CD33-specific-shRNA. Co-culture of autologous HPCs with CD33 shRNA-treated MDS-MDSCs resulted in a 2-3 fold increase in BFU-E and CFU-GM colony recovery compared to those cultured with scrambled shRNA-treated and non-transduced MDS-MDSCs and healthy donor BM MDSCs (Figure 2D). Moreover, production of IL-10, TGF-β, and arginase was reduced in CD33 shRNA-treated MDS-MDSC compared to control cells (Figure 2E, F, G). Collectively, these data delineate a role for CD33 in MDSC activation and expansion in MDS and directing hematopoietic impairment.

S100A9 is a native ligand for CD33. Although these investigations showed that CD33/Siglec 3 is a key receptor involved in functional activation of MDSC, its native ligand was unknown. Therefore, to identify potential ligand(s) for this receptor, a chimeric fusion protein

with the ectodomain of CD33 and the Fc portion of human IgG (here on referred to as CD33-fusion) was produced. BM cell lysates from MDS patients were immunoprecipitated with the CD33-fusion followed by high throughput mass-spectrometric analysis on associated peptides. S100A9, an inflammatory signaling molecule known to activate MDSC, was among the most prominent protein bands identified (Figure 3A). To confirm the specificity of the binding of this DAMP to CD33 both S100A8 and S100A9 transfectants were prepared in the rhabdomyosarcoma cell line SJCRH30, which lacks detectable expression of endogenous CD33, S100A8 or S100A9. The CD33-fusion (APC) stained only S100A9 transfected cells, but not S100A8 transfected cells, confirming binding specificity (Figure 3B. Transfectants were stained with FITC and specific binding by the CD33-fusion was stained with APC, (nuclei were stained with DAPI). Direct binding of S100A9 to CD33 was confirmed further in a sandwich ELISA where the capture antibody was anti-S100A9 (Figure 3C) as well as by dot blot analysis of transfected cell lysates with CD33-fusion (Figure 3D), demonstrating the specificity of the interaction. To fully corroborate the binding of this pair, a reverse immune-precipitation was performed on CD33 transfected cells showing that S100A9 co-precipitated with CD33 only in S100A9 co-transfected cells (Figure 3E). To validate clinically the ligand specificity in MDS patients, the pull-down was compared with CD33-fusion from healthy PBMC and BM as well as MDS patients. As expected, the highest amount of S100A9 was precipitated from the BM of MDS patient specimens (Figure 3F). Next, to understand the kinetics of S100A9 and CD33 interactions, SJCRH30 cells were transfected with either vector or CD33 and incubated with recombinant human (rh) S100A9 tagged with DDK (DYKDDDDK epitope, same epitope as Flag). This resulted in a time-dependent increase in binding of rhS100A9 to stable SJCRH30-CD33 cells but no binding to vector transfected cells (Figure 3G). To demonstrate the functionality of this ligation pair, rhS100A9 was added to SJCRH30-CD33 cells which triggered CD33 mediated up-regulation of IL10 and TGFβ expression (Figure 3H and I). To confirm that rhS100A9 can recapitulate these observation of the secretion of these cytokines after cross-linking CD33, the experiments were repeated in U937 cells with rhS100A9 and an increase in production of both cytokines was again found (Figure 3J and K). Importantly, BM plasma concentration of S100A9 was significantly increased in MDS patients compared to BM plasma from healthy donors (Figure 3L). Moreover, the engagement of CD33 with rhS100A9 in MDS-MDSC from patient BM resulted in a time-dependent co-localization of this ligand/receptor pair in primary MDS-BM cells (Figure 3M). It is well recognized that CD33 signals through phosphorylation of ITIMs that recruit SHP-1 (Src homology region 2 domain-containing

phosphatase-1). rhS100A9 ligation correspondingly increased the recruitment of SHP-1 confirming that CD33 signals through its ITIM after S100A9 ligation in MDS-BM (Figure 3N). In addition, directly treating CD33-transfected SJCRH30 with the BM plasma of MDS patients triggered the recruitment of SHP-1 to ITIM when compared to cells treated with the plasma of healthy donors, suggesting that increased secretion of S100A9 in the local BM microenvironment may have a role in the activation of CD33-ITIM signaling (Figure 3O).

S100A8/S100A9 engagement of CD33 triggers MDS-MDSC activation. Having established S100A9 and CD33 as a functional ligand/receptor pair, the role of this interaction in replicating the functional responses observed with receptor crosslinking was explored. CD33 overexpression was again induced in healthy BM cells through adenovirus transfection and their immunesuppressive properties with or without the addition of rhS100A9 was studied. Forced expression of CD33 induced a parallel increase in gene expression and secretion of the suppressive cytokines, IL-10 and TGFβ (light grey bars, Figure 4A-D), which was greatly increased by the addition of rhS100A9 (black bars). Secretion of the suppressive cytokine TGFβ was only observed after rhS100A9 treatment of CD33 transfected cells (Figure 4D), accompanied by an increase in the expression of NOS2 and ARG2, consistent with the suppressive cytokine profile (Figure 4E and F). Figure 4G-H demonstrates the transfection efficiency of the CD33 adenovirus at both the gene and protein expression level measured by QPCR and GFP by flow cytometry, respectively.

To further delineate the specific role of S100A9's ligation with CD33 compared to its other ligands, RAGE, TLR4, CD33 as well as each pair were blocked with antibodies before treating healthy BM cells with rhS100A9. These data show that blockade of CD33 reduced both IL-10 and TGFβ production, while treatment with anti-RAGE and anti-TLR4 had no significant effects on IL-10 production but displayed modest suppression of TGFβ secretion and expression (Figure 4I and J). These findings suggest that although CD33 plays a critical role in the secretion of both cytokines, other receptors associated with local bone marrow inflammation may also have a contribution. To confirm that S100A9 expression contributes to inflammation in the BM microenvironment, S100A8 and S100A9 were knocked down in MDS-MDSC using gene specific shRNAs (Figure 4K). Given that S100A9 usually pairs with S100A8 as a heterodimer and are concomitantly regulated, it was not surprising that there was reciprocal changes in gene expression with down-regulation in expression of the alternate protein. Importantly, reduction of S100A8/S100A9 expression profoundly attenuated IL-10 and TGF-β production (Figure 4L and M) and rescued autologous BFU-E and CFU-GM colony formation (Figure 4N). These data

show that inflammation-associated S100A8/S100A9 signaling plays a critical role in the activation of MDS-MDSC and suppress normal hematopoiesis.

S100A9 transgenic mice recapitulate features of human MDS. Given the findings that S100A8/S100A9 triggers CD33/Siglec 3 signaling and is involved in MDSC activation (Ehrchen, J.M., et al. 2009. J Leukoc Biol 86:557-566; Vogl, T., et al. 2007. Nat Med 13:1042-1049; Cheng, P., et al. 2008. J Exp Med 205:2235-2249), S100A9 transgenic mice (S100A9Tg) were generated to study MDSC-associated inflammation (Cheng, P., et al. 2008. J Exp Med 205:2235-2249). Since MDS is an age-associated disease, changes in the proportion of BM MDSC ($Gr1^+CD11b^+$ cells) with age were analyzed in S100A9Tg compared to S100A9 knockout (S100A9KO)(Manitz, M.P., et al. 2003. Mol Cell Biol 23:1034-1043) or wild-type (WT) mice at 6, 18 or 24 weeks of age. This resulted in a marked age-dependent accumulation of MDSC in the BM of S100A9Tg mice, but not in S100A9KO or WT mice, that reached its maximum by 24 weeks (Figure 5A). Similarly, the proportion of MDSC in PBMC and spleen also increased with age (Figure 5B). Although changes in the proportion of MDSC in the spleen was comparatively less than in the BM, it was accompanied by a decrease in the proportion of mature cells (Figure 5C and 5D), effectively increasing the ratio of immature to mature cells in this hematopoietic organ. Functionally, only the MDSC from 24-week old S100A9Tg mice, but not S100A9KO or WT mice, significantly inhibited BFU-E (Figure 5E) and CFU-GM formation, which was rescued after depletion of MDSC in the S100A9Tg group (Figure 5E). Importantly, as further evidence of the role of S100A9 as an essential inflammatory factor regulating MDSC expansion and suppressive activity, IL-10 and TGF-β secretion was significantly increased in S100A9Tg mice compared to KO or wild-type animals (Figure 5F).

To evaluate the *in vivo* consequences of S100A9 over-expression on hematopoiesis, serial complete blood counts (CBC) were analyzed from WT and S100A9Tg mice at 6, 18 and 24 weeks of age. S100A9Tg mice developed progressive multilineage cytopenias characterized by decreasing hemoglobin (Hgb), red blood cell (RBC) number, neutrophil and platelet counts evident as early as 6 weeks of age. By 18 weeks, S100A9Tg mice exhibited severe anemia and thrombocytopenia with a greater than 22.0% decrease in RBC, 20.1% decrease in Hgb, and 77.8% decrease in platelets (Table 2). Histological examination of BM aspirates and biopsy sections from WT mice displayed normal morphology and cytological features (Figure 5G-J). In contrast, the BM of S100A9Tg mice was hyper-cellular (95% cellularity) accompanied by tri-lineage cytological dysplasia (Figure 5K-N). Megakaryocyte morphology recapitulated the dysplastic features characteristic of human MDS, with a preponderance of mononuclear or

hypolobated forms. Erythroid precursors displayed megaloblastoid maturation with abnormal hemoglobination and occasional binucleation. Nuclear budding and bizarre mitotic forms were also apparent (Figure 5K-N). Cytopenias worsened with age and by 24 weeks S100A9Tg mice developed severe pan-cytopenia (detailed descriptions summarized in the figure legend). Although this model closely replicates the inflammatory milieu observed in human MDS, HSPC from S100A9Tg mice also express the S100A9 protein. Given that the provenance of this protein in human MDS is not known, cellular expression of S100A9 in MDS BM-MNC was investigated by flow cytometry. S100A9 intracellular staining was detected in $CD33^+$ cells, whereas $CD34^+$ HSCs had no demonstrable S100A9 expression (Figure 5O and 5P). S100A9 expression was not detected in other immune cells such as $CD3^+$ lymphocytes, $CD19^+$ B cells or $CD56^+$ NK cells.

Table 2. Complete peripheral blood count of S100A9Tg and wt-mice

Test	Units	6 weeks		18 weeks		24 weeks	
		WT	S100A9-Tg	WT	S100A9-Tg	WT	S100A9-Tg
WBC	$10^3/\mu l$	5.4±0.5	4.2±1.5	6.0±1.4	2.9±0.2*	6.3±0.8	3.0±0.4*
LYM	$10^3/\mu l$	3.9±0.5	2.6±1.2	4.7±1.1	2.4±0.1*	4.8±0.7	2.5±0.3*
MONO	$10^3/\mu l$	0.4±0.1	0.3±0.2	0.4±0.1	0.2±0.1*	0.4±0.1	0.2±0.1*
GRAN	$10^3/\mu l$	1.1±0.6	1.2±1.2	0.9±0.3	0.3±0.2*	1.1±0.4	0.3±0.1**
HCT	%	48.1±3.2	42.4±2.1	45.7±0.7	35.5±3.0**	45.4±3.5	32.1±2.7**
MCV	fl	51.4±1.6	49.8±2.0	50.3±0.5	50.0±1.2	50.0±1.3	50.0±1.6
RDWa	fl	35.0±0.7	33.2±2.2	34.0±1.3	32.5±1.7	33.3±1.4	32.2±1.5
RDW%	%	16.3±0.7	15.9±0.1	16.3±0.5	15.5±0.5	16.0±0.5	15.4±0.6
HGB	g/dl	14.2±0.8	13.0±0.7	13.9±0.3	11.1±0.7**	13.7±0.6	10.3±0.5**
MCHC	g/dl	29.5±1.1	30.6±1.3	30.4±0.4	31.5±0.9	30.3±1.0	32.3±1.1
MCH	pg	15.1±0.3	15.2±0.1	15.3±0.1	15.8±0.3	15.2±0.2	16.2±0.4
RBC	$10^6/\mu l$	9.4±0.7	8.5±0.4	9.1±0.1	7.1±0.6**	9.1±0.3	6.4±0.2***
PLT	$10^3/\mu l$	555.7±96.6	412.0±124.0	431.3±33.9	95.7±35.0***	437.0±41.9	61.0±23.5***

All data are means ± SEM (n=3-5 mice). Peripheral blood samples were prepared from both S100A9Tg and control (WT) mice in ages of 6, 18 and 24 weeks and analyzed on a Hema True Hematology Analyzer (Heska). * $p<0.05$; ** $p<0.01$;*** $p<0.001$ vs wt-mice

Analysis of the role of MDSC by adoptive transfer of enriched HSC from S100A9Tg mice. To more accurately delineate the role of MDSC from S100A9Tg mice in hematopoiesis, competitive adoptive transfer was performed of enriched HSCs into lethally irradiated (900cGy) female FVB/NJ mice with age-matched WT HSC, S100A9Tg HSC or an admixture (1:1 ratio) of enriched BM HSCs from male mice. Using a male to female SRY gene expression PCR approach to monitor engraftment, all mice experienced greater than 80% engraftment (Figure 8). After engraftment (defined as WBC $>3x10^3$ cells/uL in WT recipients at 8 weeks), recipients of WT HSC had proportions of both BM derived $Gr1^+Cd11b^+$ and HSCs (Figure 6A and C) that were comparable to levels in un-transplanted WT mice (Figure 5A). In contrast, adoptive transfer with S100A9Tg enriched HSCs generated a high proportion of GFP expressing

$Gr1^+Cd11b^+$ MDSCs (Figure 6B) accompanied by a reduced proportion of HSCs, findings analogous to our observations in older transgenic mice (Figure 6C). However, mice that received the admixed HSC population had a proportion of MDSCs approaching that in WT adoptively transferred mice (~30%). Notably, nearly 50% of MDSCs lacked GFP expression, indicating origination from WT HSPCs (Figure 6B), whereas the remaining GFP^+ MDSC derived from S100A9Tg donor cells. Although the total MDSC population did not increase to the level observed in the S100A9Tg adoptively transferred mice, a decreased proportion of HSCs to levels found in mice transplanted with S100A9Tg donor cells was observed (Figure 6C). These findings indicate that the smaller population of activated MDSCs from S100A9Tg donor cells had sufficient suppressive activity to yield a comparable impairment of hematopoietic integrity. These findings were supported by sequential analyses of peripheral blood counts in which mixed source transplant recipients had cytopenias that were intermediate in severity relative to those in mice receiving the S100A9Tg or WT donor cells (Figure 6D, E, F). Interestingly, while mixed donor recipients had the same proportion of HSCs after engraftment as Tg transplanted mice, their WBC counts were higher than mice transplanted with S100A9Tg HSC and lower than levels in WT HSC recipients. Similarly, onset of anemia was delayed in recipients of the mixed versus S100A9Tg donor cells. These findings suggest that normal HSC from WT mice are able to partially rescue hematopoiesis, but with time hematopoiesis is suppressed by accumulating MDSC derived from S100A9Tg donor cells.

To address whether S100A9 alone has direct effects on HSCs, BM CD34+ (MDSC depleted, MDSC-) from MDS patient specimens were treated with rhS100A9 for 24 and 48 hours and assessed apoptosis by flow cytometry. A decrease in the number of $CD34^+$ HSPCs was observed after treatment compared to controls accompanied by a corresponding increase in the apoptotic fraction among surviving cells after 48 hours exposure (Figure 6G and H). In order to corroborate these findings, healthy bone marrow-derived $CD34^+$ cells (Lonza, Wakerfield) were cultured with rhS100A9 and a decrease in viable cells was again observed after treatment (50.7% viability in control cells versus 24.7% in rhS100A9 treated cells, Figure 6I). These findings suggest that S100A9 has a direct apoptotic effect in human HSCs.

Forced maturation of MDSC restores hematopoiesis. To confirm the effector role of MDSC and investigate the potential benefit of targeted suppression of MDSC, S100A9Tg mice were treated with *all*-trans-retinoic acid (ATRA). ATRA induces MDSC differentiation into mature myeloid cells and neutralizes ROS production, thereby extinguishing MDSC through forced terminal differentiation (Nefedova, Y., et al. 2007. Cancer Res 67:11021-11028; Mirza,

N., et al. 2006. Cancer Res 66:9299-9307). To this end, it was examined whether ATRA would induce MDSC differentiation in S100A9Tg mice and improve hematopoiesis. S100A9Tg and WT mice were treated with ATRA (250μg/200μl) or vehicle control orally for five consecutive days. Two days after completion of the treatment, ATRA reduced the total number of MDSC while numbers in WT mice remained at basal levels (Figure 7A). Reductions in MDSC number in S100A9Tg mice were coupled to an increase in mature cells following ATRA treatment (Figure 7B). Treatment of primary MDS BM specimens with ATRA also reduced *in vitro* MDSC accumulation. Importantly, BM progenitor cultures from ATRA-treated S100A9Tg mice showed significantly improved BFU-E recovery compared to vehicle-treated controls (Figure 7C). Analysis of changes in peripheral blood counts showed that RBC, WBC and platelet counts significantly increased compared to vehicle treated controls (Figure 7D), indicating that terminal differentiation of MDSCs can restore effective hematopoiesis.

Investigations showed that MDSC employ CD33-associated ITIMs to inhibit their own cellular maturation (Figure 3N and O). However, ITIM signals can be over-ridden by stimulatory immunoreceptor tyrosine-based activation motif (ITAM)-mediated signals (Lanier, L.L. 2005. Annu Rev Immunol 23:225-274; Ravetch, J.V., et al. 2000. Science 290:84-89). Some CD33-related receptors, such as certain Siglecs, lack ITIMs and instead function as activating receptors. Mouse Siglec-H and human Siglec-14 have been shown to interact with DAP12 (Blasius, A.L., et al. 2006. Blood 107:2474-2476; Blasius, A.L., et al. 2006. Trends Immunol 27:255-260; Angata, T., et al. 2006. Faseb J 20:1964-1973; Lanier, L.L., et al. 1998. Nature 391:703-707), an ITAM-containing adaptor that can promote myeloid cell maturation (Figure 9) and inhibit TLR-4 activation (Turnbull, I.R., et al. 2007. Nat Rev Immunol 7:155-161). Rhe *DAP12* gene expression of purified MDS-MDSC (n=5) was compared to age-matched healthy donor MDSC (n=5). *DAP12* mRNA was significantly lower in MDS-MDSC in all specimens tested (Figure 7E). It was reasoned that overriding CD33-ITIM signaling via DAP12 would induce the differentiation of these immature myeloid cells and improve hematopoiesis. To test this, a constitutively active form of DAP12, named P23, was created and AD293 cells transfected with either GFP, WT-*DAP12*, or active-*DAP12* P23 viral vectors. The results show that P23 binds Syk kinase and activates downstream signaling in transduced AD293 cells without external stimulation (Figure 7F). Furthermore, P23 promotes primary human DC maturation as demonstrated by up-regulation of CD80, CD83, and CCR7 antigens (Figure 10) (Blasius, A.L., et al. 2006. Blood 107:2474-2476; Blasius, A.L., et al. 2006. Trends Immunol 27:255-260). Based on these findings, it is possible that P23 could induce the maturation of MDS-MDSC and

thereby prevent or disrupt hematopoietic suppression. To test this, expression of the human monocytic and granulocytic surface markers CD14 and CD15 were analyzed after transfection (Araki, H., et al. 2004. Blood 103:2973-2980) and results showed that while WT-*DAP12* transfection alone was sufficient to induce up-regulation of CD14 and CD15, P23 transfection induced even greater expression of both maturation markers (Figure 7G). Moreover, P23 promoted the maturation of primary MDS-MDSC as demonstrated by up-regulation of CD80, CD83, and CCR7 maturation markers (Figure 7H). Lastly, to test whether DAP12-mediated MDSC maturation relieved suppression of erythropoiesis, MDS-MDSC were purified from seven MDS patients and infected with control, WT-*DAP12* or P23 lentiviral constructs. To assess the suppressive function of the mature MDS-MDSCs on hematopoiesis, colony forming capacity was assessed after culture of infected cells with autologous, MDSC-depleted BM cells. P23-infected MDS-MDSC co-cultures yielded significantly higher colony numbers than control viral vector or WT-*DAP12*-infected MDS-MDSC co-cultures (Figure 7I). These findings indicate that DAP12 overrides CD33-associated ITIM signaling to stimulate MDSC maturation, and reverse the suppressive effects on HPC colony forming capacity.

Discussion

Inflammatory stimuli within the BM microenvironment are recognized as important biological signals stimulating progenitor cell proliferation and apoptosis in MDS. A recent population-based study extended this further by demonstrating a strong linkage between chronic immune stimulation and MDS predisposition (Kristinsson, S.Y., et al. 2011. J Clin Oncol 29:2897-2903). Definitive evidence that niche intrinsic abnormalities per se can alone account for development of MDS in a cell non-autonomous fashion are limited. Raaijmakers and colleagues showed that selective osteo-progenitor dysfunction caused by deletion of *Dicer1* in the mesenchymal component of the BM microenvironment was sufficient to perturb hematopoiesis and lead to development of myeloid dysplasia, followed by secondary emergence of myeloid-restricted genetic abnormalities (Raaijmakers, M.H., et al. 2010. Nature 464:852-857).

The disclosed studies show that $Lin^{-}HLA\text{-}DR^{-}CD33^{+}$ MDSC accumulate in the BM of MDS patients, derive from a population that is distinct from the neoplastic clone, and serve as cellular effectors that suppress hematopoiesis, promote T cell tolerance and serve as a key source of myelosuppressive and inflammatory molecules such as IL-10, TGF-β, NO, and arginase. Using multiple biological and biochemical approaches, it was shown that S100A9, also known as migration inhibitory factor-related protein 14 (MRP-14) or calgranulin-B, can serve as an

endogenous native ligand for CD33/Siglec 3. Furthermore, forced expansion of MDSC by over-expression of the S100A9 in transgenic mice initiates development of hematologic features that phenocopy human MDS, specifically progressive age-dependent ineffective and dysplastic hematopoiesis. These findings indicate that expansion of a single cellular constituent of the BM microenvironment is sufficient to foster neoplastic change in heterologous myeloid progenitors through niche-conducive oncogenesis. The time dependent accumulation of MDSC in the transgenic mouse model parallels recent human findings that MDSCs expand with age accompanied by rising serum levels of proinflammatory cytokines (e.g., TNF-α, IL-6, and IL-1β), providing evidence that such senescence dependent changes driving MDSC expansion may play an important role in the age dependent pathogenesis of MDS (Verschoor CP, et al. 2013. J Leukoc Biol 93(4):633-7). Importantly, the $LIN^-HLA\text{-}DR^-CD33^+$ phenotype did not alone confer suppressor cell function, as evidenced by lack of $LIN^-HLA\text{-}DR^-CD33^+$ MDSC suppression from age-matched healthy donors or non-MDS cancer patients. The disclosed studies demonstrate the necessity for activation of innate immune signaling and generation of pro-inflammatory molecules, such as S100A9, for the induction of MDS-MDSC-mediated suppressor function. Furthermore, the disclosed finding that primary human MDS-MDSC lack molecular genetic abnormalities intrinsic to the malignant clone indicate that MDSC derive from non-neoplastic HSC, and that MDSC activation and expansion likely precedes emergence of genetically distinct MDS clones.

CD33, a Siglec receptor expressed by many immune cells including MDSC, is shown herein to be markedly over-expressed by MDS-MDSC, and this receptor is shown to control the suppressive functions of MDS-MDSC through disruption of ITIM-mediated signaling. Additionally, the disclosed findings that rhS100A9 directly triggers apoptosis in human HPCs, indicates that this ligand exerts dual roles in the promotion of ineffective hematopoiesis that involve both cellular (MDSC) and humoral mechanisms (CD33, TLR4). Moreover, cellular response to CD33 ligand engagement appears cell type specific, i.e., apoptosis in HPC versus activation and proliferation in MDSC. Compensatory regeneration within the myeloid compartment could account for the increased proliferative index observed in MDS (Raza et. al. 1995. Blood 86(1):268-276) and preferential myeloid skewing that occurs with age. Over-expression of CD33 may therefore impair maturation signals from ITAM associated receptors that is critical to expansion of immature MDSC (Figure 7G and H). Consistent with this, shRNA silencing of CD33 reduced myelosuppressive cytokine elaboration, and importantly, restored hematopoietic progenitor colony forming capacity. Moreover, constitutively active DAP12

signaling was sufficient to override CD33-ITIM inhibition and induce MDSC differentiation, which restored erythropoiesis upon active-DAP12 transfection into MDS-MDSC. More importantly, DAP12 activation can inhibit TLR-mediated signaling pathways, which may also play a role in the inflammation-mediated BM suppression (Turnbull, I.R., et al. 2007. Nat Rev Immunol 7:155-161; Hamerman, J.A., et al. 2006. J Immunol 177:2051-2055).

Mounting evidence implicates activation of innate immune signaling in the pathogenesis and biologic features of human MDS (Hofmann, W.K., et al. 2002. Blood 100:3553-3560; Gondek, L.P., et al. 2008. Blood 111:1534-1542; Starczynowski, D.T., et al. 2008. Blood 112:3412-3424). In del(5q) MDS, allelic deletion of miR-145 and miR-146a results in de-repression of the respective targets, TIRAP and TRAF6. Of particular importance, Starcznowski and colleagues showed that knockdown of these specific miRs or over-expression of TRAF6 in murine HSPC recapitulated hematologic features of del(5q) MDS in a transplant model through both cell-autonomous and non-autonomous mechanisms involving interleukin-6 (Starczynowski, D.T., et al. 2010 Nat Med 16:49-58; Starczynowski, D.T., et al. 2010. Hematol Oncol Clin North Am 24:343-359). The disclosed studies show that the heterodimeric DAMP S100A8/S100A9, specifically released at BM inflammatory sites, is not only aberrantly expressed in MDS but serves as a native ligand for CD33. This finding provides evidence that S100 proteins contribute directly to MDS pathogenesis through microenvironment-directed, cell non-autonomous mechanisms involving MDSC (Ehrchen, J.M., et al. 2009. J Leukoc Biol 86:557-566; Viemann, D., et al. 2007. Blood 109:2453-2460). Moreover, TLR activation suppresses osteoblast differentiation, while instructing myeloid commitment in HSC (Bandow, K., et al. 2010. Biochem Biophys Res Commun 402:755-761; De Luca, K., et al. 2009. Leukemia 23:2063-2074). Prolonged activation of innate immune signaling with age, therefore, may disrupt the BM endosteal niche supporting maintenance of hematopoietic stem cells, and favor translocation of myeloid progenitors to an angiogenic niche characteristic of MDS (Bellamy, W.T., et al. 2001. Blood 97:1427-1434). This is supported by the disclosed findings of age dependent development of cytopenias with emergence of dysplastic cytological features in the S100A9Tg mice. More importantly, the competitive transplant experiments showed that admixture of S100A9Tg with WT donor HSCs delays, albeit with time still impairs hematopoiesis.

The disclosed findings support a model for MDS pathogenesis in which sustained activation of innate immune signaling in the BM microenvironment creates a permissive inflammatory milieu that is sufficient for development of myelodysplasia. Cell autonomous neoplastic hematopoietic progenitors may emerge following acquisition of secondary genetic

abnormalities in the myeloid compartment. S100A9Tg mice simulate human MDS and can serve as an *in vivo* model to study MDS pathogenesis and development of novel therapeutics. Nevertheless, therapeutic interventions that promote MDSC maturation may have remitting potential when applied early in the disease course.

Example 2

Active caspase-1 (Table 3) and IL-1β generation (Table 4) were assessed in four populations: stem cells (CD34+CD38-), progenitors (CD34+CD38+), erythroids (CD71+), and myeloid cells (CD33+). Mean fluorescent intensity (MFI) values are shown in Table 3.

Table 3. Treatment with CD33-IgG decreases active caspase-1 generation in an MDS specimen.

	Stem Cells	Progenitors	Erythroids	Myeloids
Ancestry Subset Value Type For	LIVE/CD34+/STEM Geom. Mean <FITC-A> FAM FLICA	LIVE/CD34+/PROGENITORS Geom. Mean <FITC-A> FAM FLICA	LIVE/CD71+ Geom. Mean <FITC-A> FAM FLICA	LIVE/CD33+ Geom. Mean <FITC-A> FAM FLICA
UNSTAINED	731	5760	189	3908
PLASMA ONLY	7062	61966	4170	44708
1μg IgG	4316	38250	2836	37161
0.1μg CD33-IgG	5232	43019	3339	40221
0.5μg CD33-lgG	5015	48556	3135	41516
1μg CD33-lgG	3444	24089	2247	19533

Table 4. Treatment with CD33-IgG decreases IL-1β generation in an MDS specimen.

Ancestry Subset Value Type For	LIVE/CD34+/STEM Geom. Mean <PE-A> IL-1b-PE	LIVE/CD34+/PROGENITORS Geom. Mean <PE-A> IL-1b-PE	LIVE/CD71+ Geom. Mean <PE-A> IL-1b-PE	LIVE/CD33+ Geom. Mean <PE-A> IL-1b-PE
UNSTAINED	1457	25484	45.5	9979
PLASMA ONLY	201	9682	56.6	8884
1μg IgG	126	6667	15.5	8051
0.1μg CD33-IgG	191	6380	48.2	8472
0.5μg CD33-lgG	151	10343	24.4	9073
1μg CD33-lgG	119	3092	12.6	3766

As shown in Figure 12, fold change of active caspase-1 and IL-1β generation normalized to plasma treated control in four cell populations . Active caspase-1 and IL-1β generation were assessed in four populations by flow cytometry after treatment with CD33-IgG: stem cells (CD34+CD38-), progenitors (CD34+CD38+), erythroids (CD71+), and myeloid cells (CD33+). Fold change of active caspase-1 MFI (Fig. 12A) and IL-1β generation (Fig. 12B).

As shown in Figure13, fold change of active caspase-1 and IL-1β generation normalized to plasma treated control in four cell populations . Active caspase-1 and IL-1β generation were assessed in four populations by flow cytometry after treatment with a related pathway inhibitor:

stem cells (CD34+CD38-), progenitors (CD34+CD38+), erythroids (CD71+), and myeloid cells (CD33+). Fold change of active caspase-1 MFI (Fig. 13A) and IL-1β generation (Fig. 13B).

Active caspase-1 and IL-1β generation were assessed in four populations: stem cells (CD34+CD38-), progenitors (CD34+CD38+), erythroids (CD71+), and myeloid cells (CD33+). Mean fluorescent intensity (MFI) values are found in the Tables 3 and 4.

As shown in Figure 14, neutralization of plasma S100A9 by CD33 Chimera trap enhances colony forming capacity in MDS patient specimens. Figures 14A to 14C show erythroid burst-forming units (BFU-E) (Fig. 14B), multipotential colony forming units (CFU-GEMM) (Fig. 14A), and granulocyte/macrophage colony forming units (CFU-GM) (Fig. 14C) in MDS patient specimens treated with IgG, plasma, or 0.1, 0.5, or 1.0μg of CD33-IgG chimeric trap.

Unless defined otherwise, all technical and scientific terms used herein have the same meanings as commonly understood by one of skill in the art to which the disclosed invention belongs. Publications cited herein and the materials for which they are cited are specifically incorporated by reference.

Those skilled in the art will recognize, or be able to ascertain using no more than routine experimentation, many equivalents to the specific embodiments of the invention described herein. Such equivalents are intended to be encompassed by the following claims.

WHAT IS CLAIMED IS:

1. A recombinant fusion protein, comprising:

(a) at least two S100A9-binding moieties selected from the group consisting of an extracellular domain of human CD33, an extracellular domain of toll like receptor 4 (TLR4), and an extracellular domain of Receptor for Advanced Glycation End Products (RAGE); and

(b) an immunoglobulin Fc region.

2. The fusion protein of claim 1, comprising a formula selected from the group consisting of:

eCD33 – eTLR4 – Fc,

eCD33 – eRAGE – Fc,

eTLR4 – eRAGE – Fc,

eRAGE – eTLR4 – Fc,

eCD33 – eTLR4 – eRAGE – Fc,

eCD33 – eRAGE – eTLR4 – Fc,

eTLR4 – eCD33 – eRAGE – Fc,

eRAGE – eCD33 – eTLR4 – Fc,

eTLR4 – eRAGE – eCD33 – Fc, and

eRAGE – eTLR4 – eCD33 – Fc,

wherein "eCD33" comprises the extracellular domain of human CD33,

wherein "eTLR4" comprises the extracellular domain of TLR4,

wherein "eRAGE" comprises the extracellular domain of RAGE,

wherein "Fc" comprises the immunoglobulin Fc region, and

wherein "–" consists of a peptide linker or a peptide bond.

3. The fusion protein of claim 1 or 2, further comprising a biotin acceptor peptide that can be biotinylated with biotin ligase (BirA) in the presence of biotin and ATP.

4. A recombinant fusion protein, comprising:

(a) an S100A9-binding moiety selected from the group consisting of an extracellular domain of human CD33, an extracellular domain of toll like receptor 4 (TLR4), and an extracellular domain of Receptor for Advanced Glycation End Products (RAGE);

(b) a biotin acceptor peptide that can be biotinylated with biotin ligase (BirA) in the presence of biotin and ATP; and

(c) an immunoglobulin Fc region.

5. The fusion protein of claim 4, comprising a formula selected from the group consisting of:

eCD33 – Fc – Avi,

eTLR4 – Fc – Avi,

eRAGE – Fc – Avi,

eCD33 – eTLR4 – Fc – Avi,

eCD33 – eRAGE – Fc – Avi,

eTLR4 – eRAGE – Fc – Avi,

eRAGE – eTLR4 – Fc – Avi,

eCD33 – eTLR4 – eRAGE – Fc – Avi,

eCD33 – eRAGE – eTLR4 – Fc – Avi,

eTLR4 – eCD33 – eRAGE – Fc – Avi,

eRAGE – eCD33 – eTLR4 – Fc – Avi,

eTLR4 – eRAGE – eCD33 – Fc – Avi, and

eRAGE – eTLR4 – eCD33 – Fc – Avi

wherein "eCD33" comprises the extracellular domain of human CD33,

wherein "eTLR4" comprises the extracellular domain of TLR4,

wherein "eRAGE" comprises the extracellular domain of RAGE,

wherein "Fc" comprises the immunoglobulin Fc region,

wherein "Avi" comprises an optional biotin acceptor peptide that can be biotinylated with biotin ligase (BirA) in the presence of biotin and ATP, and

wherein "–" consists of a peptide linker or a peptide bond.

6. The fusion protein of any one of claims 3 to 5, wherein the biotin acceptor peptide comprises the amino acid sequence SEQ ID NO:7, or an amino acid sequence having at least 90% identity to SEQ ID NO:7.

7. The fusion protein of any one of claims 1 to 6, wherein the extracellular domain of human CD33 comprises only the variable region.

8. A recombinant fusion protein, consisting essentially of:

(a) the variable extracellular domain of human CD33; and

(b) an immunoglobulin Fc region.

9. The fusion protein of any one of claims 1 to 8, wherein the extracellular domain of human CD33 comprises the amino acid sequence SEQ ID NO:1, or an amino acid sequence having at least 90% identity to SEQ ID NO:1.

10. The fusion protein of claim 9, wherein the extracellular domain of human CD33 comprises the amino acid sequence SEQ ID NO:2.

11. The fusion protein of any one of claims 7 to 8, wherein the variable region of human CD33 comprises the amino acid sequence SEQ ID NO:3, or an amino acid sequence having at least 90% identity to SEQ ID NO:3.

12. The fusion protein of claim 11, wherein the variable region of human CD33 comprises the amino acid sequence SEQ ID NO:4.

13. The fusion protein of any one of claims 1 to 12, wherein the extracellular domain of human TLR4 comprises the amino acid sequence SEQ ID NO:5, or an amino acid sequence having at least 90% identity to SEQ ID NO:5.

14. The fusion protein of any one of claims 1 to 13, wherein the extracellular domain of RAGE comprises the amino acid sequence SEQ ID NO:6, or an amino acid sequence having at least 90% identity to SEQ ID NO:6.

15. A multimeric complex comprising two or more fusion proteins of any one of claims 1 to 14 conjugated to a core molecule or particle.

16. The multimeric complex of claim 15, wherein the core molecule is streptavidin, wherein the two or more fusion proteins are biotinylated.

17. The multimeric complex of claim 15, wherein the core molecule is a liposome comprising antibodies that specifically bind the two or more fusion proteins.

18. The multimeric complex of claim 17, wherein the antibodies specifically bind the biotin acceptor peptide.

19. The multimeric complex of any one of claims 15 to 18, comprising from 2 to 5 fusion proteins conjugated to the core molecule or particle.

20. A method for treating a disease or condition caused or exacerbated by S100A9 activity, comprising administering to a subject in need thereof a composition comprising the fusion protein of any one of claims 1 to 18 or the multimeric complex of any one of claims 15 to 19.

21. The method of claim 20, wherein the method comprises treating an infection, sepsis, or a combination thereof in the patient.

22. The method of claim 20, wherein the method comprises treating an autoimmune disease in the patient.

23. The method of claim 20, wherein the method comprises treating rheumatoid arthritis in the patient.

24. The method of claim 20, wherein the method comprises treating a cancer in the patient.

25. The method of claim 20, wherein the method comprises treating a myelodysplastic syndrome (MDS) in the subject.

26. A method for treating myelodysplastic syndrome (MDS) in a subject, comprising administering to the subject a therapeutically effective amount of a composition comprising a soluble CD33 fusion protein that binds and sequesters S100A9.

27. A method for identifying an agent for treating myelodysplastic syndromes (MDS), comprising screening candidate agents for the ability to prevent S100A9 binding to CD33.

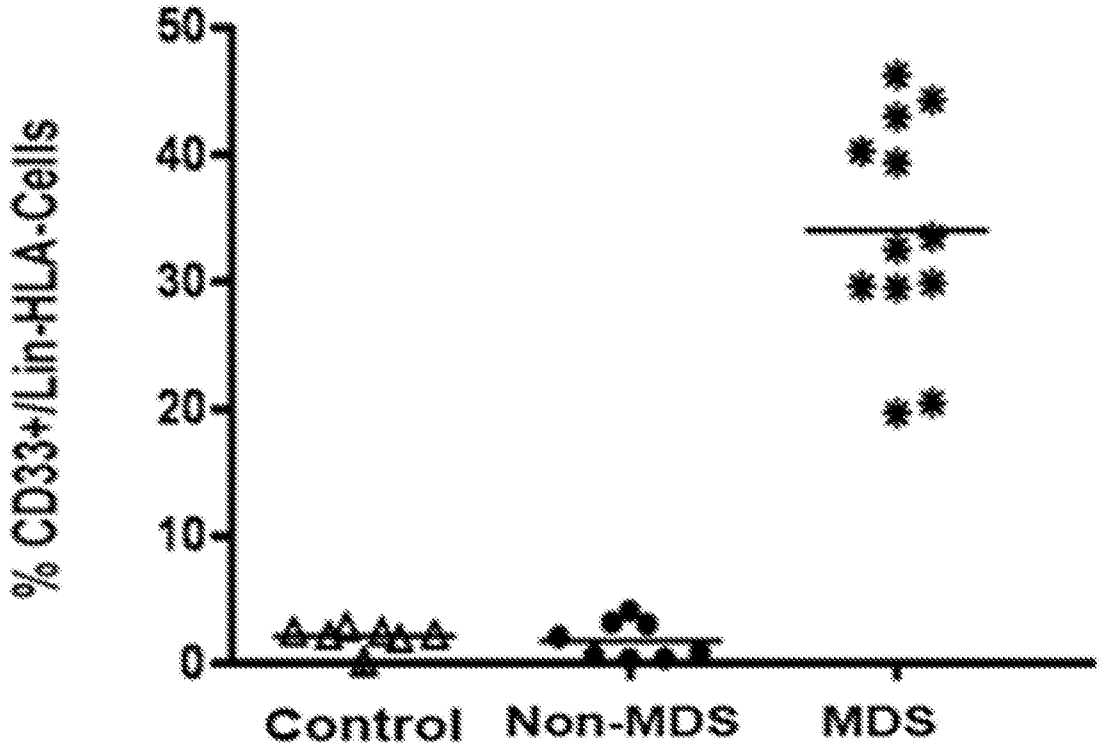

FIGURE 1A

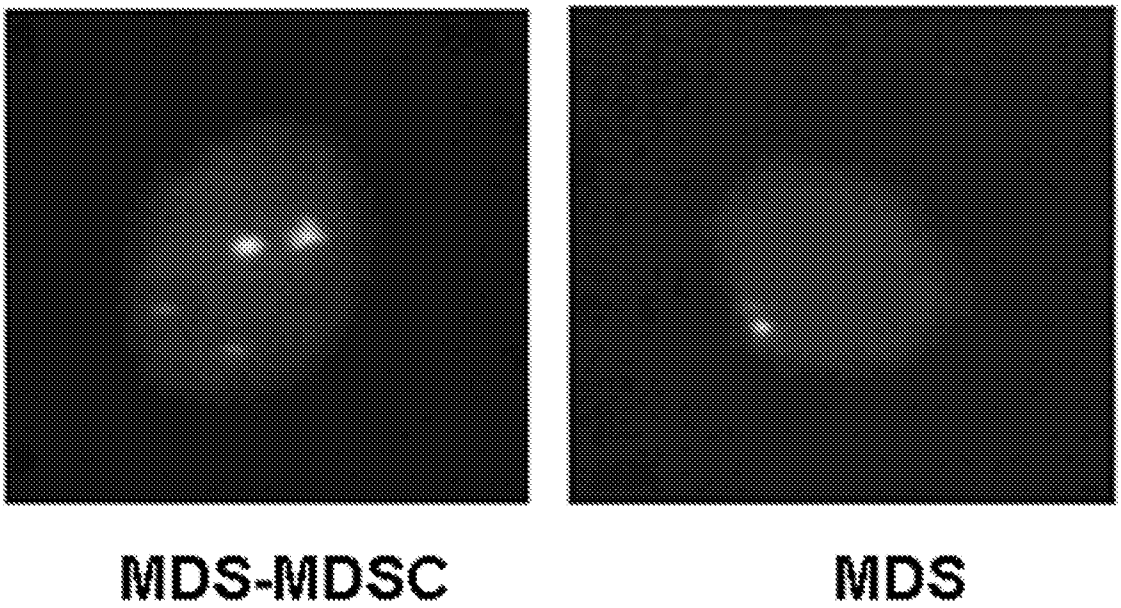

FIGURE 1B

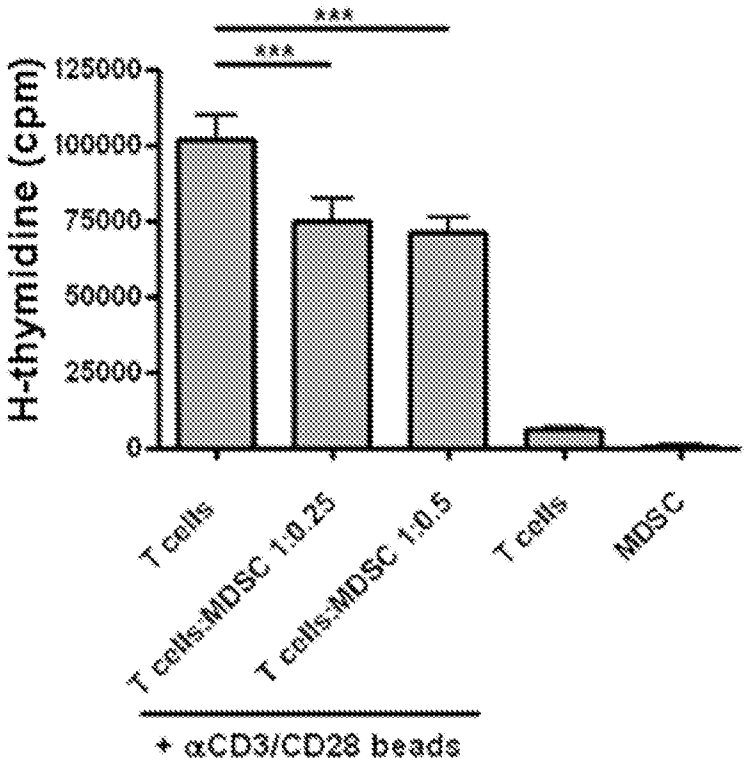

FIGURE 1C

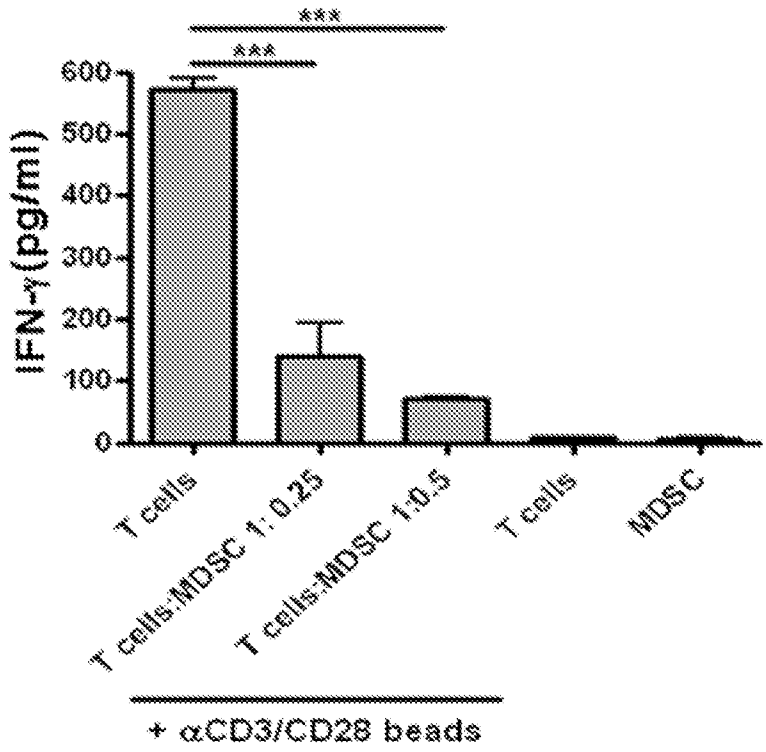

FIGURE 1D

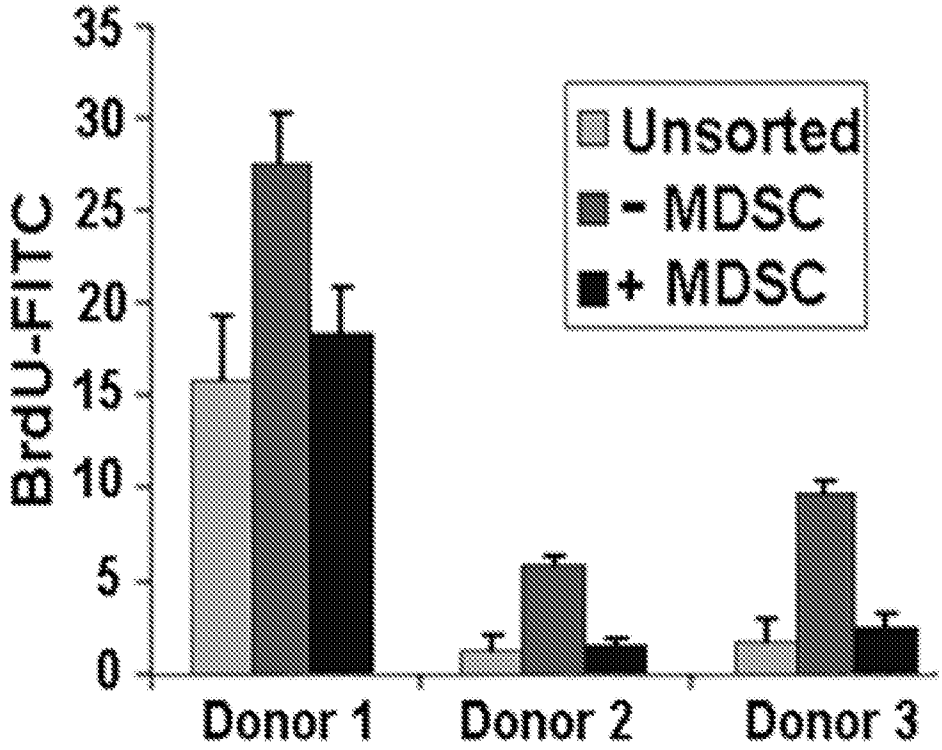

FIGURE 1E

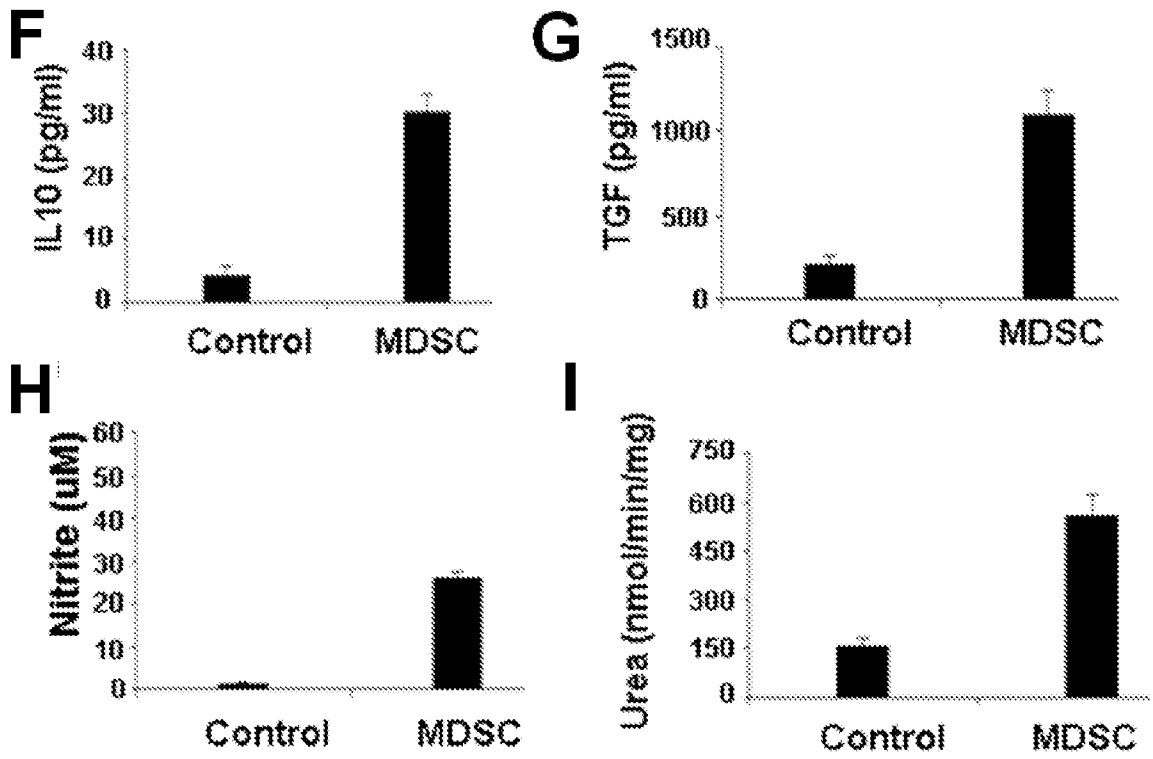

FIGURES 1F – 1I

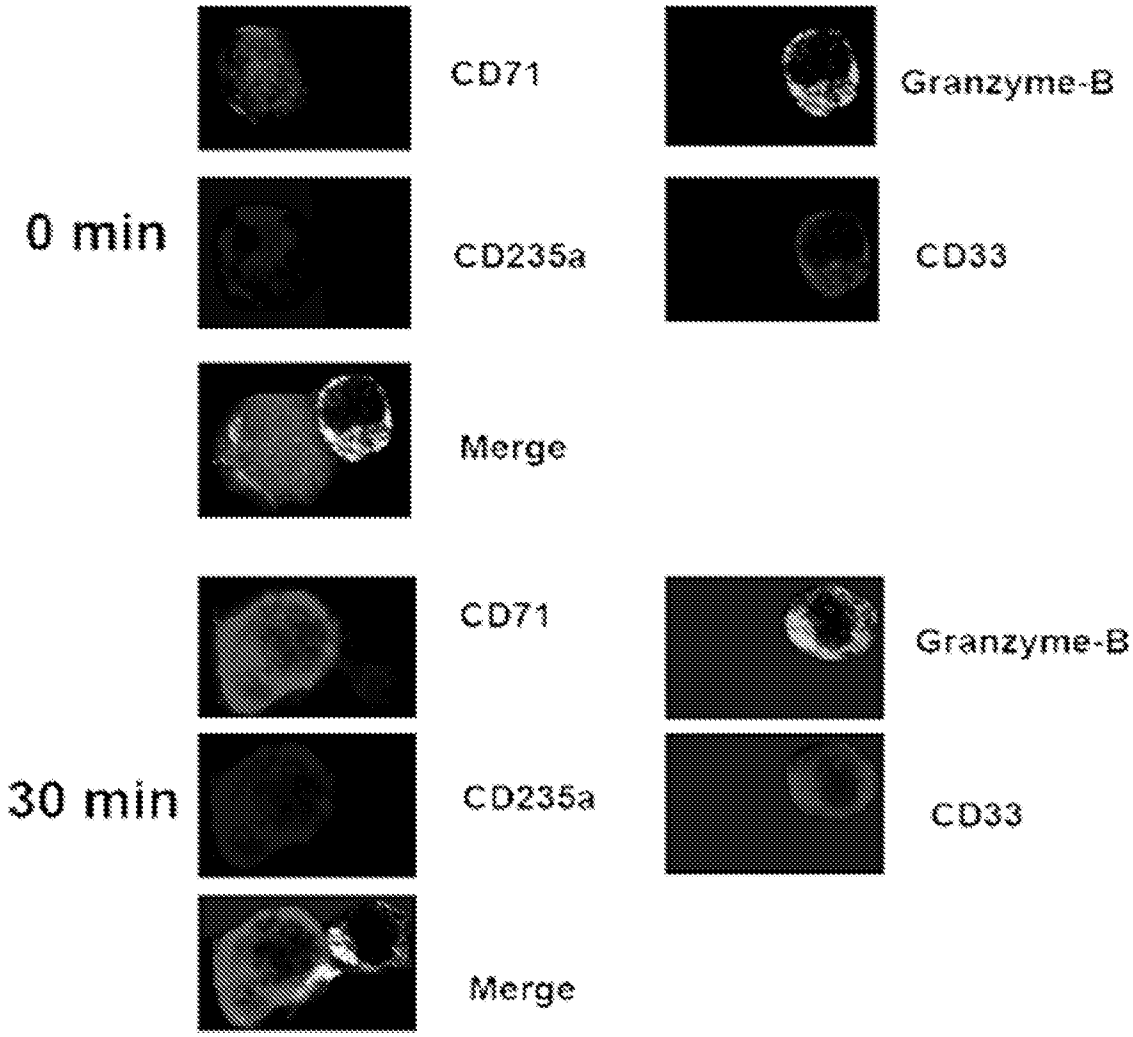
0 min
CD71
Granzyme-B
CD235a
CD33
Merge
30 min
CD71
Granzyme-B
CD235a
CD33
Merge

FIGURE 1J

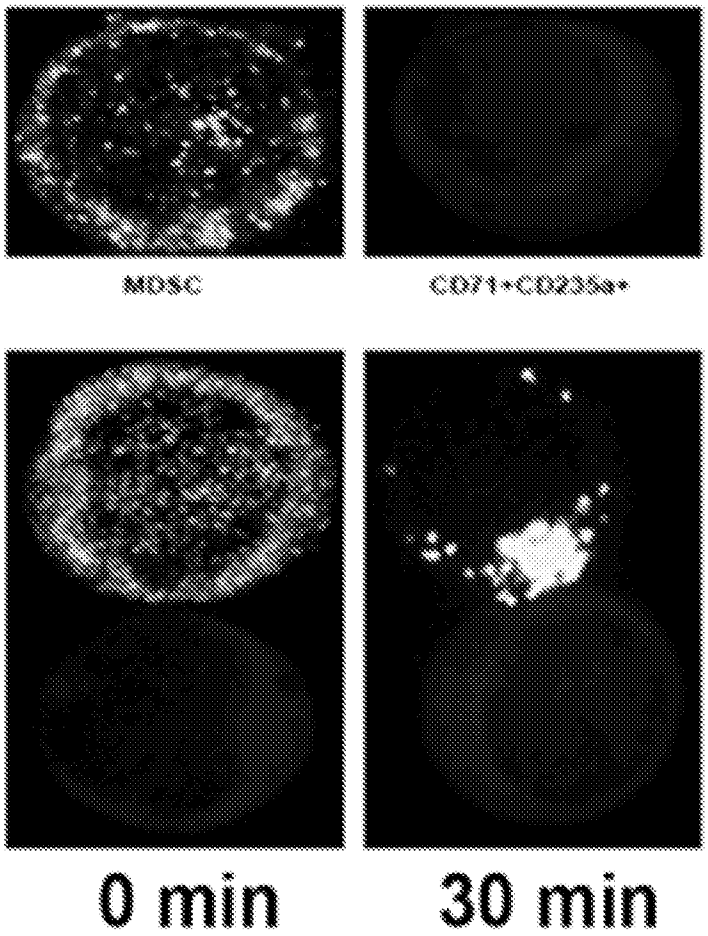

FIGURE 1K

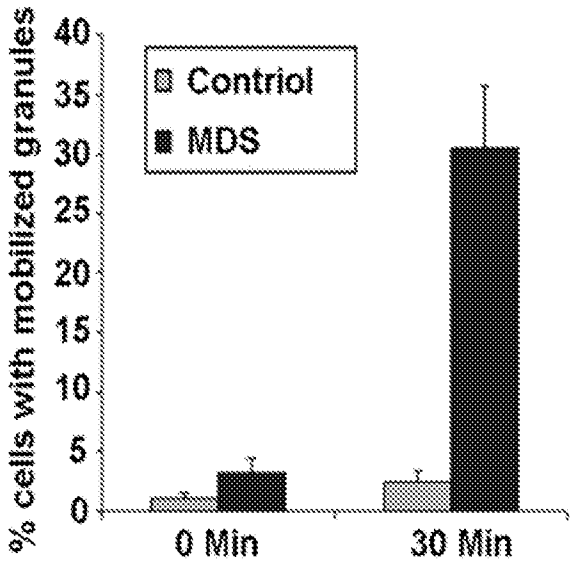

FIGURE 1L

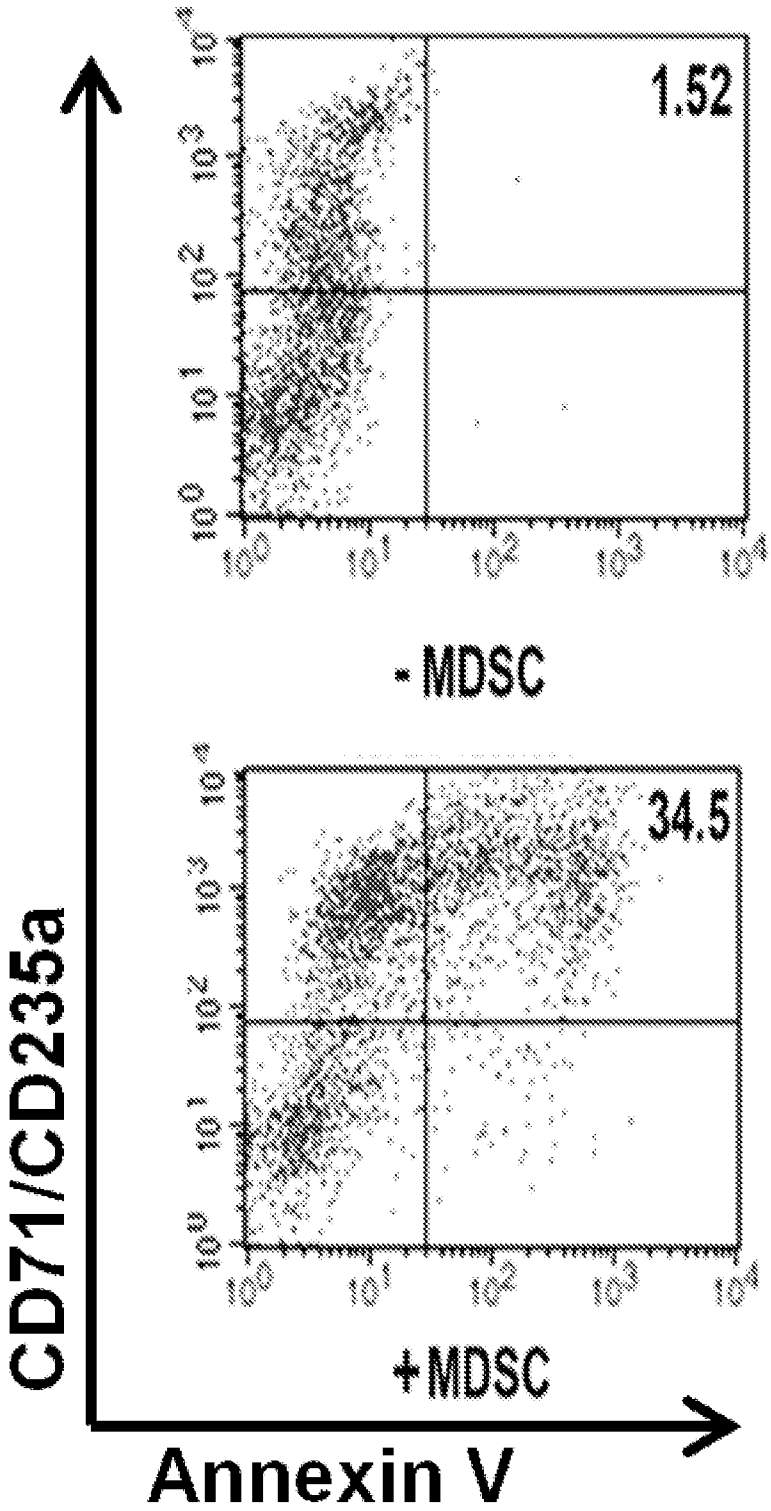

FIGURE 1M

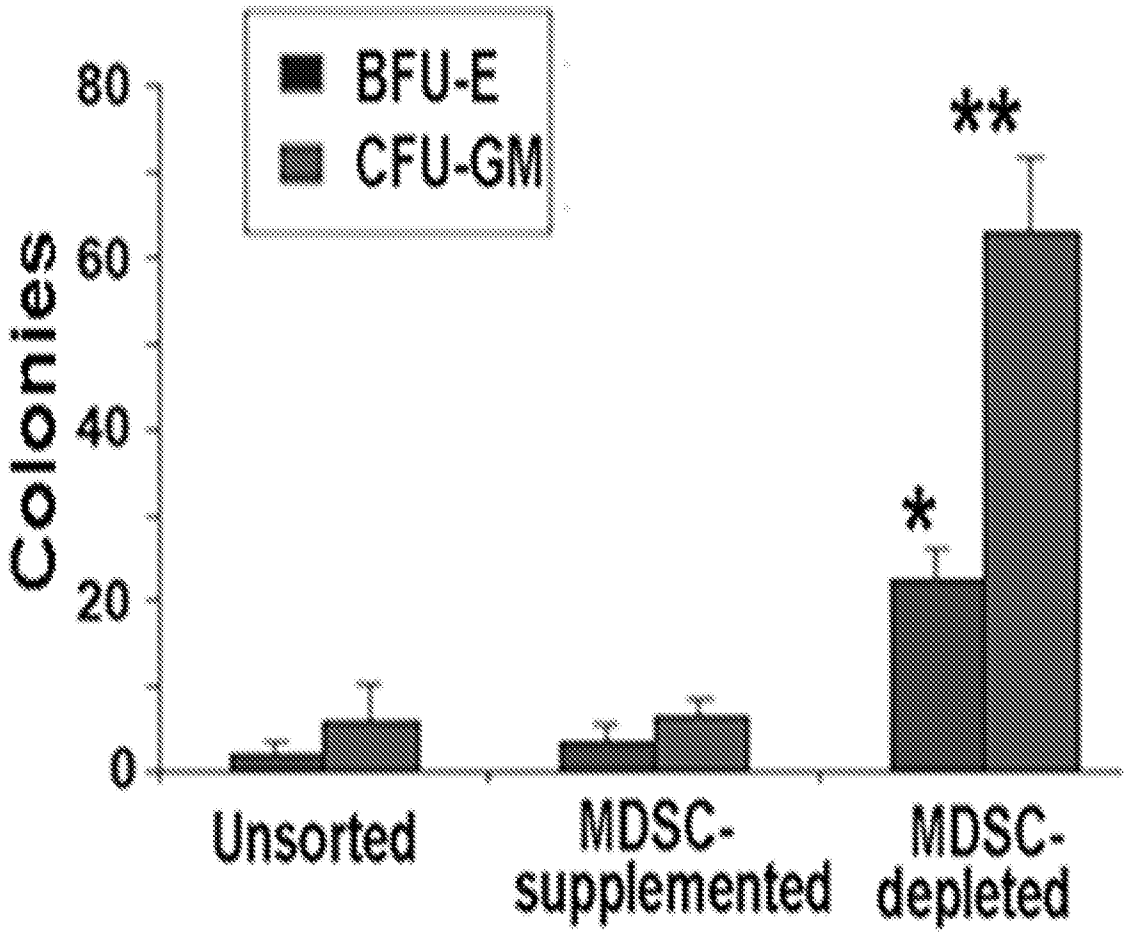

FIGURE 1N

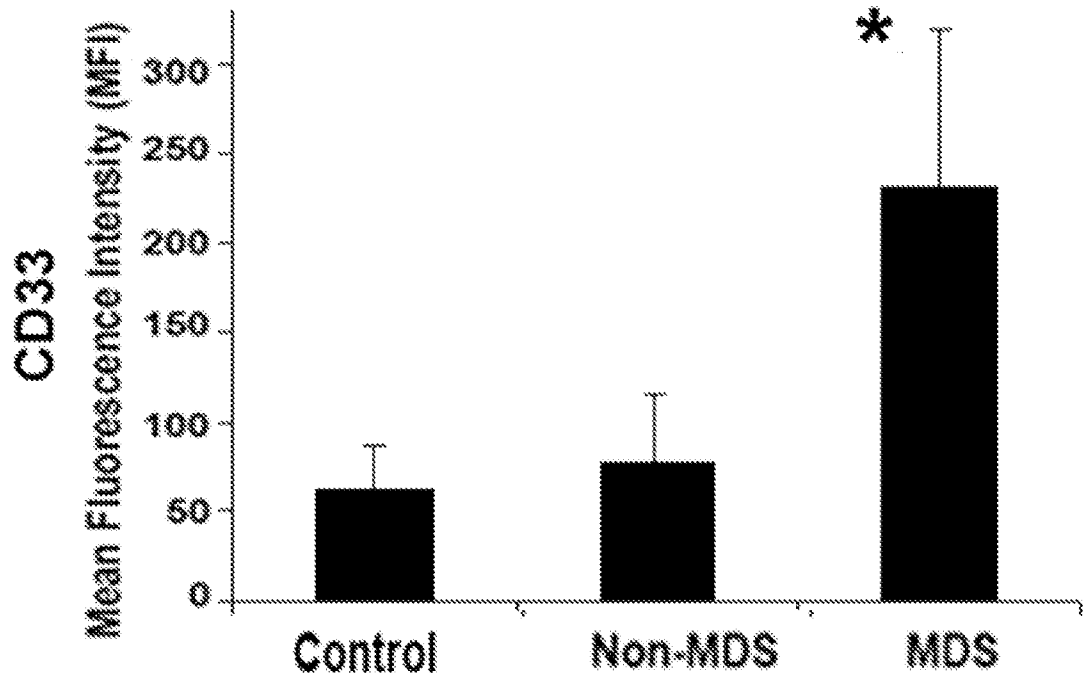

FIGURE 2A

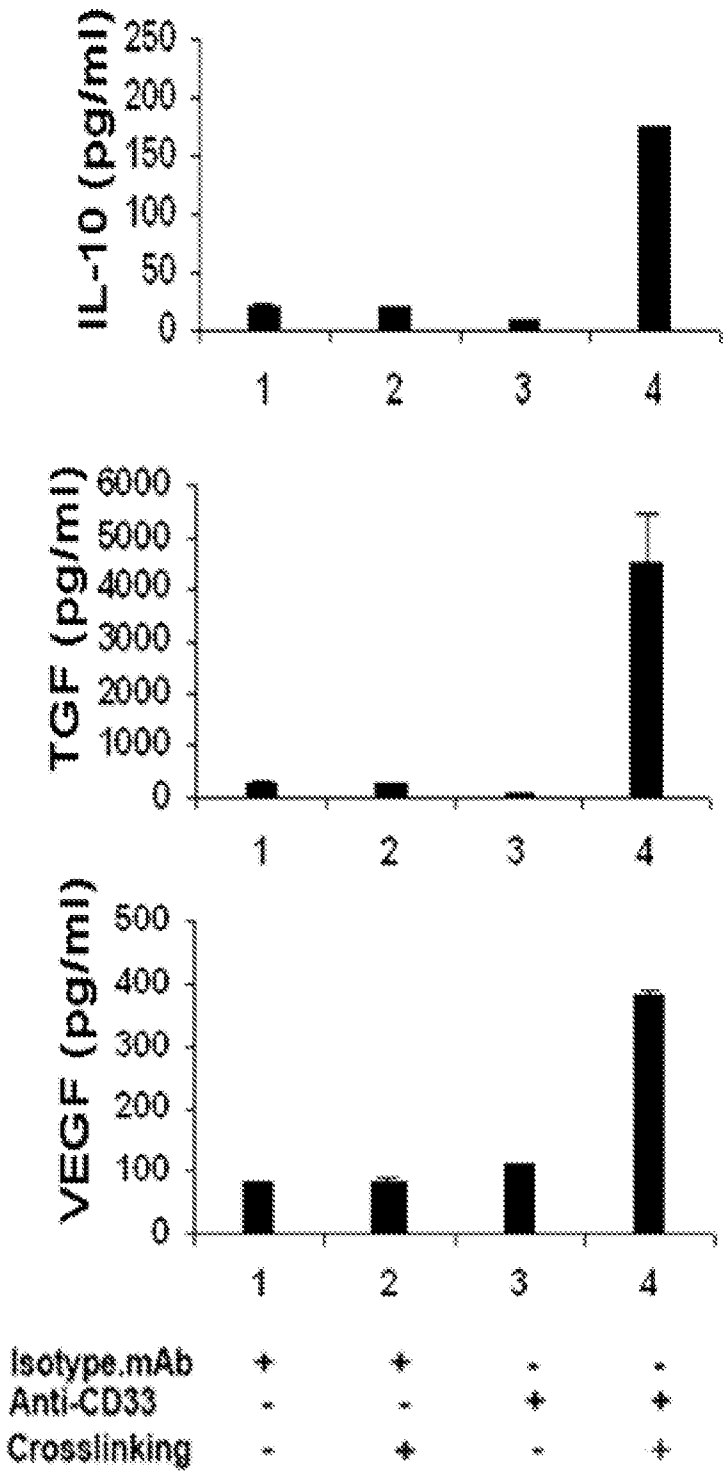
IL-10 (pg/ml)
250
200
150
100
50
0
1
2
3
4
TGF (pg/ml)
6000
5000
4000
3000
2000
1000
0
1
2
3
4
VEGF (pg/ml)
500
400
300
200
100
0
1
2
3
4
Isotype.mAb + + - -
Anti-CD33 - - + +
Crosslinking - + - +

FIGURE 2B

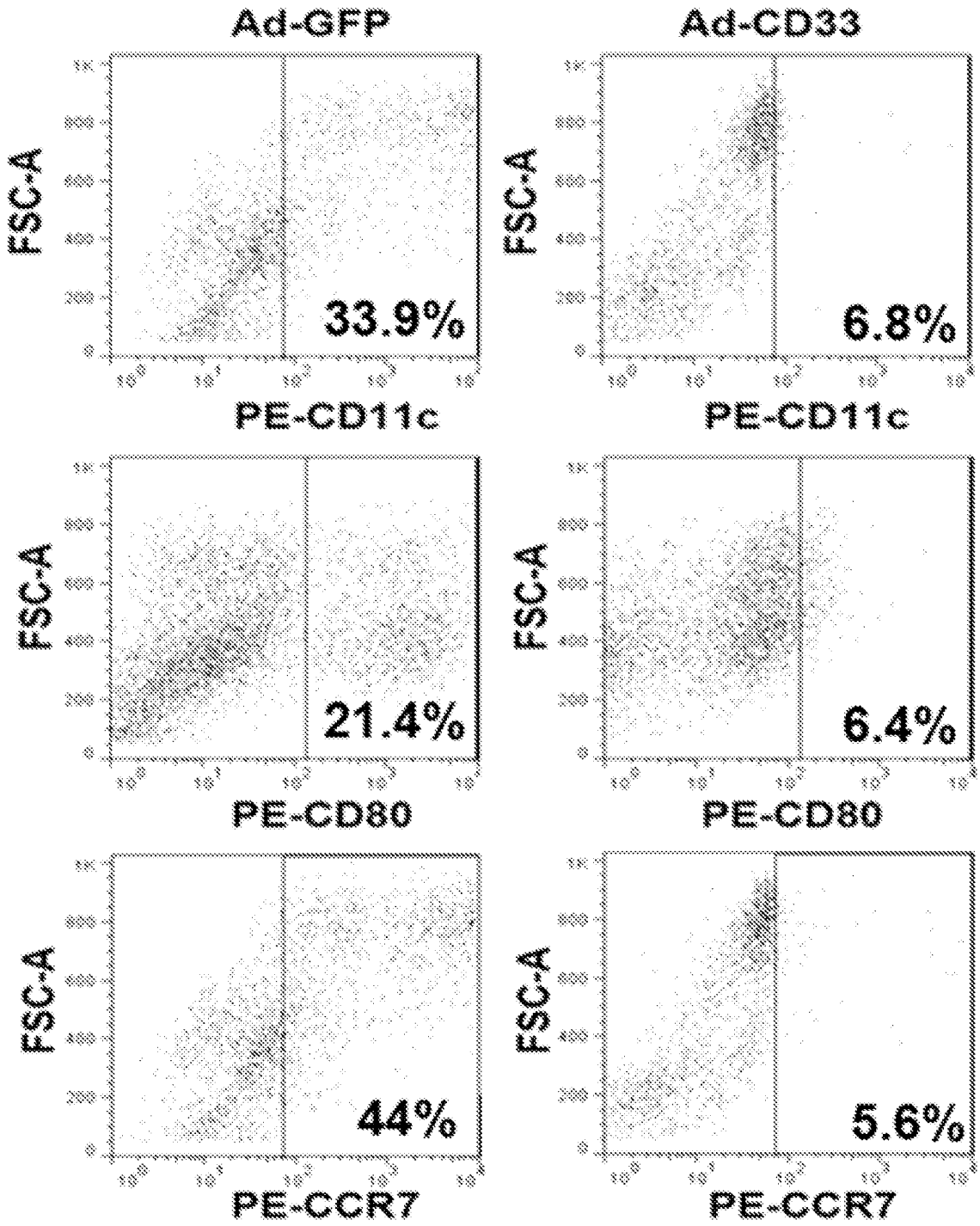

FIGURE 2C

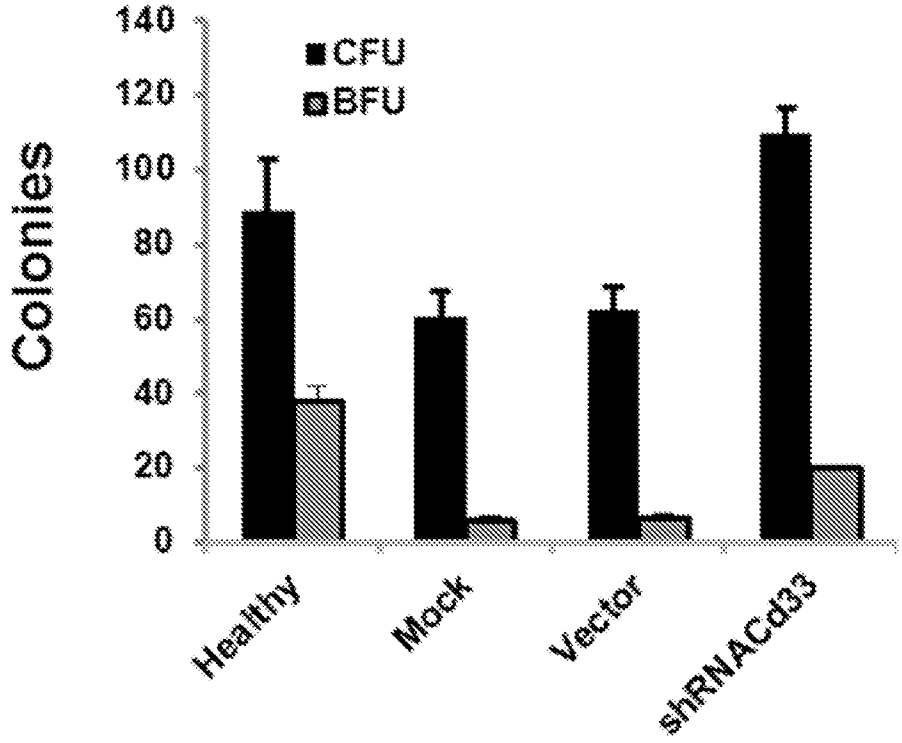

FIGURE 2D

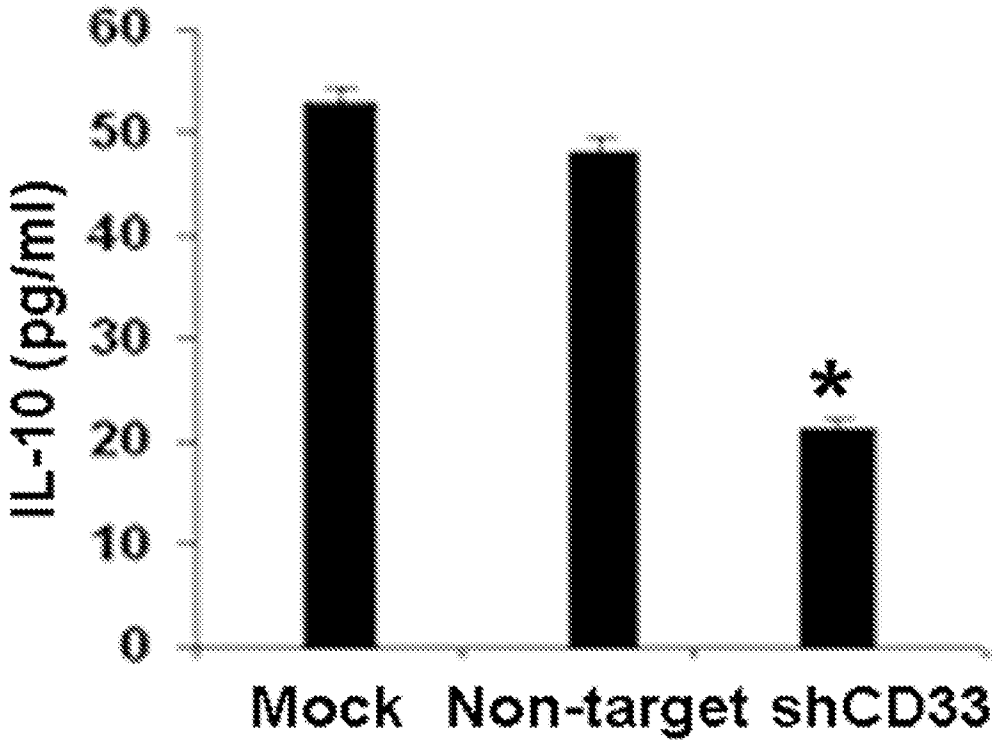

FIGURE 2E

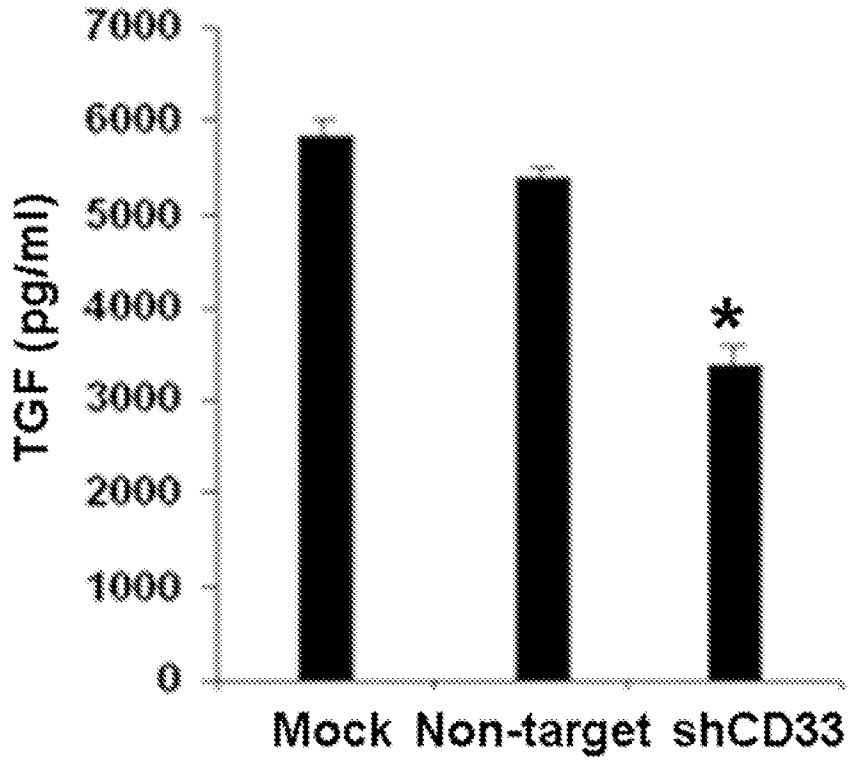

FIGURE 2F

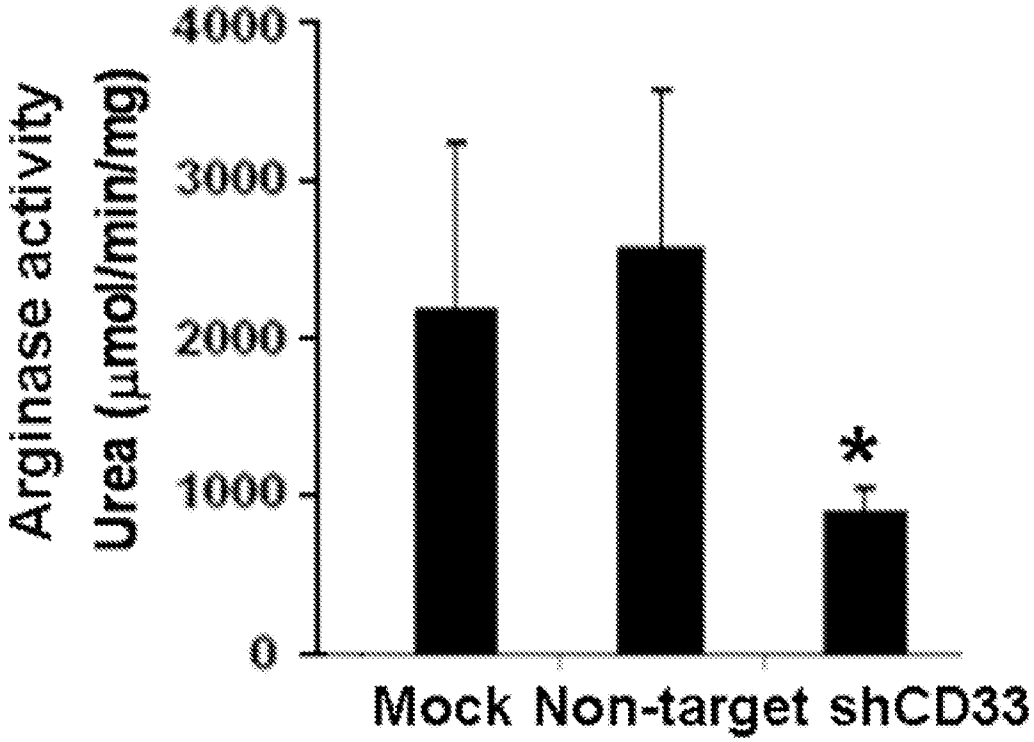

FIGURE 2G

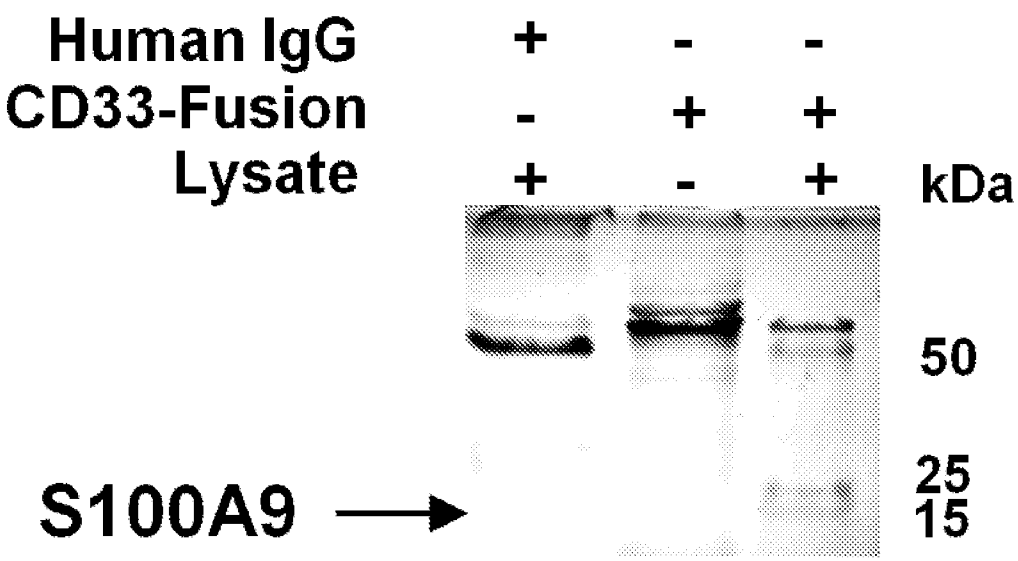

FIGURE 3A

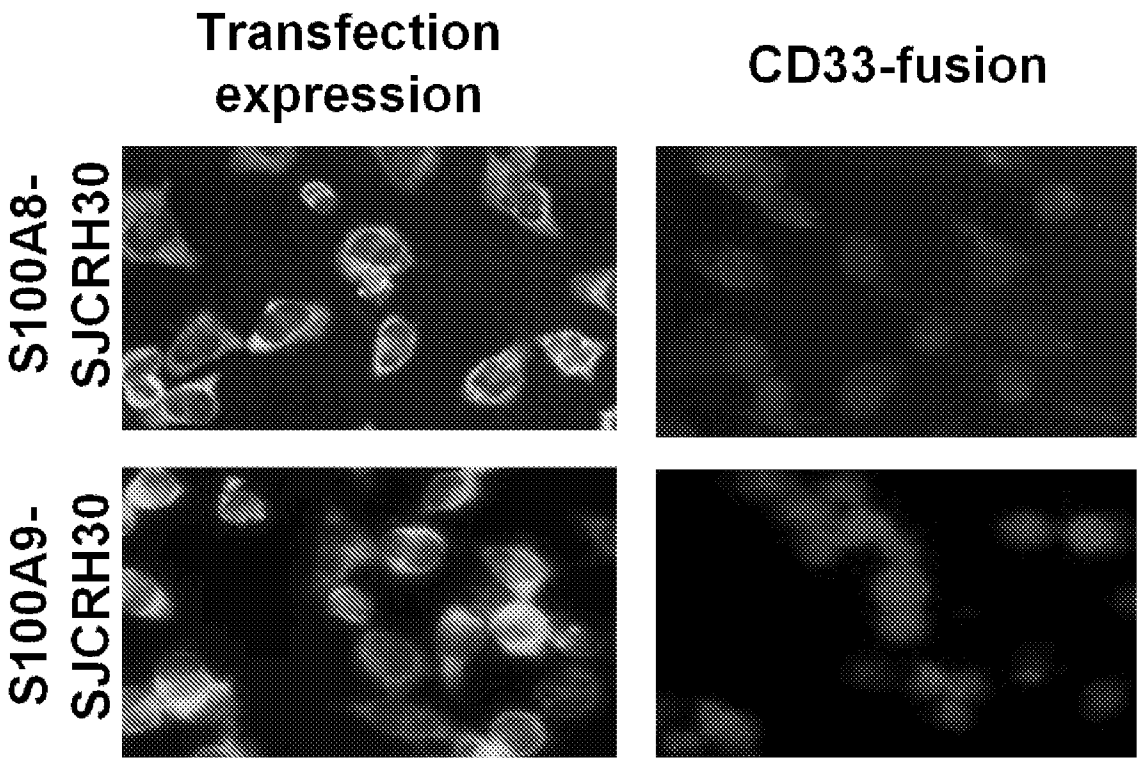

FIGURE 3B

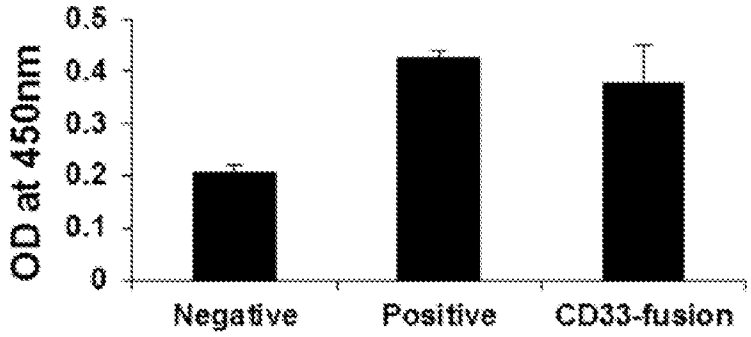

FIGURE 3C

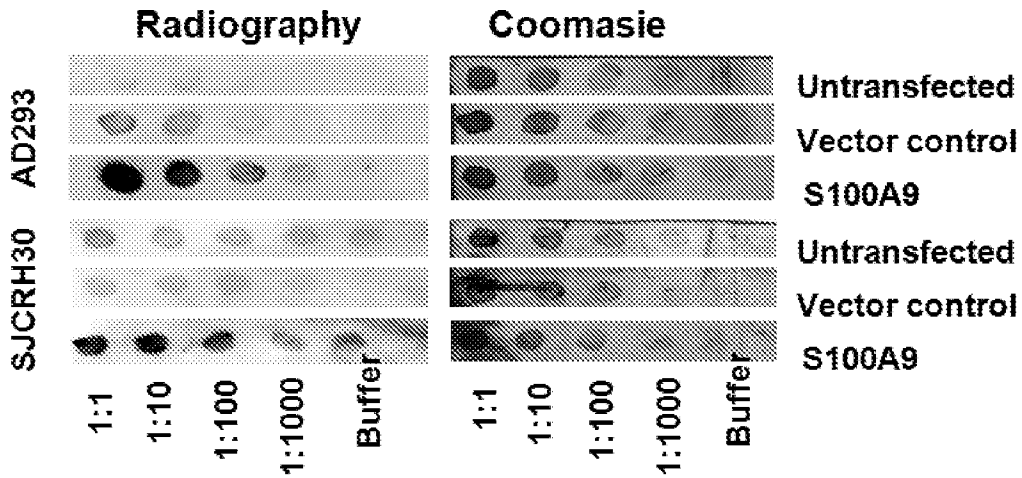

FIGURE 3D

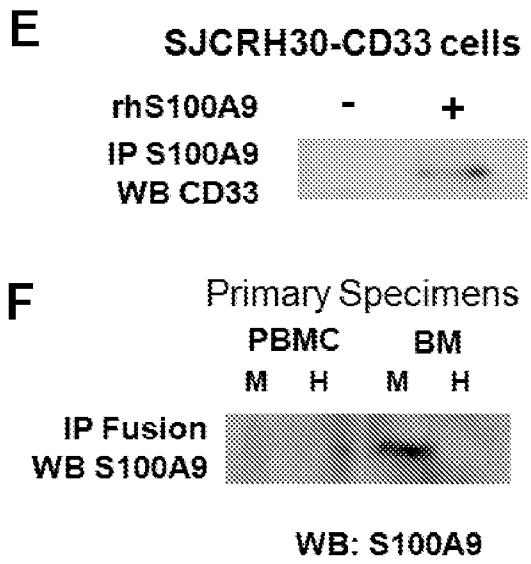

FIGURE 3E – 3F

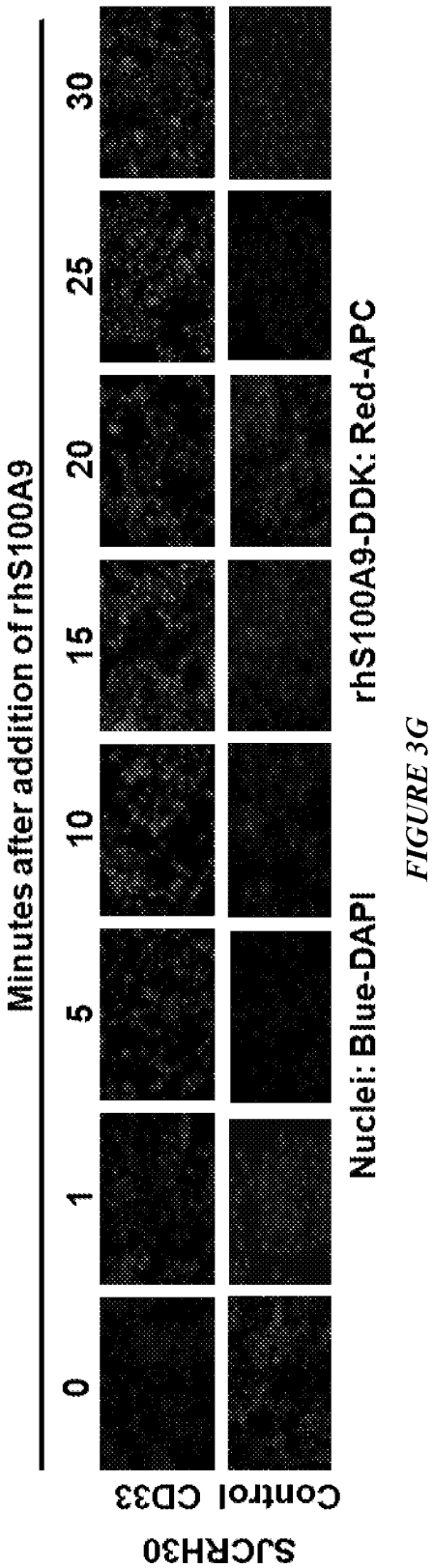
SJCRH30
Control CD33
Minutes after addition of rhS100A9
0
1
5
10
15
20
25
30
Nuclei: Blue-DAPI
rhS100A9-DDK: Red-APC

FIGURE 3G

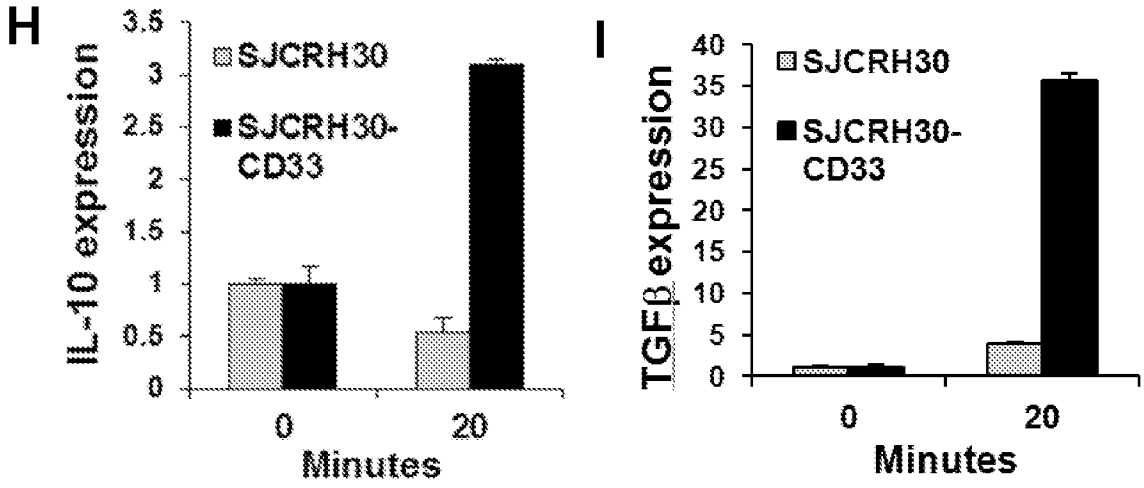

FIGURE 3H – 3I

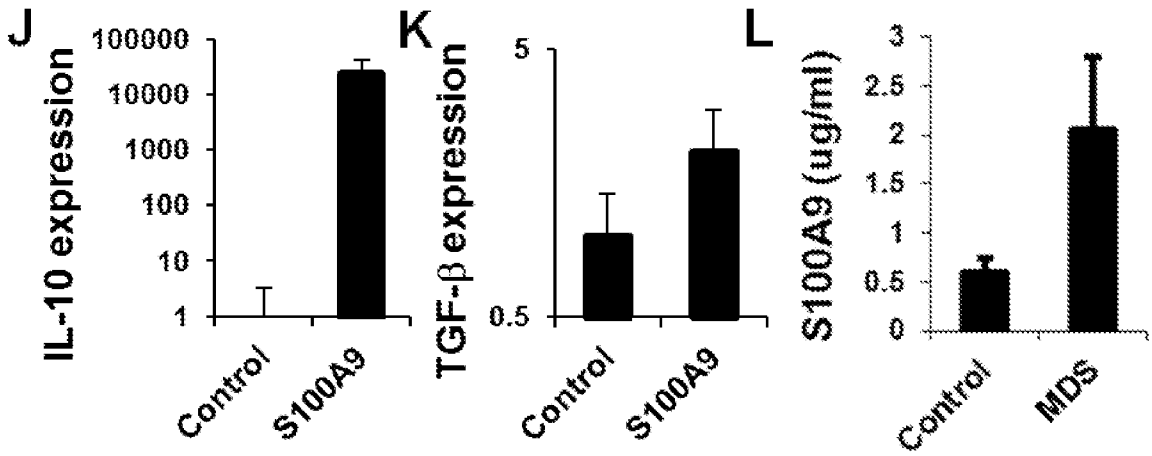

FIGURE 3J – 3L

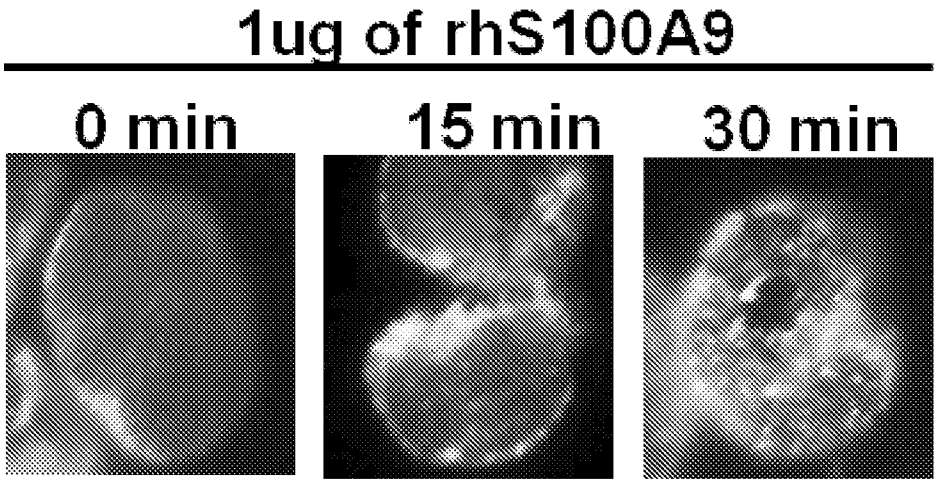

FIGURE 3M

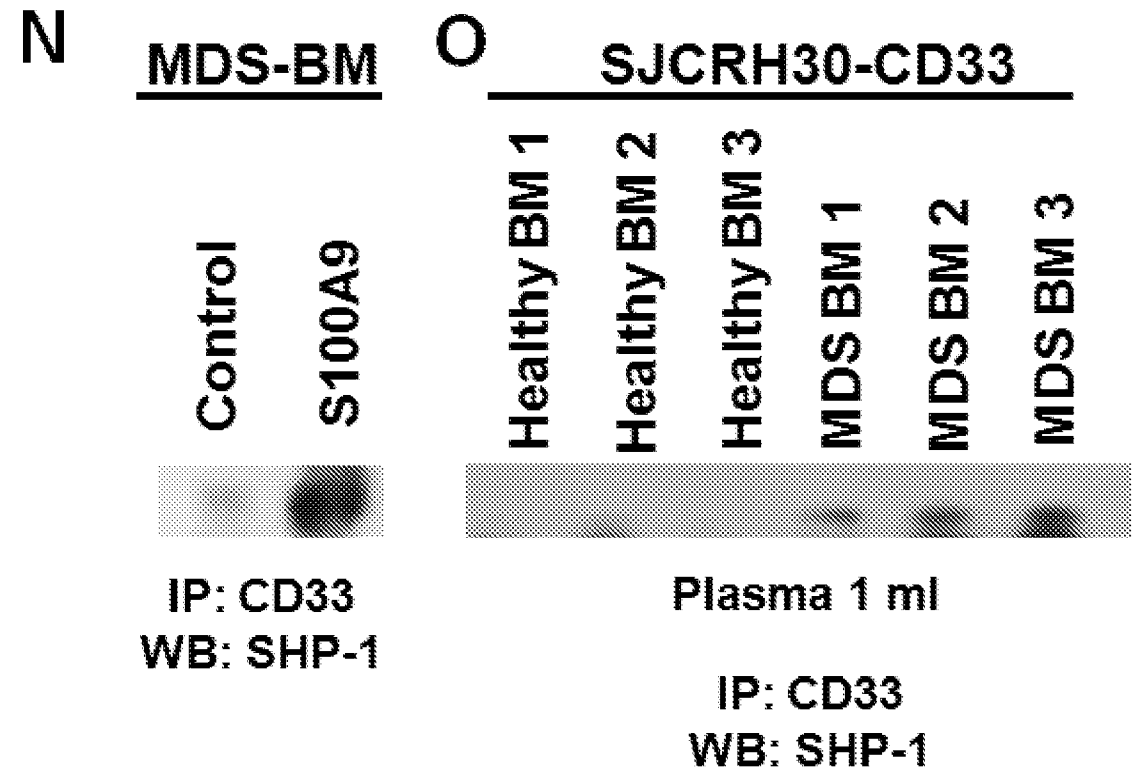

FIGURE 3N – 3O

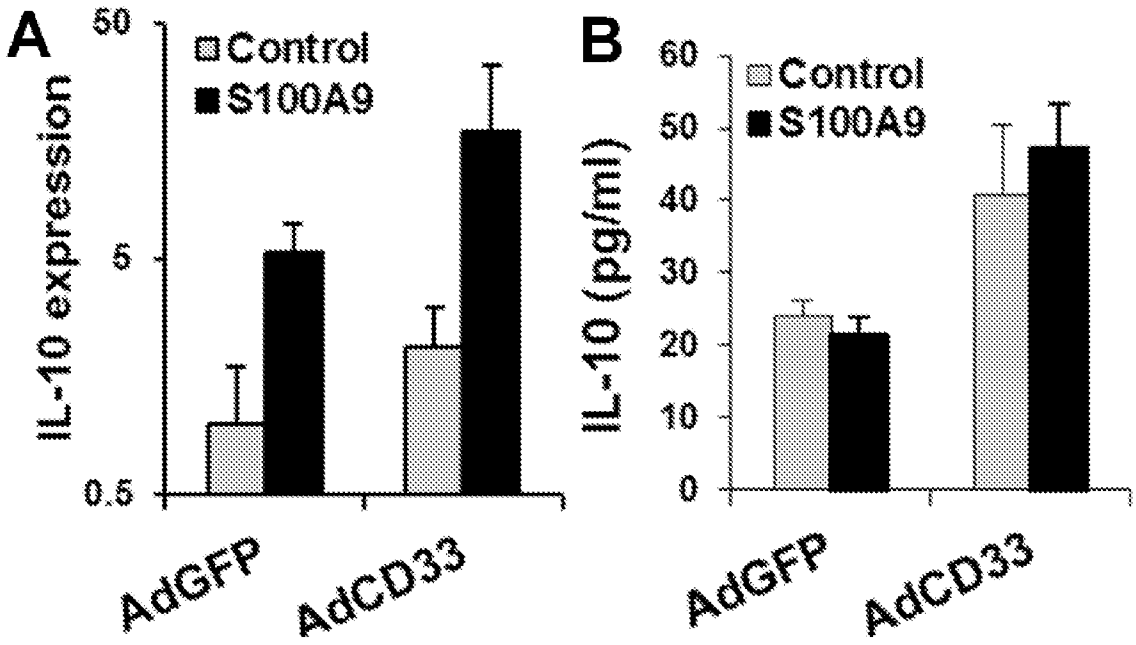

FIGURE 4A – 4B

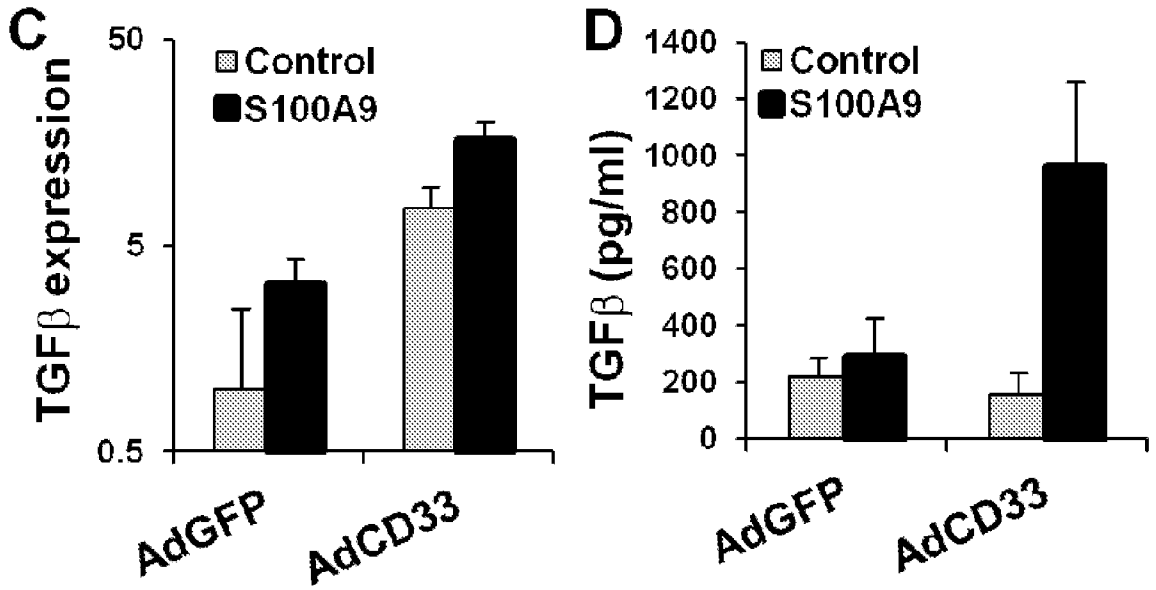

FIGURE 4C – 4D

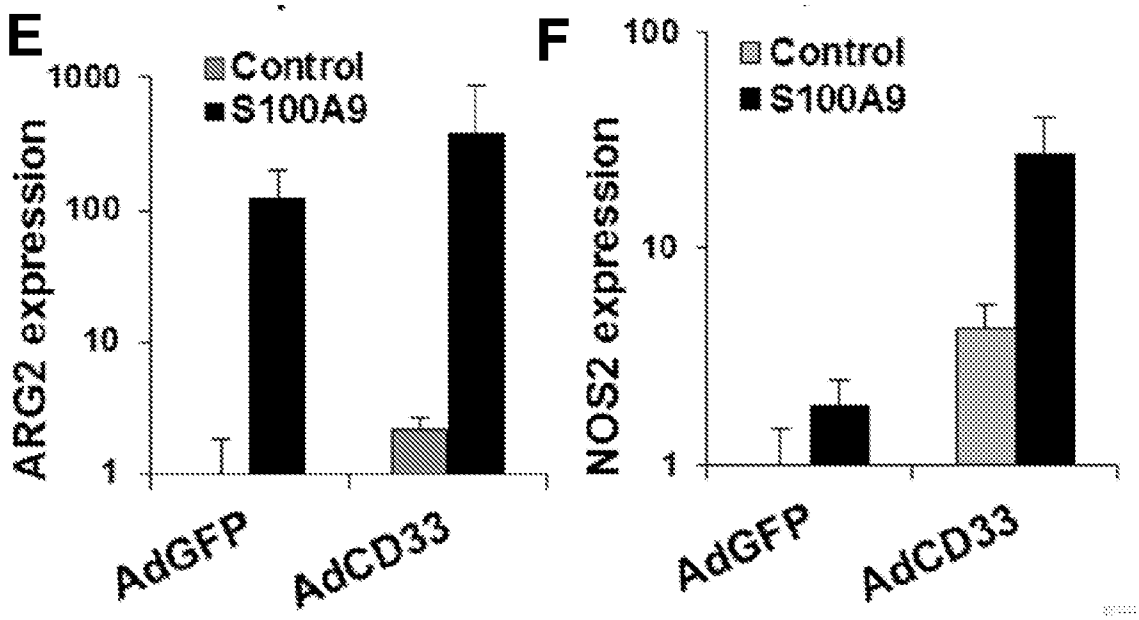

FIGURE 4E – 4F

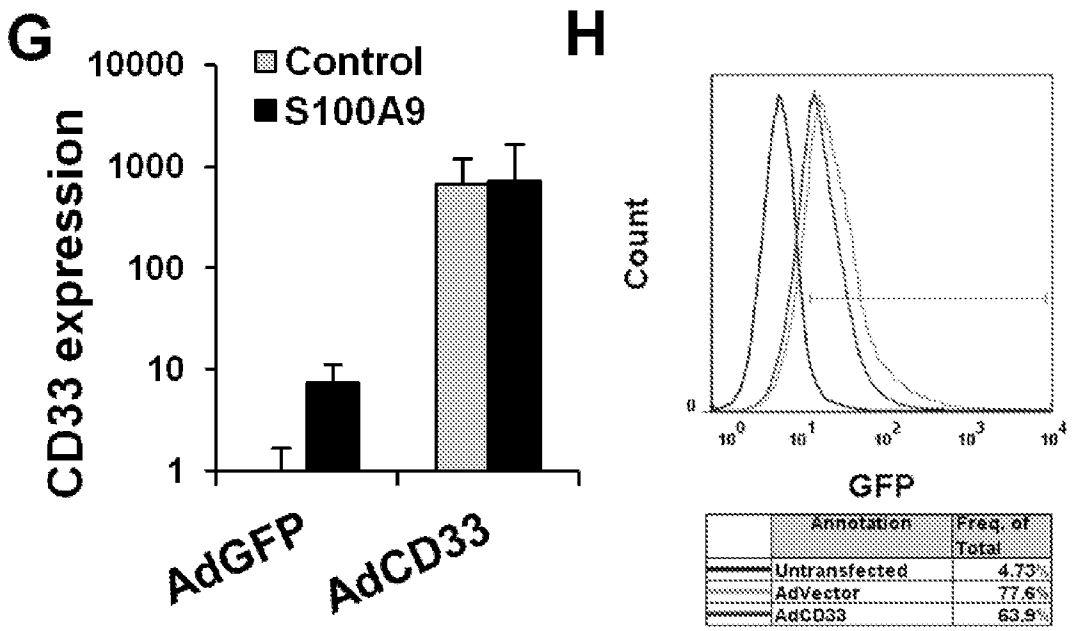
G
10000
1000
100
10
1
CD33 expression
Control
S100A9
AdGFP
AdCD33
H
Count
0
GFP
Annotation
Freq. of Total
Untransfected
4.73%
AdVector
77.6%
AdCD33
63.9%

FIGURE 4G – 4H

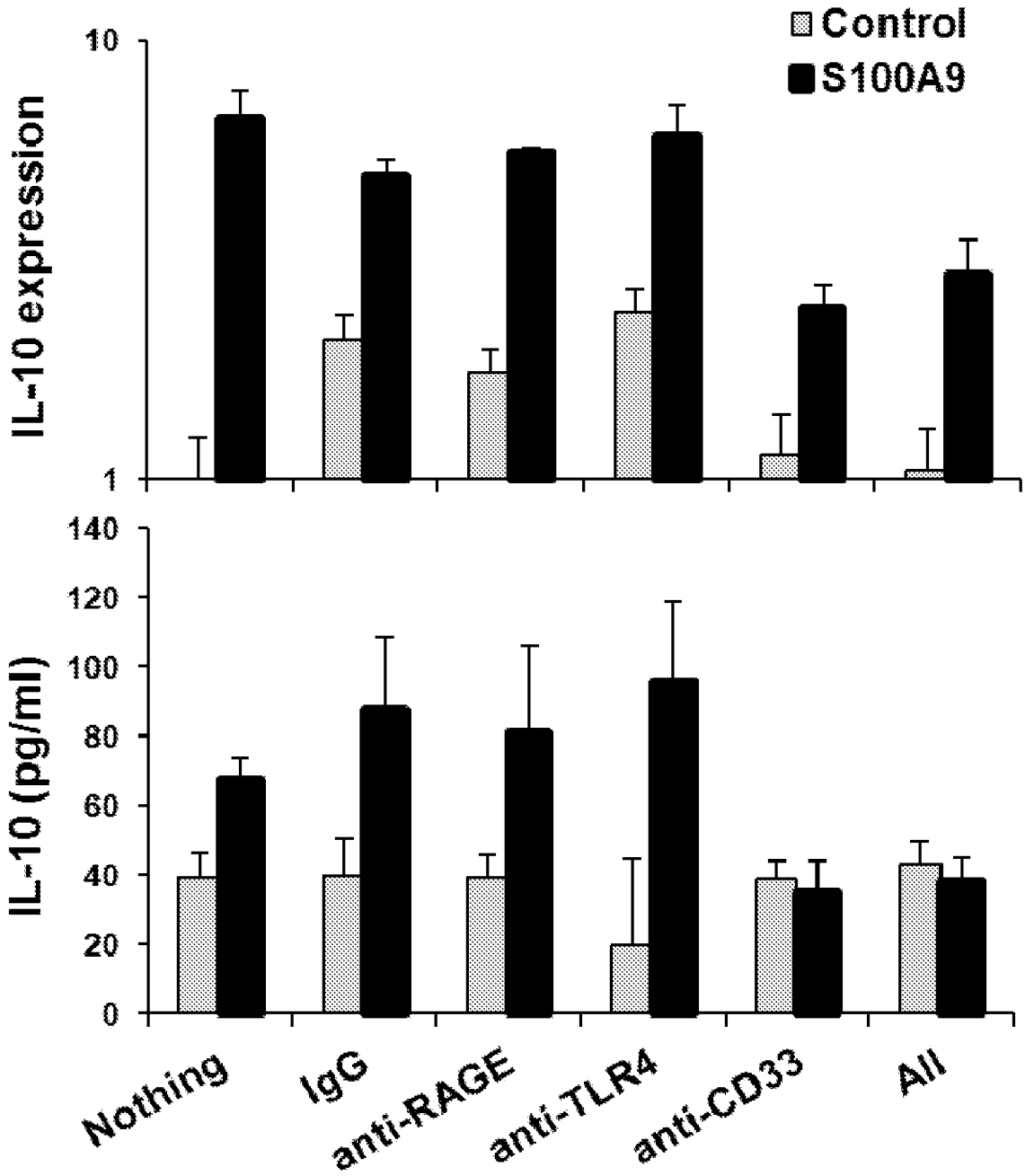
Control
S100A9
IL-10 expression
10
1
IL-10 (pg/ml)
140
120
100
80
60
40
20
0
Nothing
IgG
anti-RAGE
anti-TLR4
anti-CD33
All

FIGURE 4I

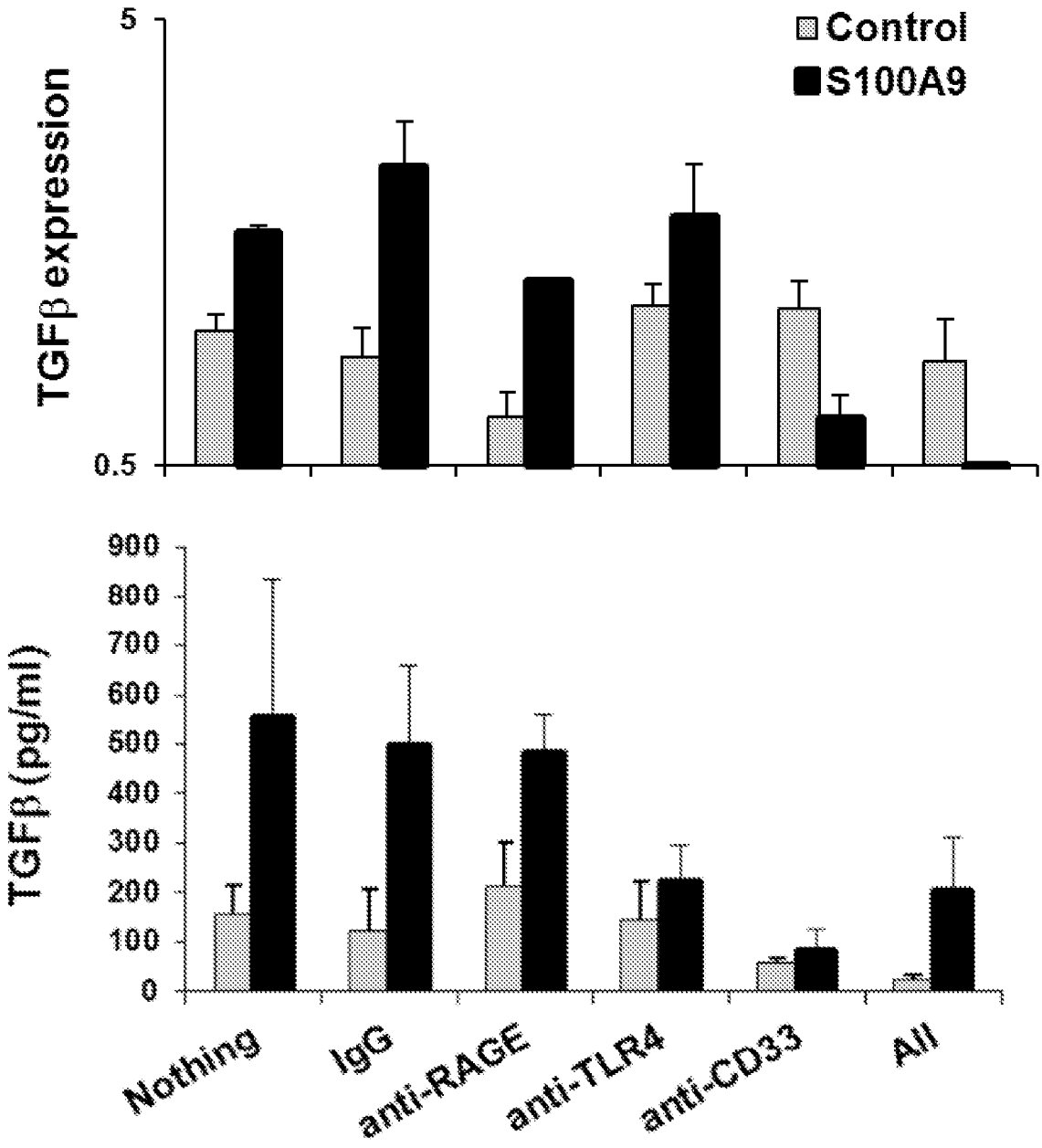
5
0.5
TGFβ expression
Control
S100A9
900
800
700
600
500
400
300
200
100
0
TGFβ (pg/ml)
Nothing
IgG
anti-RAGE
anti-TLR4
anti-CD33
All

FIGURE 4J

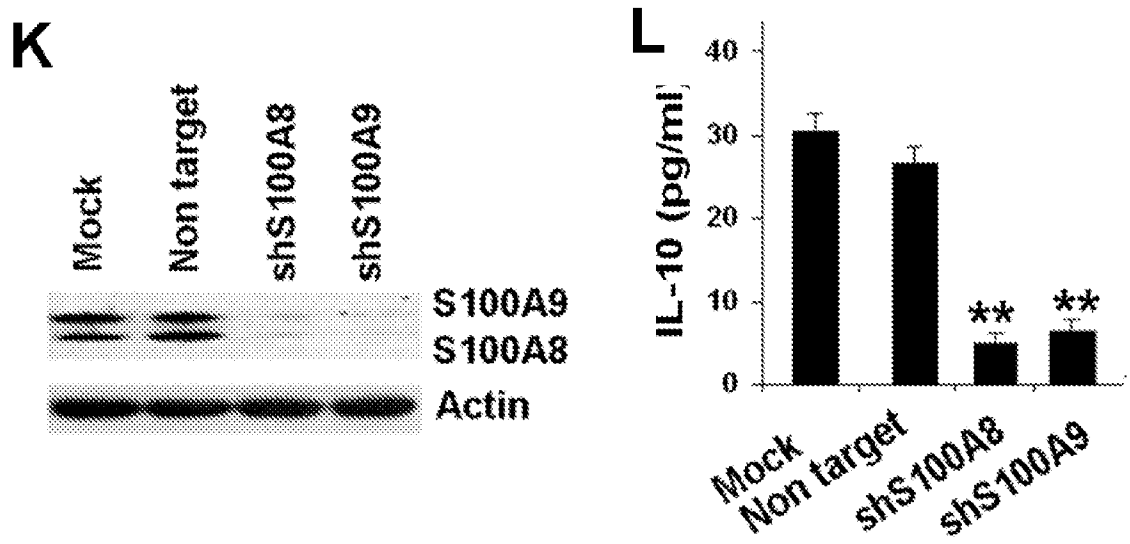

FIGURE 4K – 4L

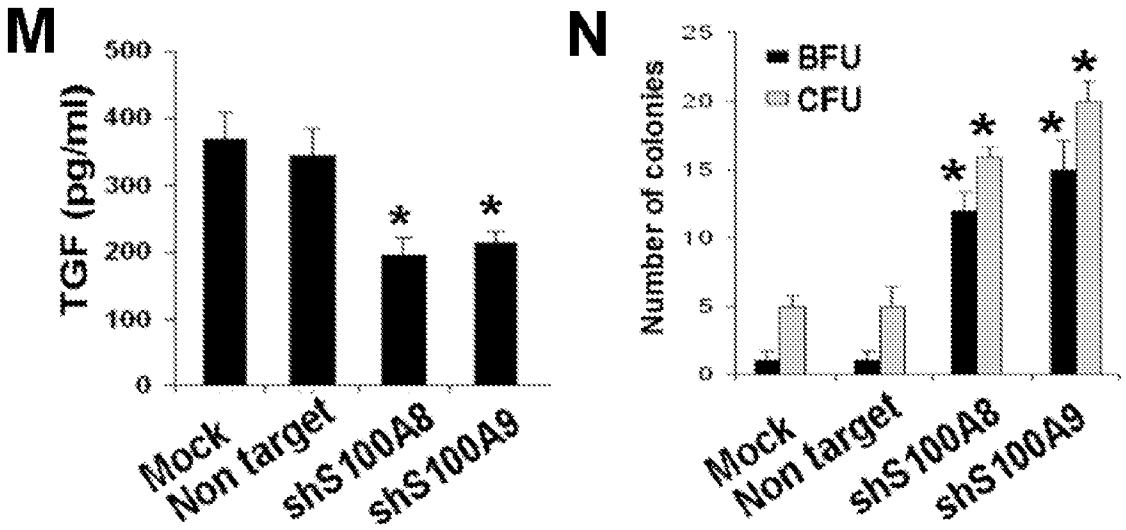

FIGURE 4M – 4N

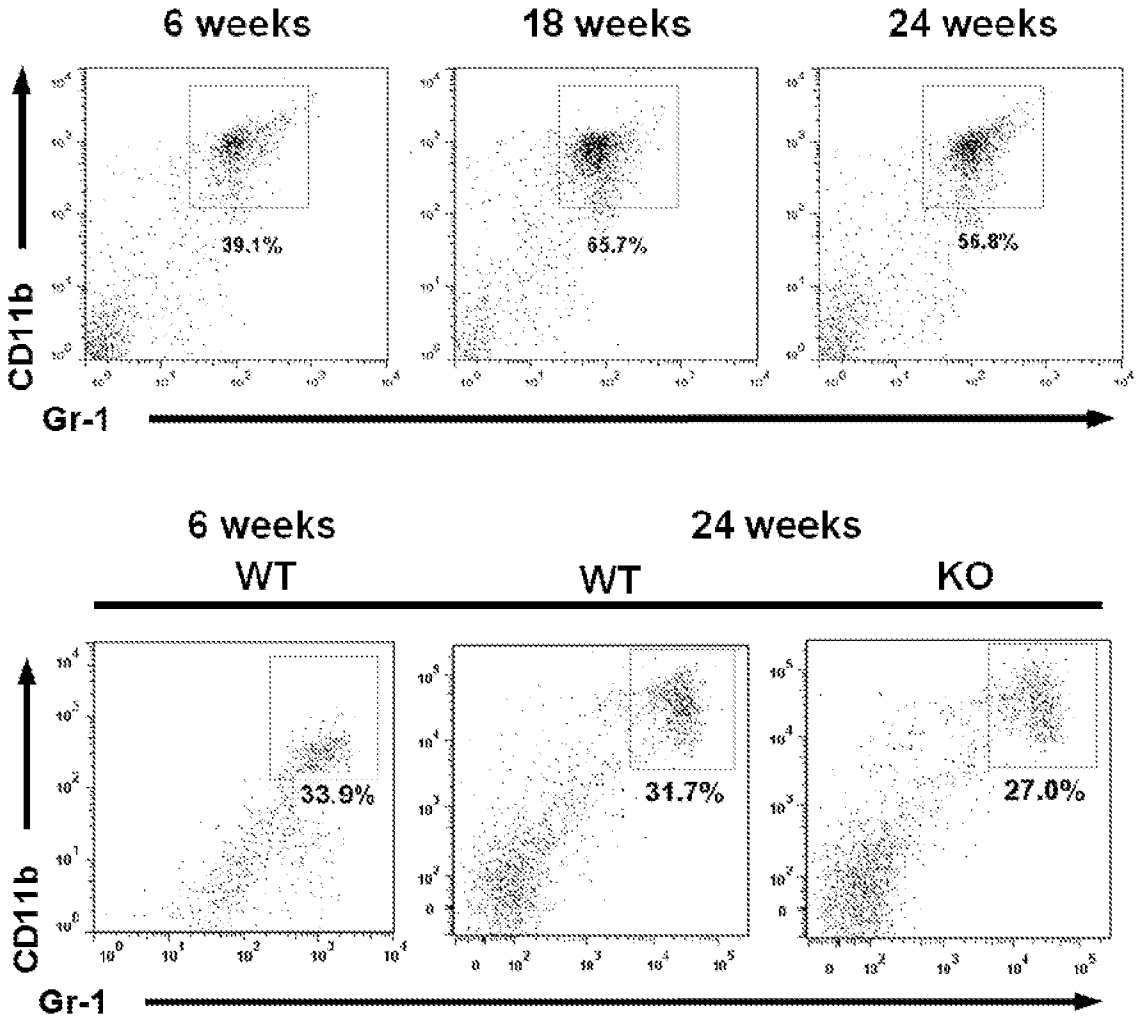

FIGURE 5A

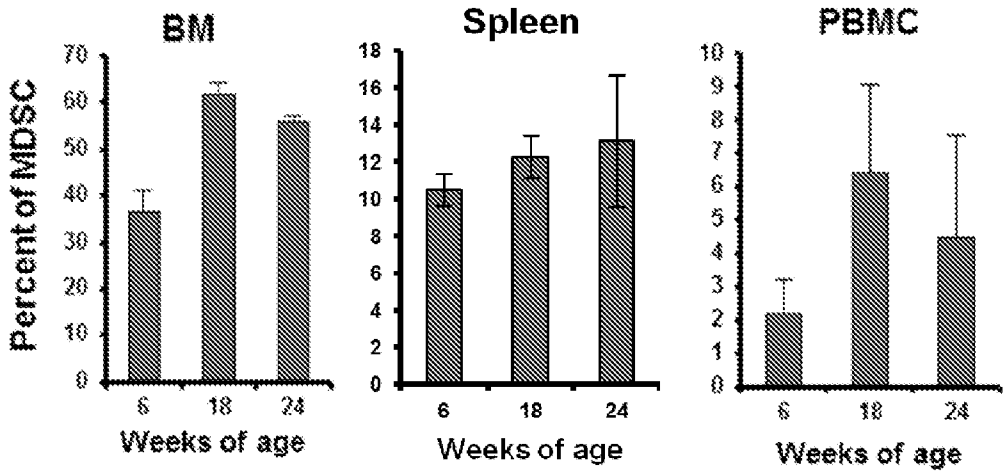

FIGURE 5B

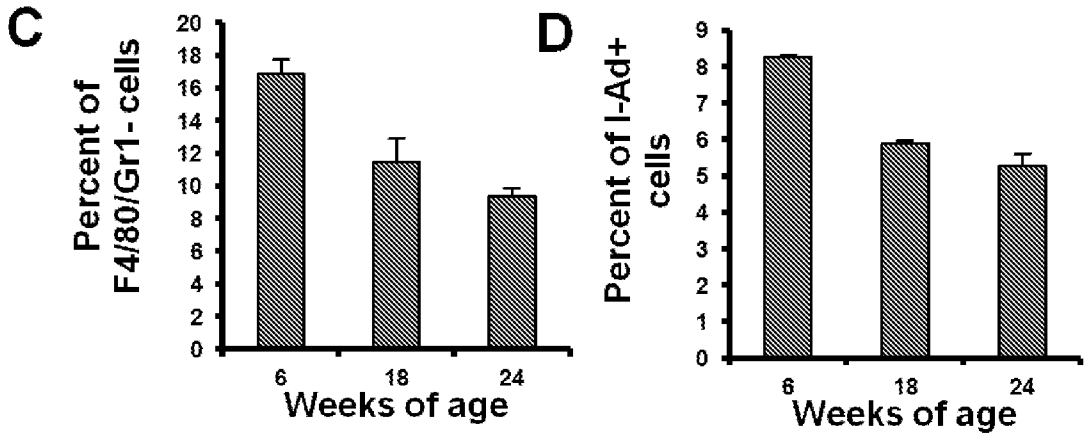

FIGURE 5C – 5D

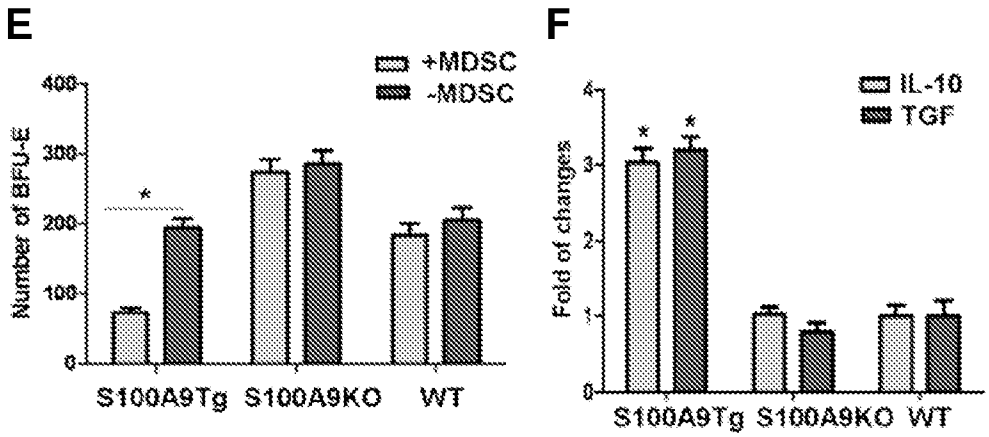

FIGURE 5E – 5F

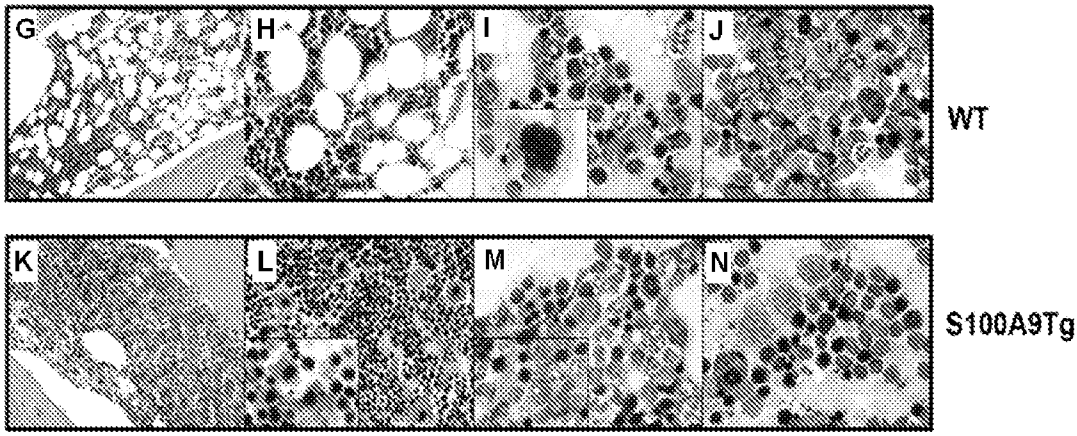

FIGURE 5G – 5N

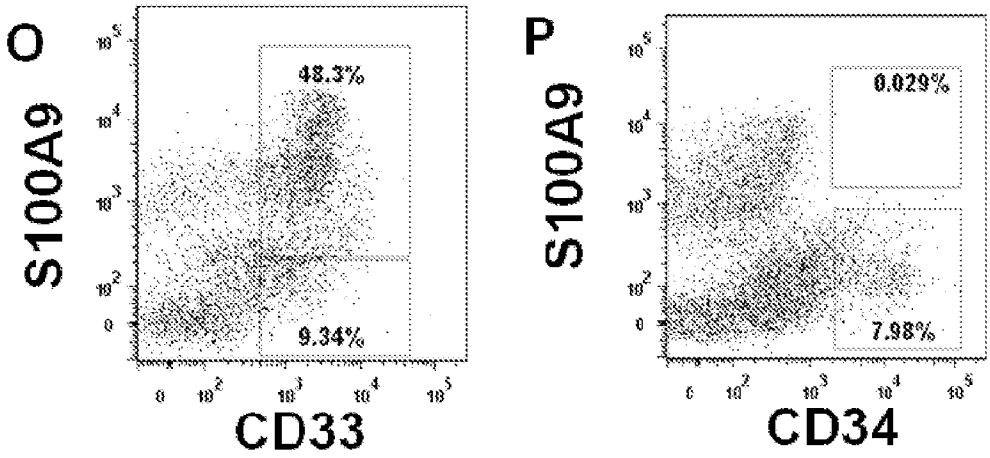

FIGURE 5O – 5P

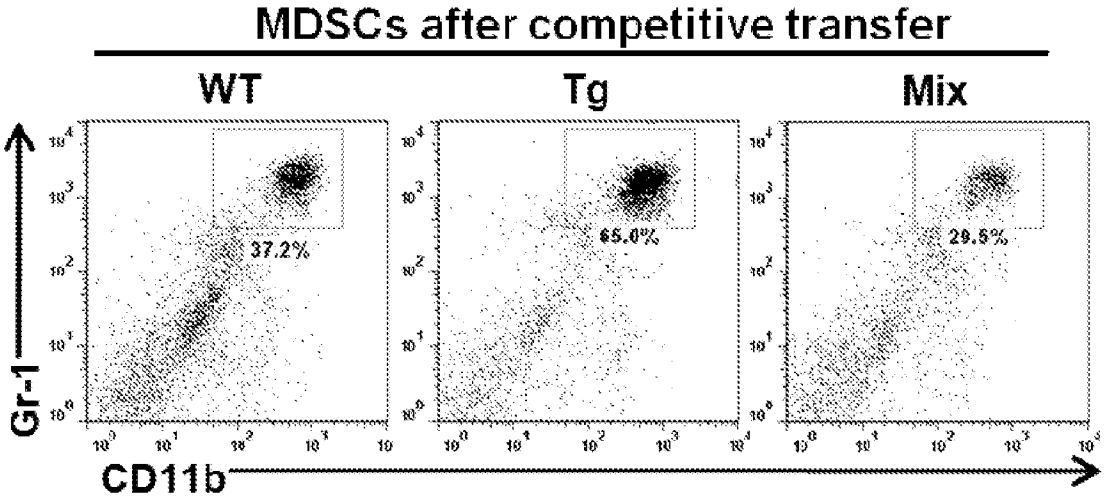

FIGURE 6A

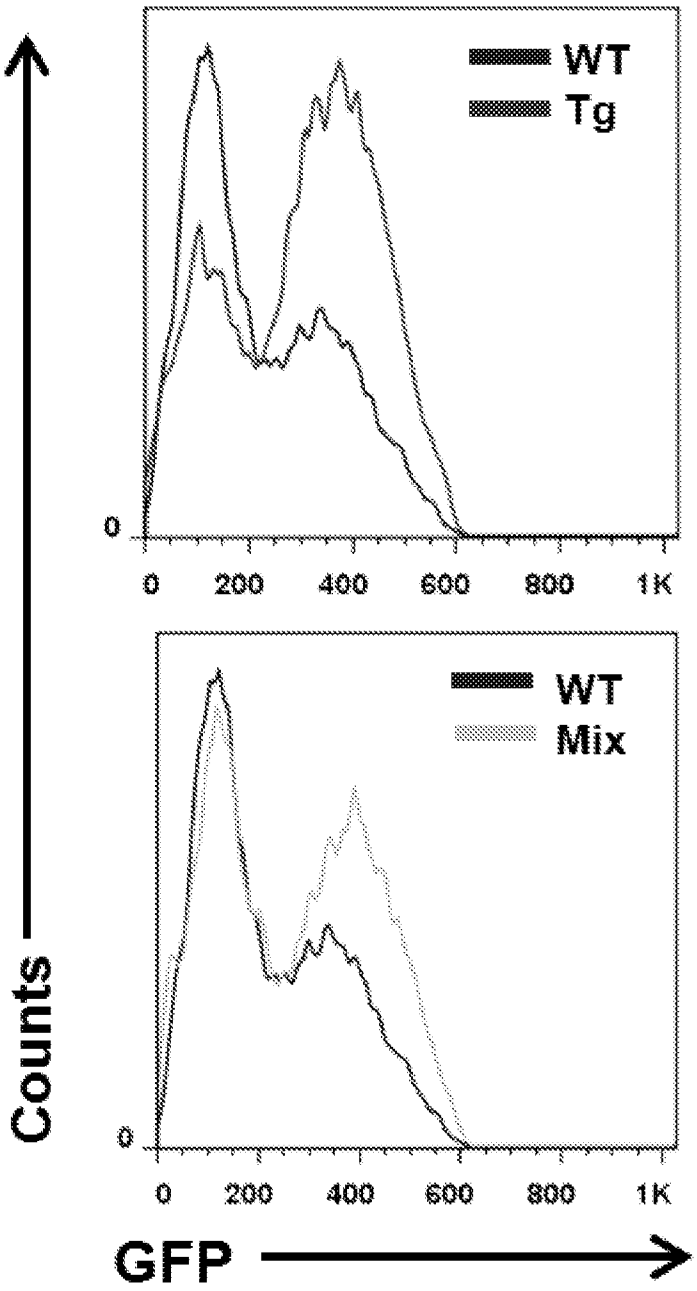
WT
Tg
0
0
200
400
600
800
1K
WT
Mix
0
0
200
400
600
800
1K
Counts
GFP

FIGURE 6B

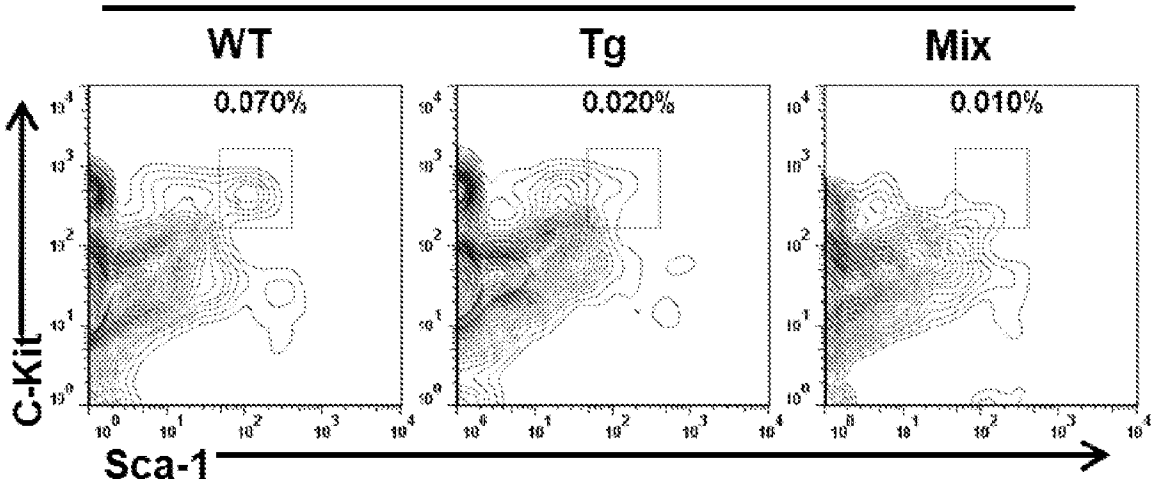

FIGURE 6C

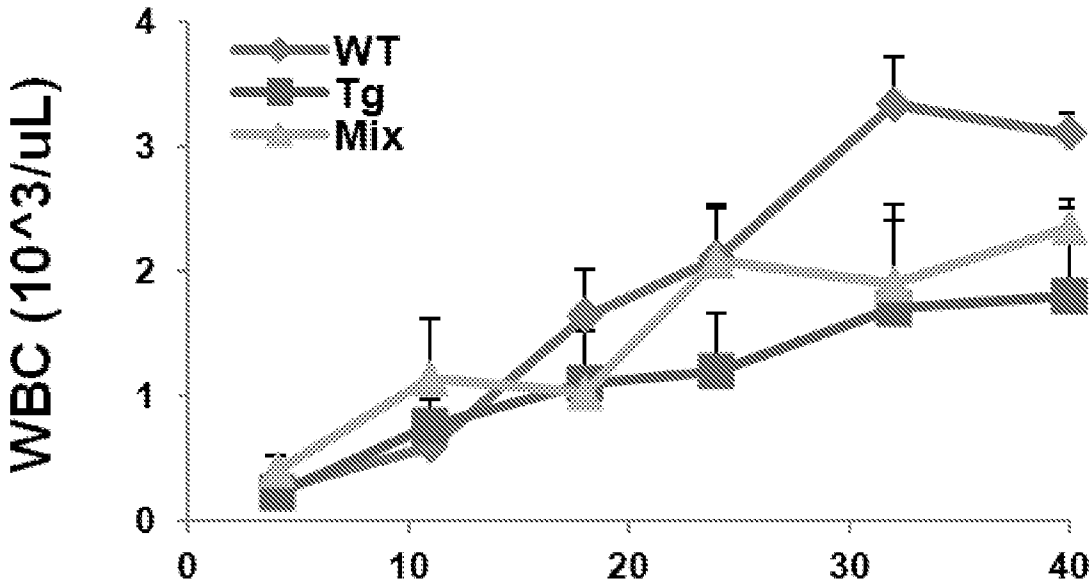

FIGURE 6D

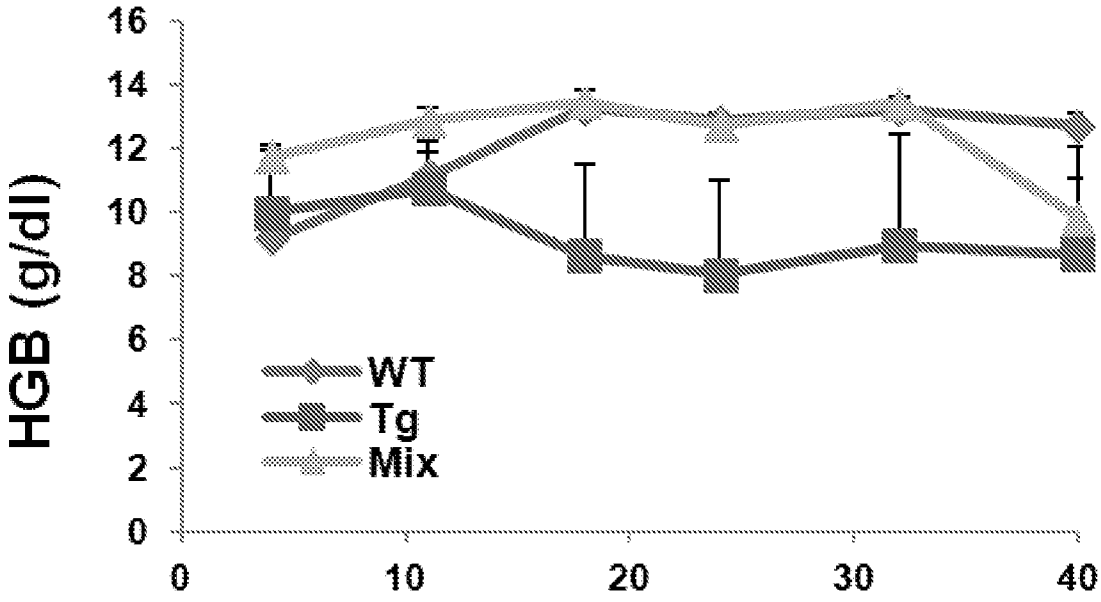

FIGURE 6E

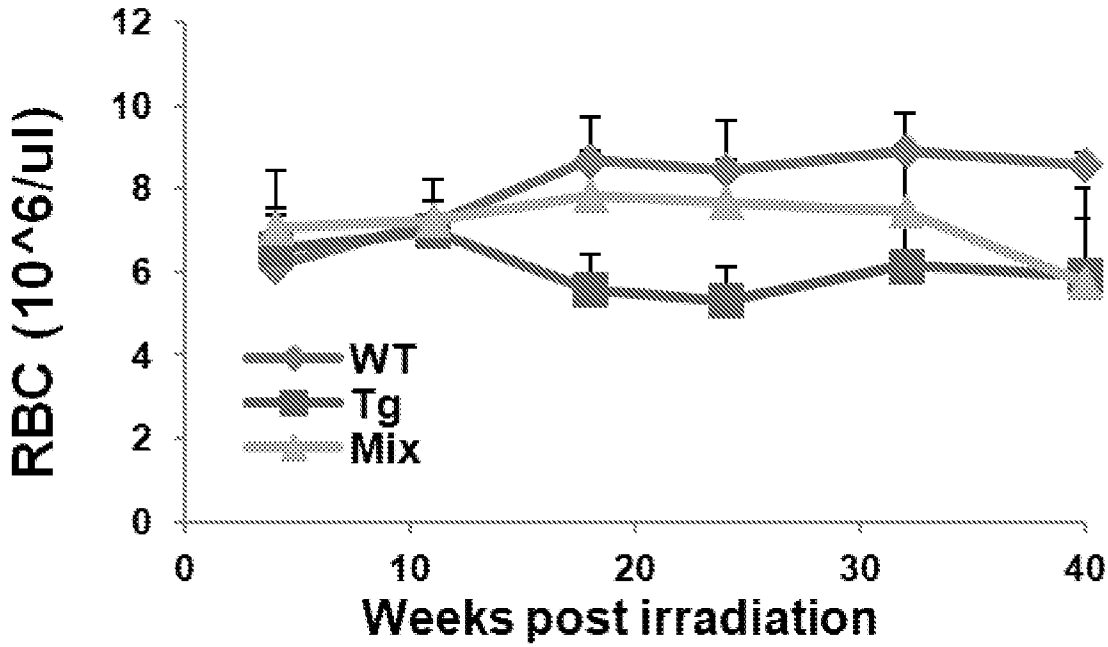

FIGURE 6F

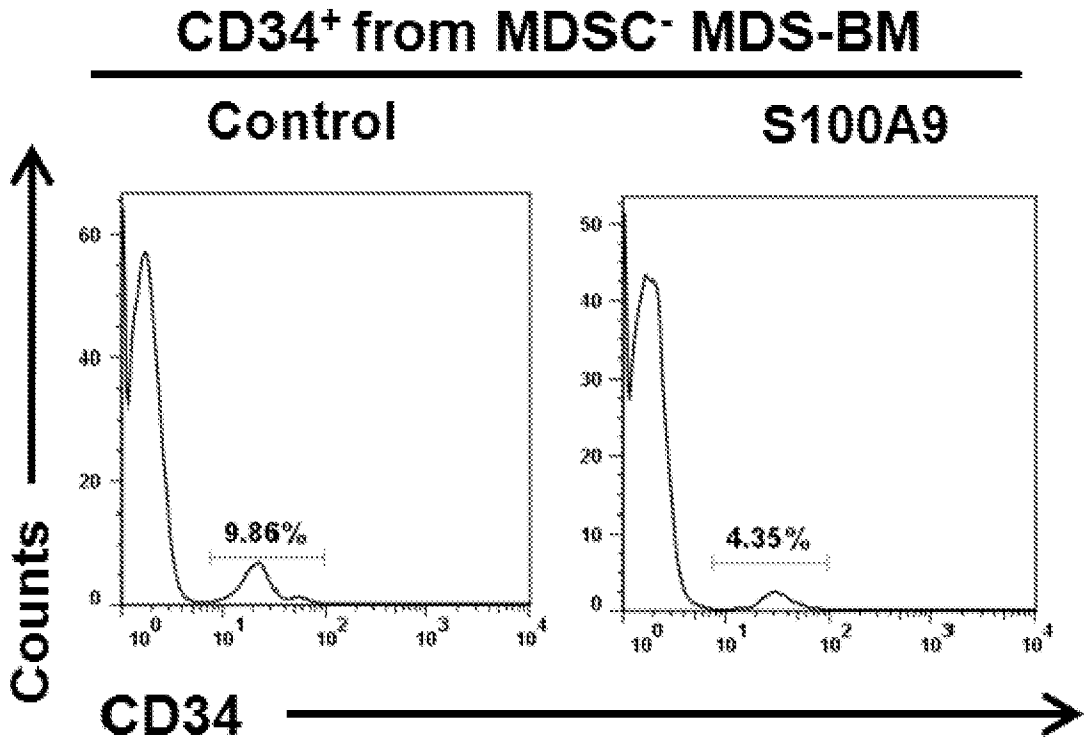

FIGURE 6G

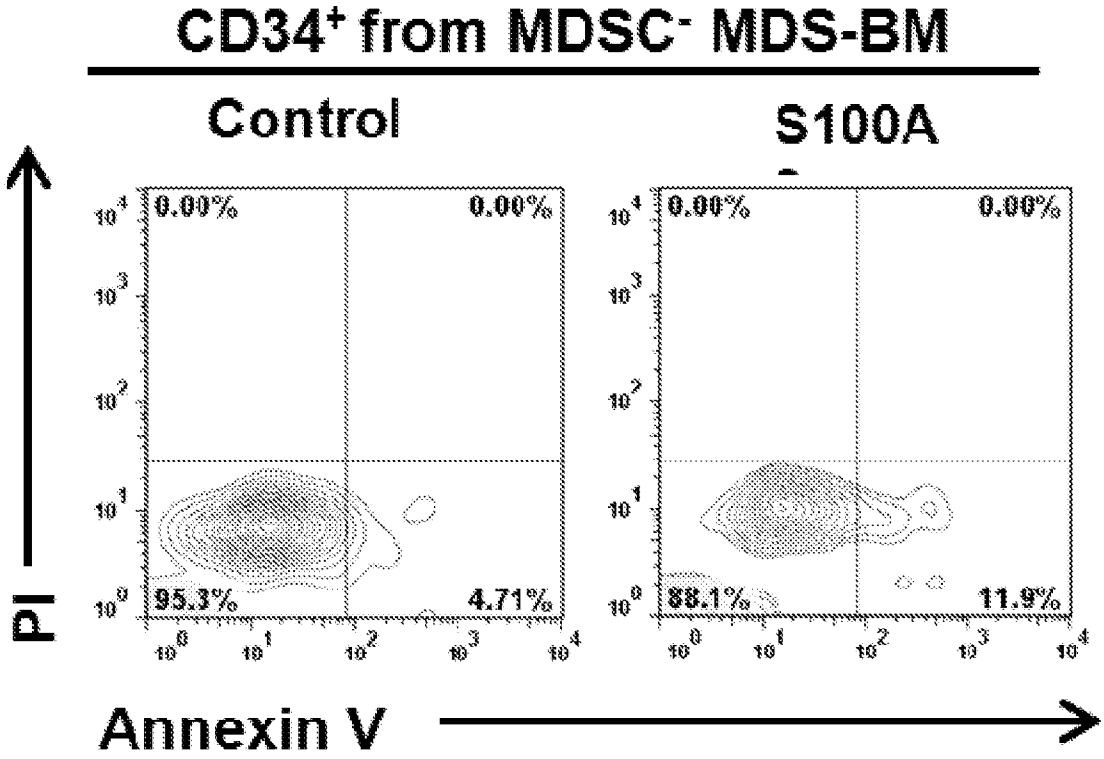

FIGURE 6H

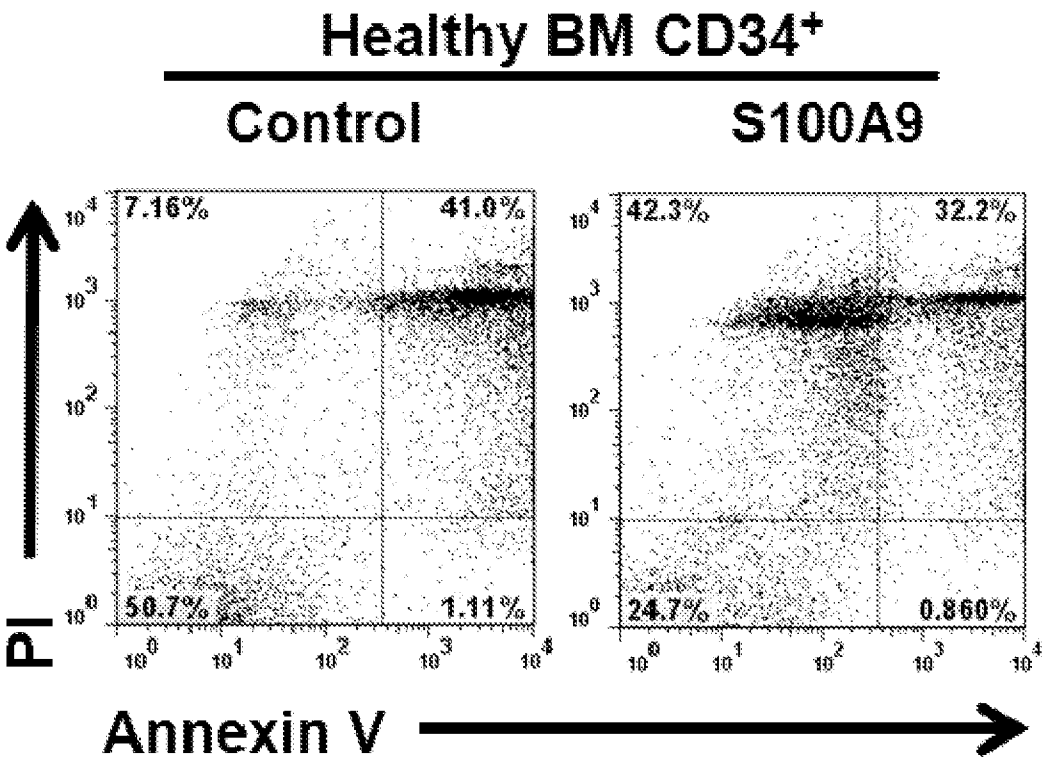
Healthy BM CD34+
Control
S100A9
7.16%
41.0%
50.7%
1.11%
42.3%
32.2%
24.7%
0.860%
PI
Annexin V

FIGURE 6I

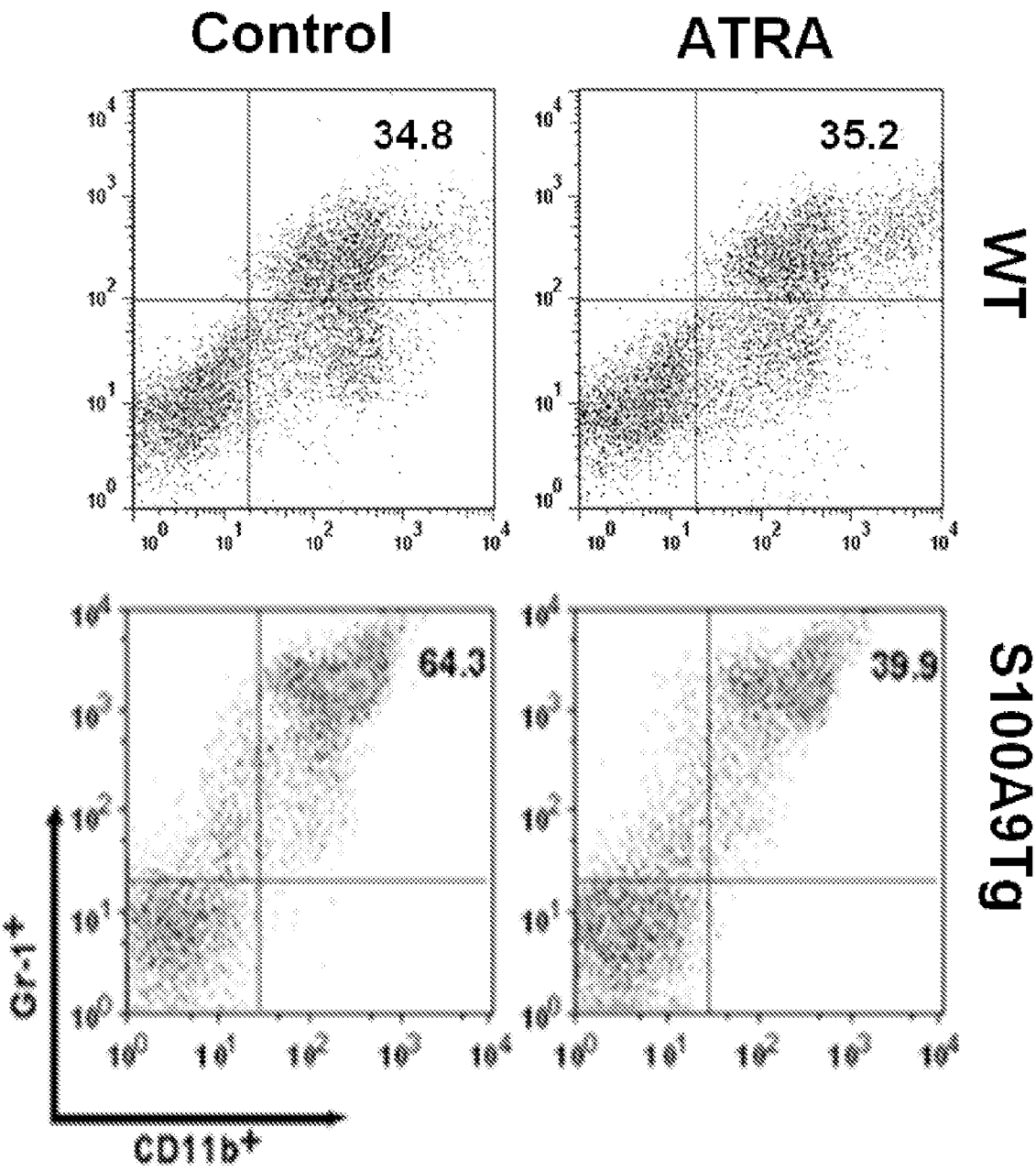

FIGURE 7A

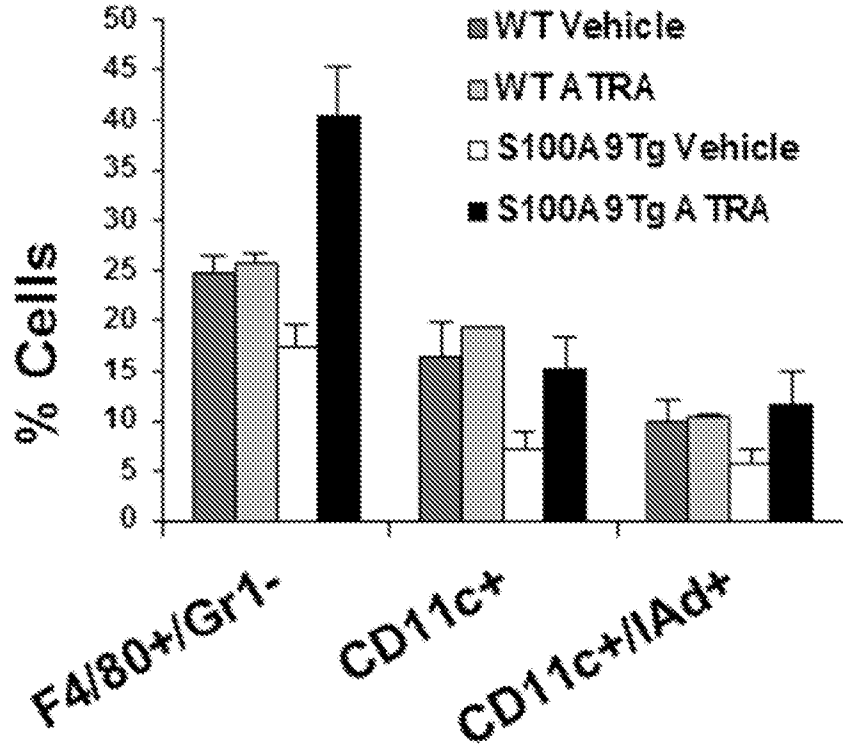

FIGURE 7B

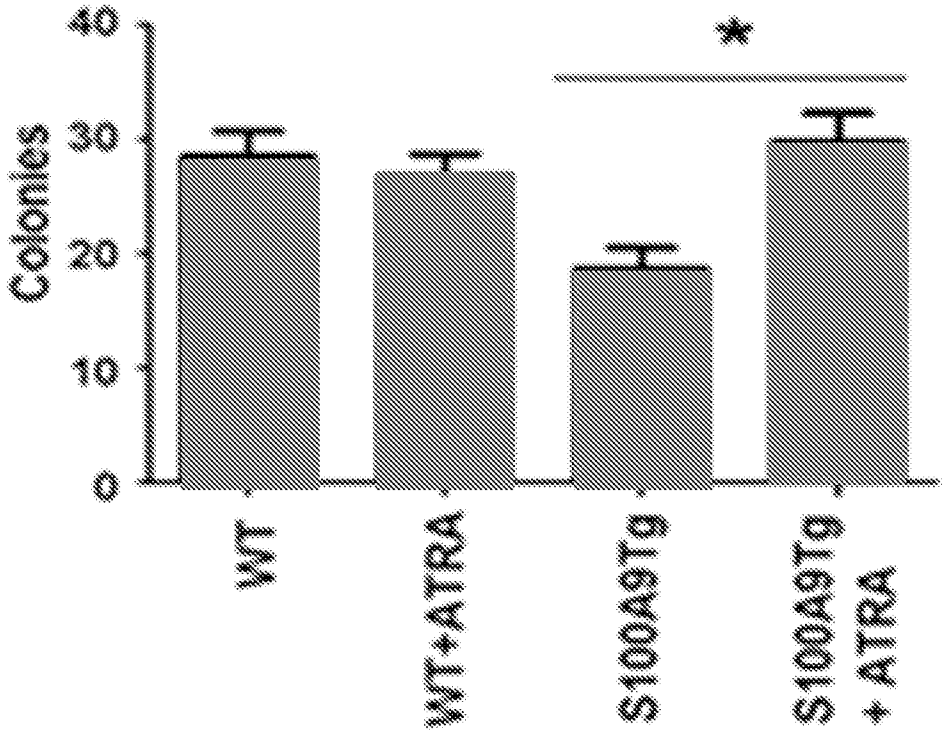

FIGURE 7C

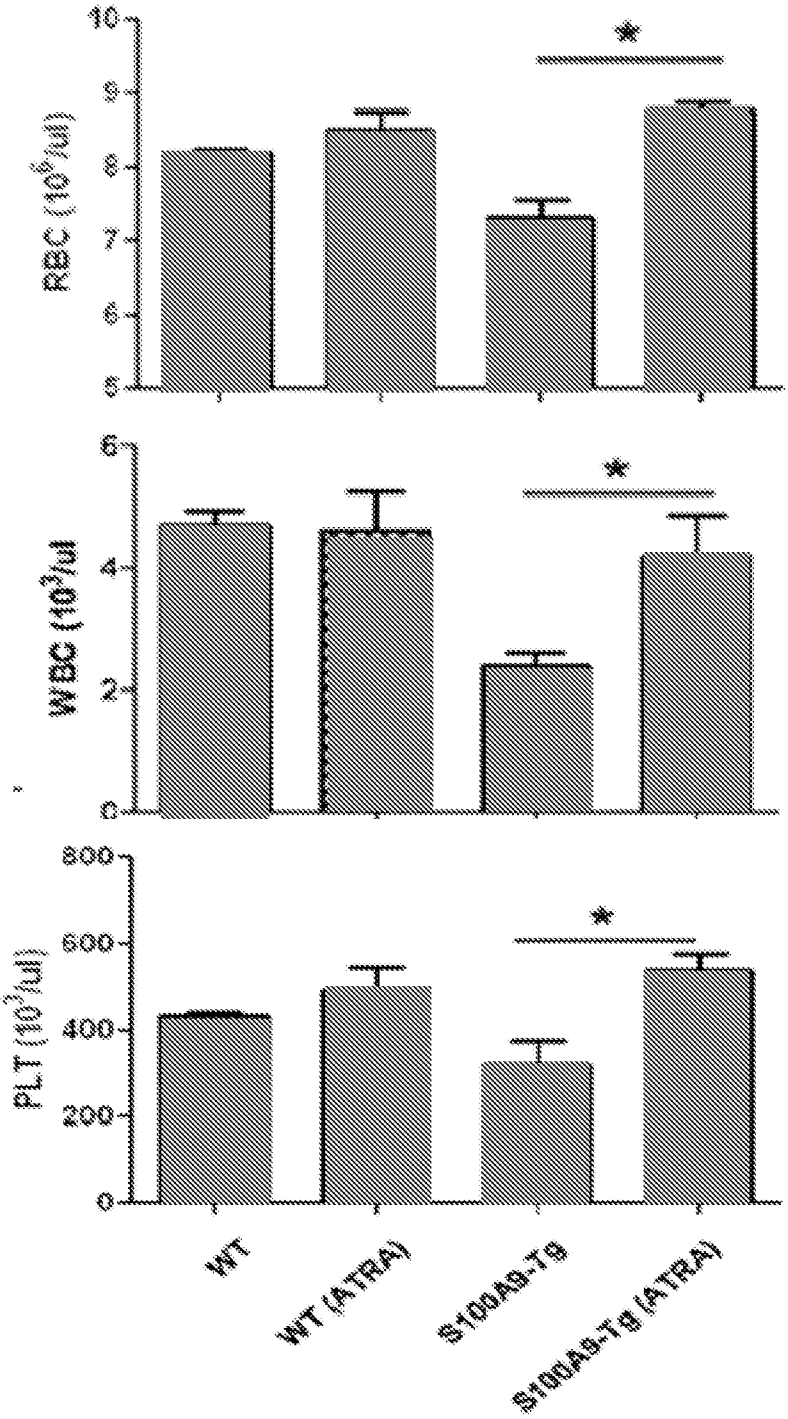
RBC (10^6/ul)
WBC (10^3/ul)
PLT (10^3/ul)
*
WT
WT (ATRA)
S100A9-Tg
S100A9-Tg (ATRA)

FIGURE 7D

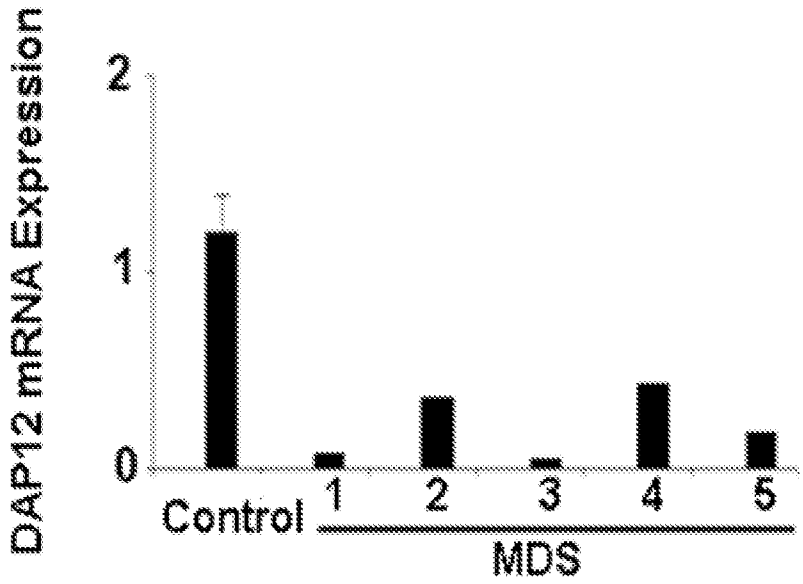

FIGURE 7E

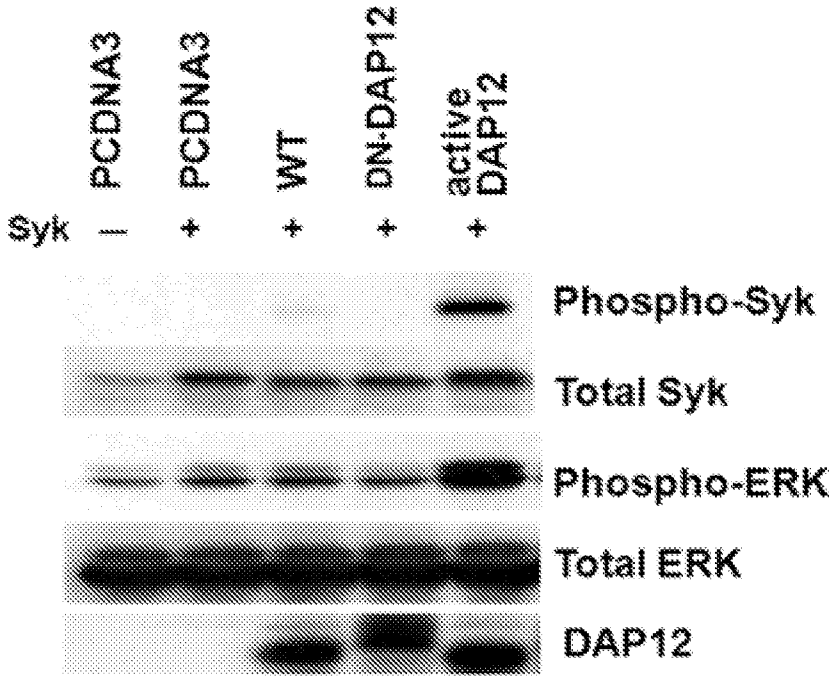

FIGURE 7F

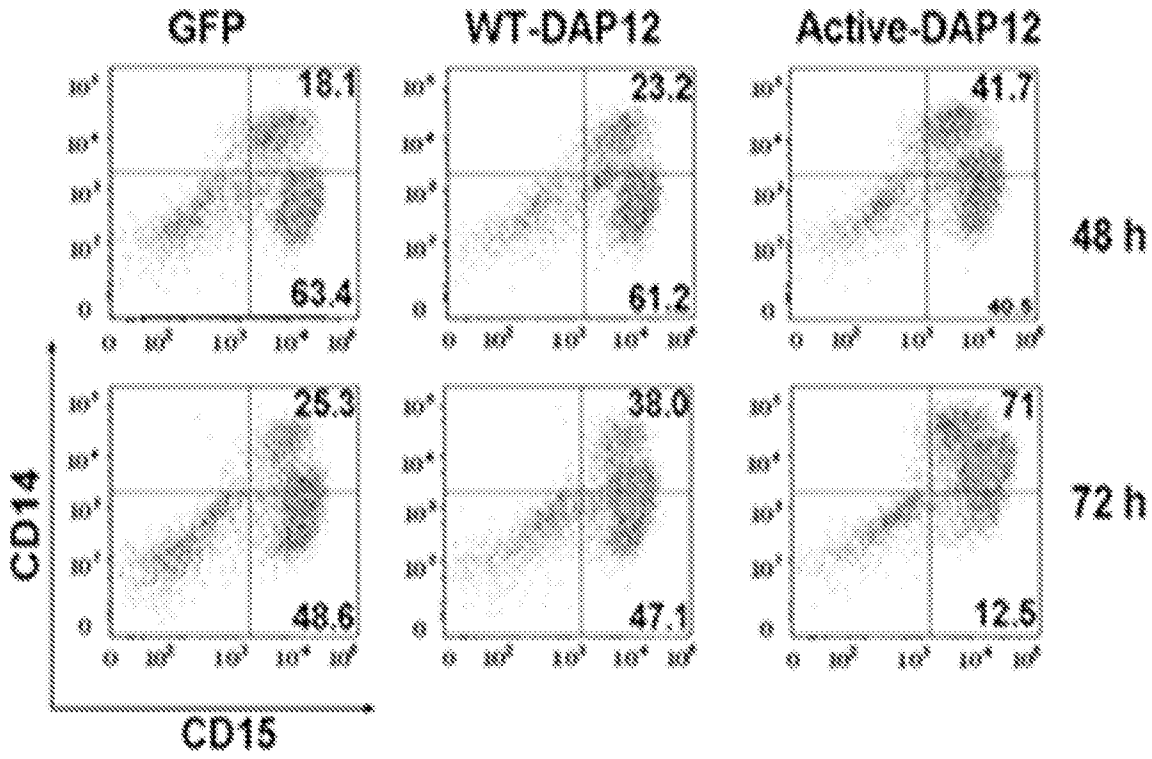

FIGURE 7G

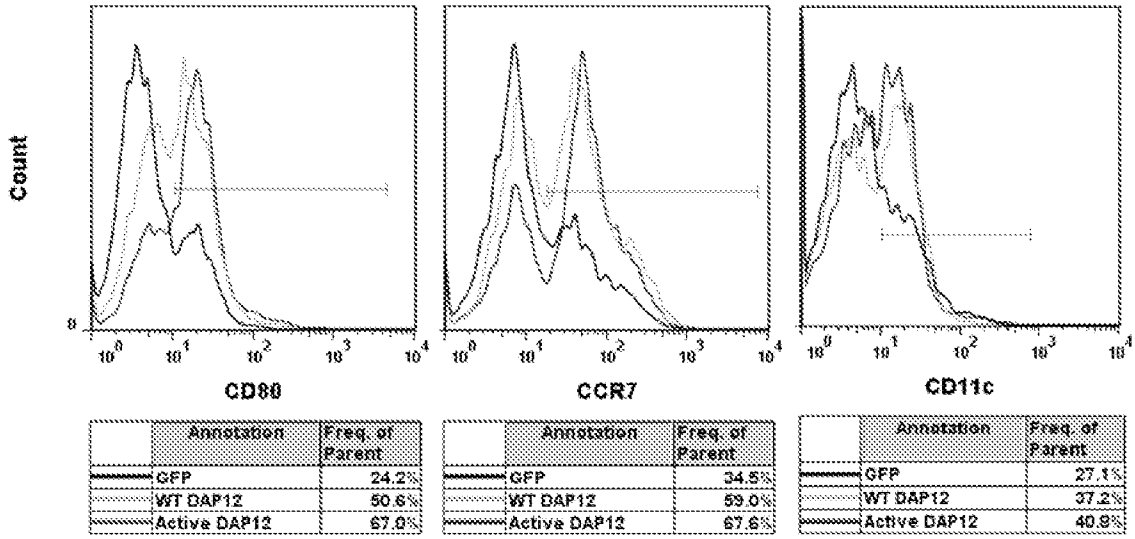

Annotation	Freq. of Parent
GFP	24.2%
WT DAP12	50.6%
Active DAP12	67.0%

Annotation	Freq. of Parent
GFP	34.5%
WT DAP12	59.0%
Active DAP12	67.6%

Annotation	Freq. of Parent
GFP	27.1%
WT DAP12	37.2%
Active DAP12	40.9%

FIGURE 7H

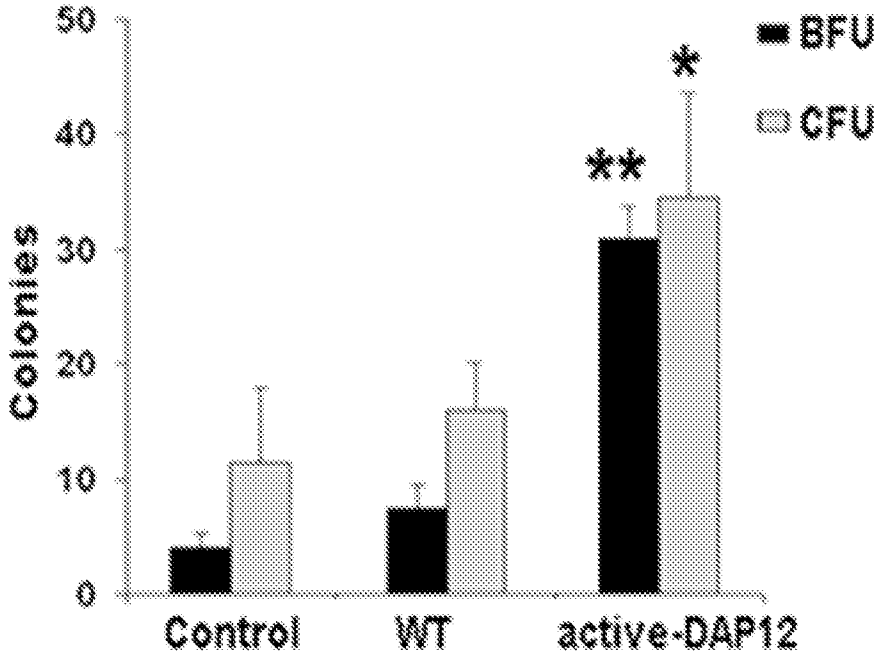

FIGURE 7I

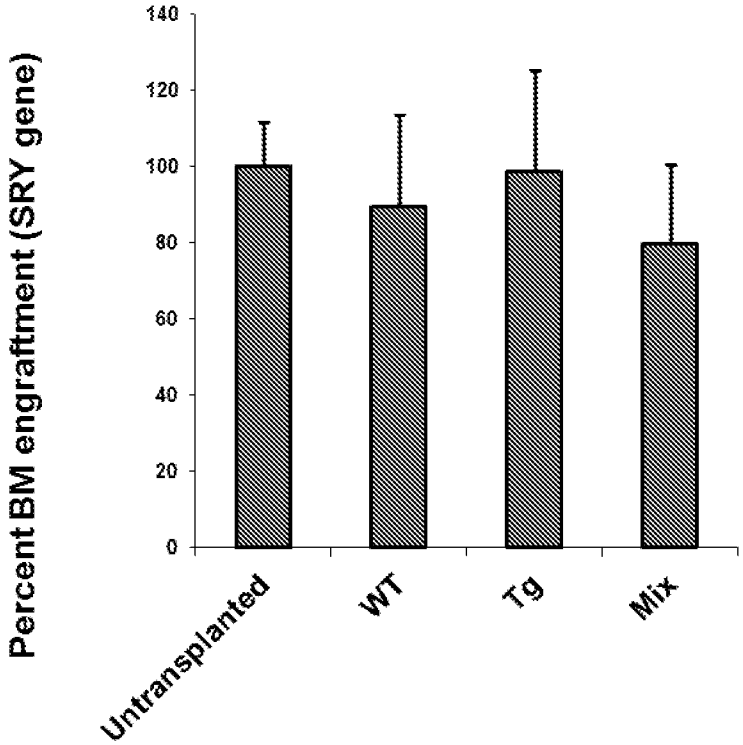

FIGURE 8

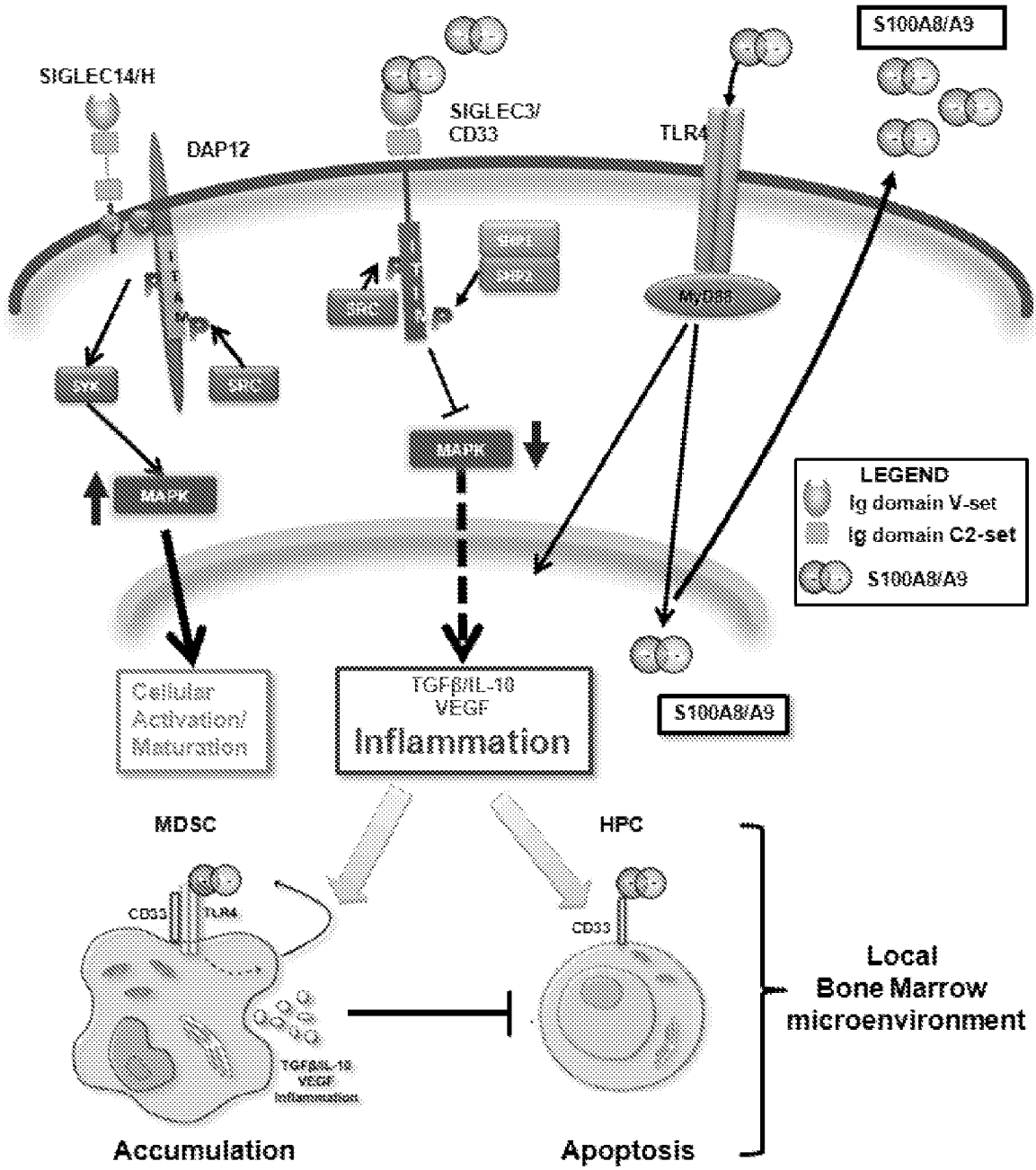
S100A8/A9
SIGLEC14/H
SIGLEC3/
CD33
TLR4
DAP12
SYK
SYK
SHP-1
SHP-2
SYK
MyD88
MAPK
MAPK
LEGEND
Ig domain V-set
Ig domain C2-set
S100A8/A9
Cellular
Activation/
Maturation
TGFβ/IL-10
VEGF
Inflammation
S100A8/A9
MDSC
HPC
CD33
TLR4
CD33
TGFβ/IL-10
VEGF
Inflammation
Local
Bone Marrow
microenvironment
Accumulation
Apoptosis

FIGURE 9

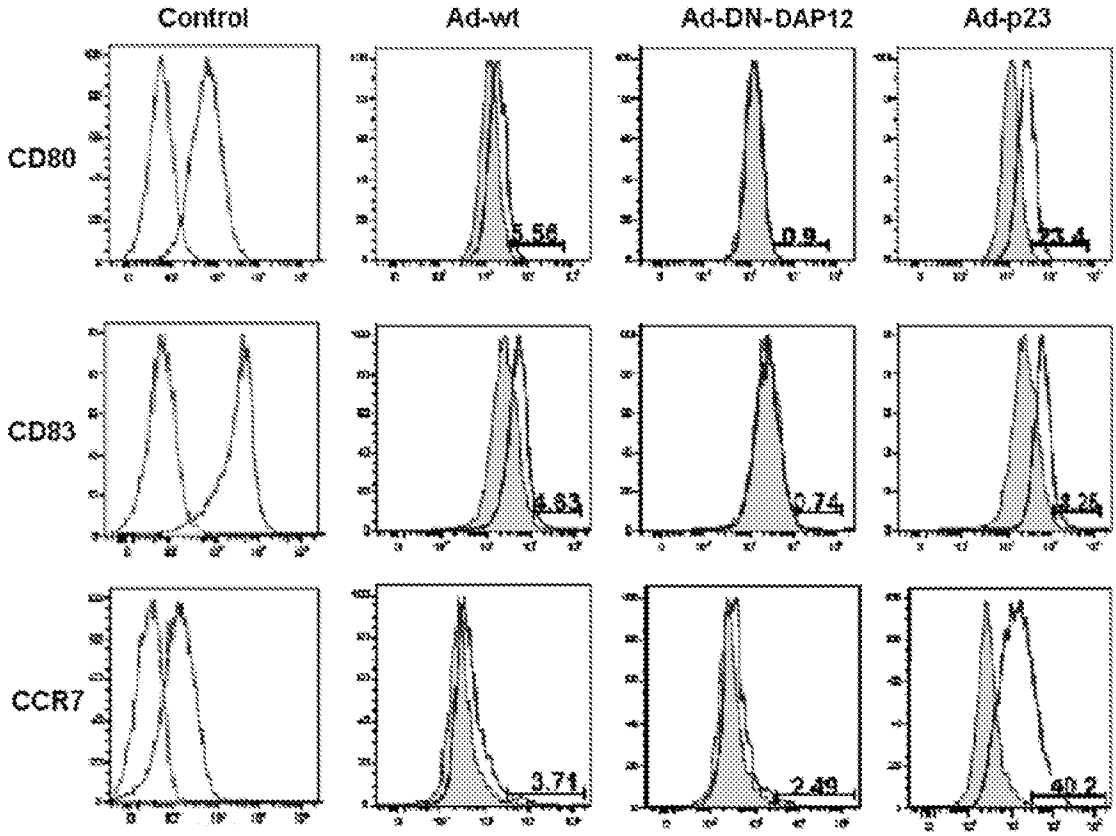
Control
Ad-wt
Ad-DN-DAP12
Ad-p23
CD80
CD83
CCR7
5.56
0.9
23.4
4.83
0.74
4.25
3.71
2.49
40.2

FIGURE 10

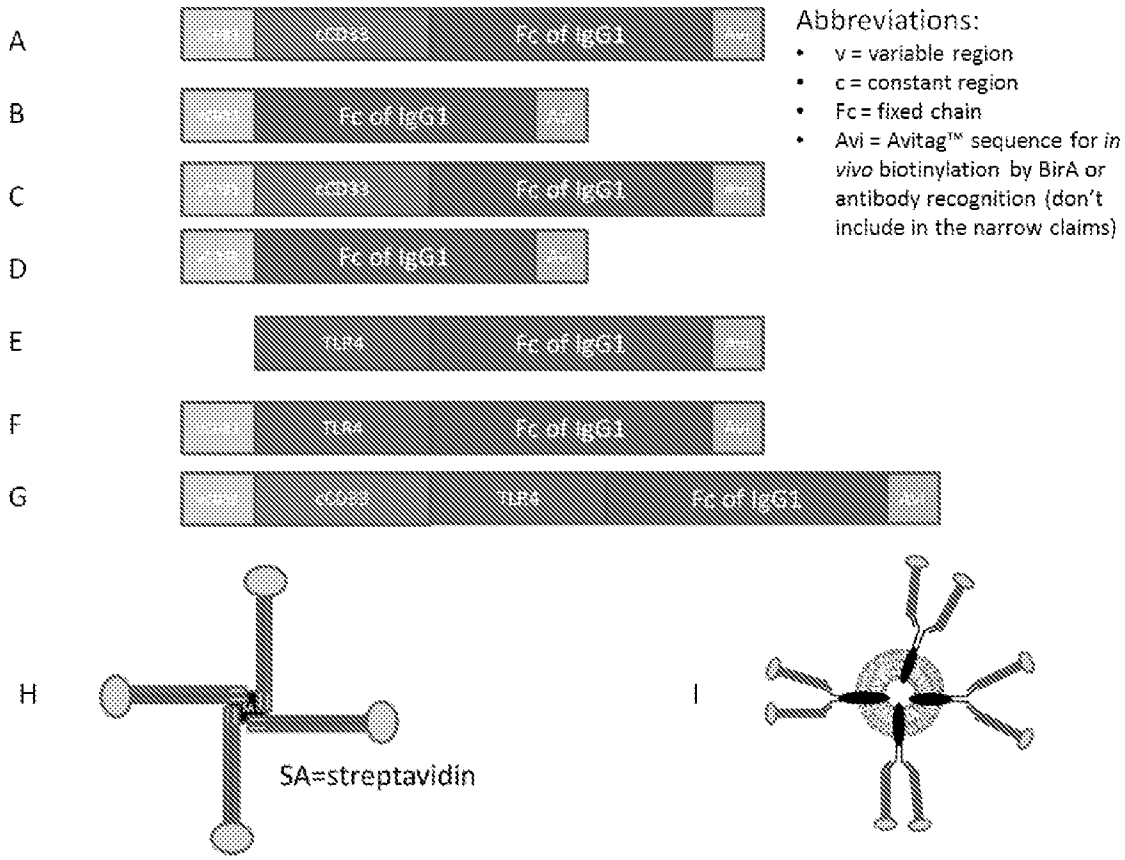

FIGURES 11A-11I

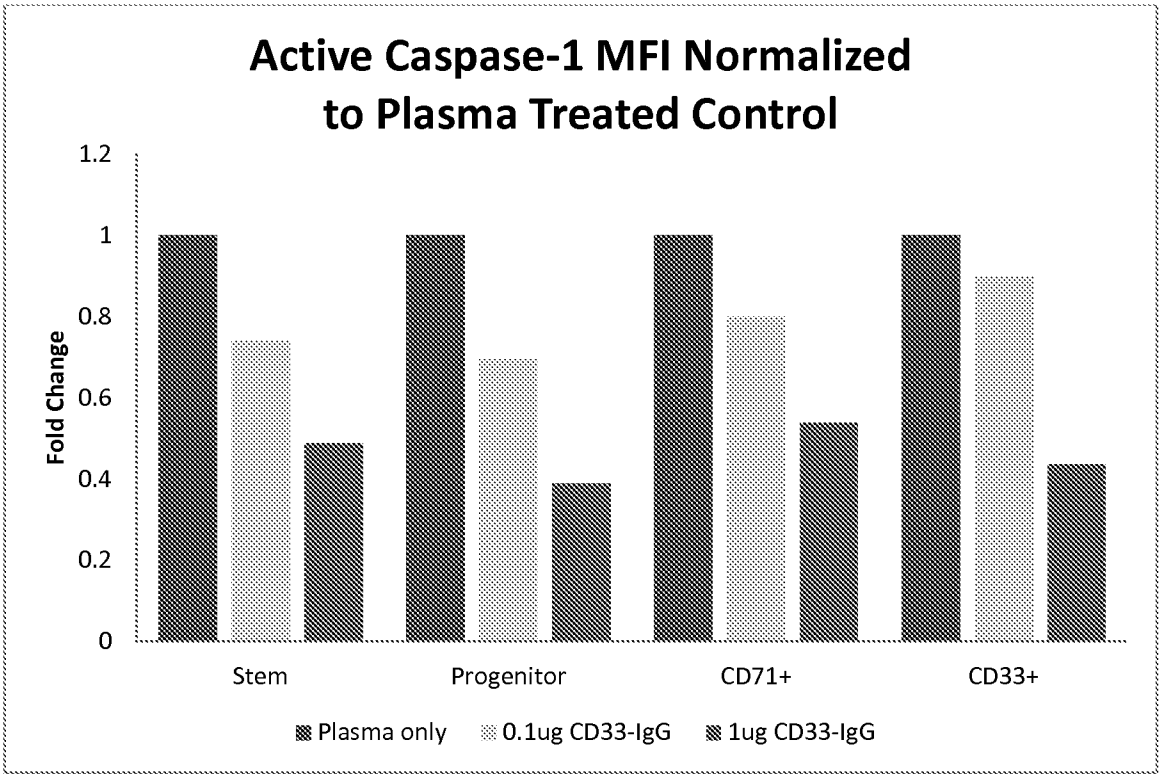

FIGURE 12A

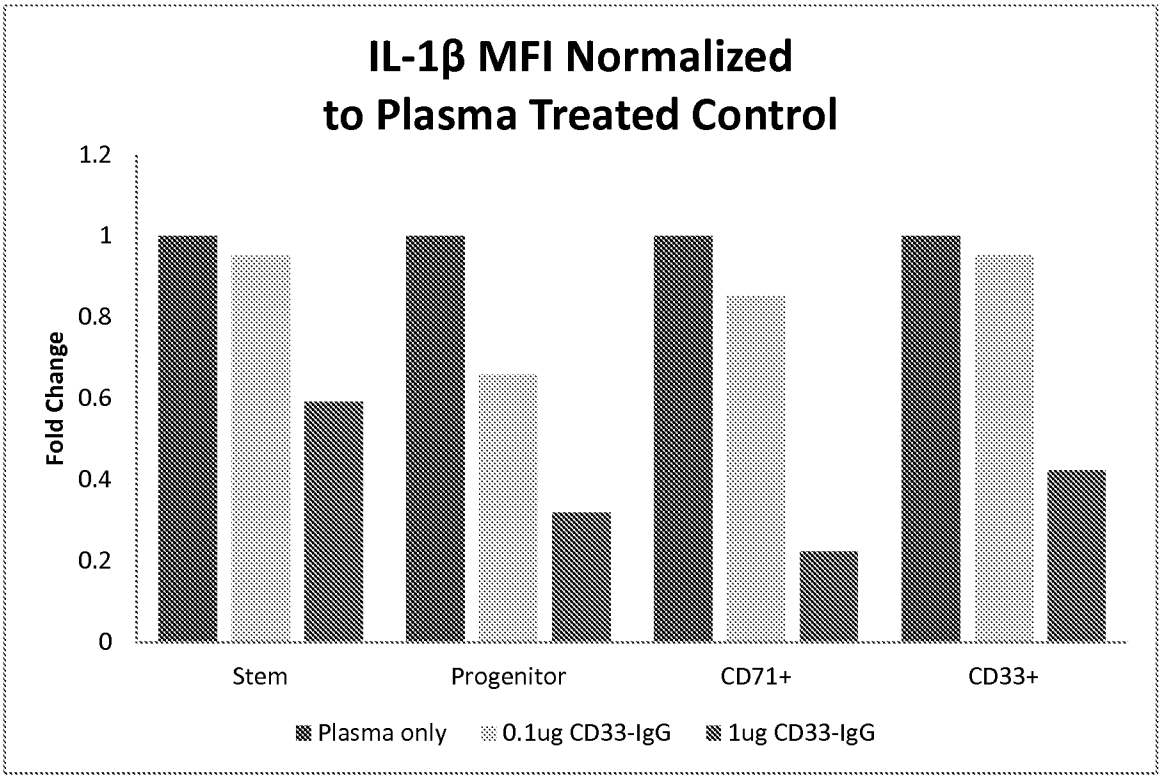

FIGURE 12B

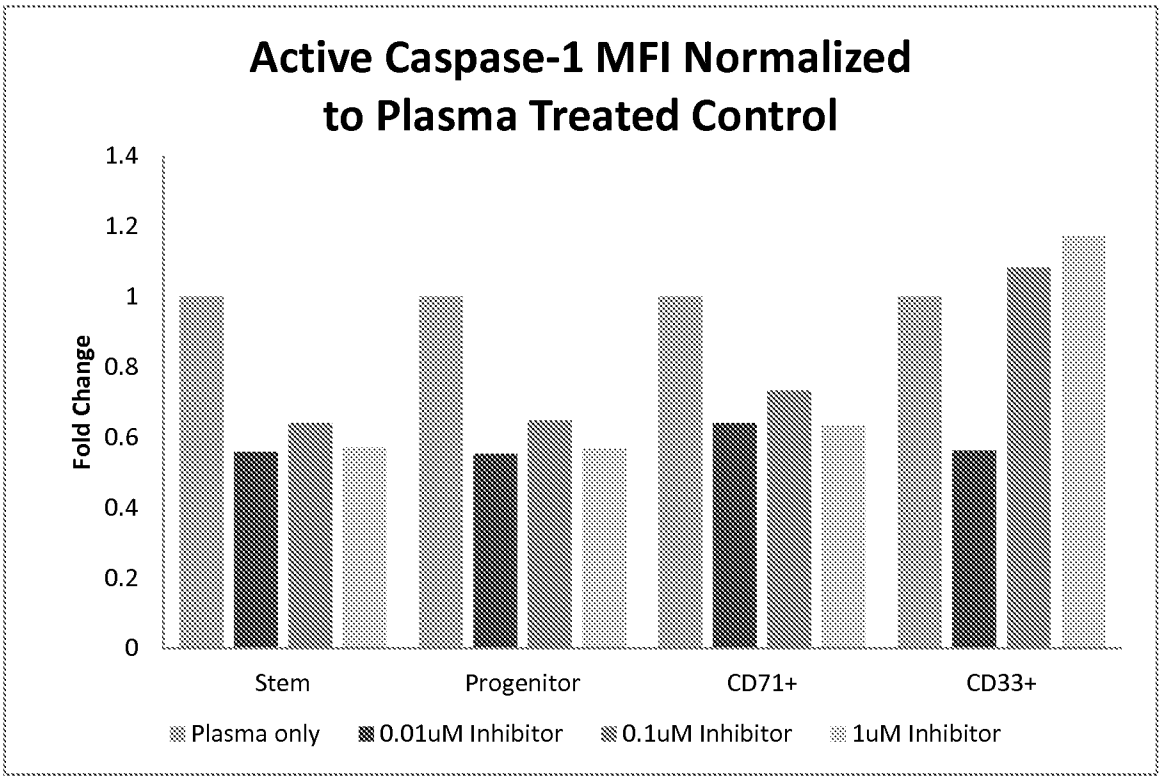

FIGURE 13A

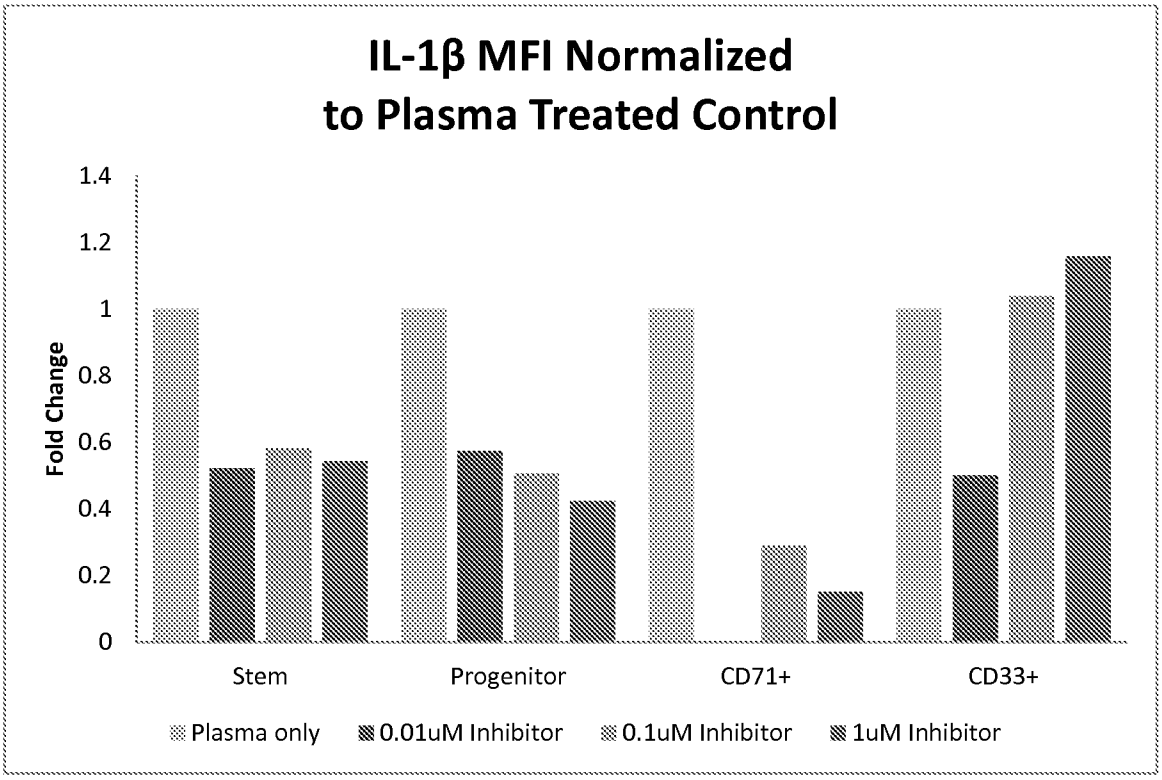

FIGURE 13B

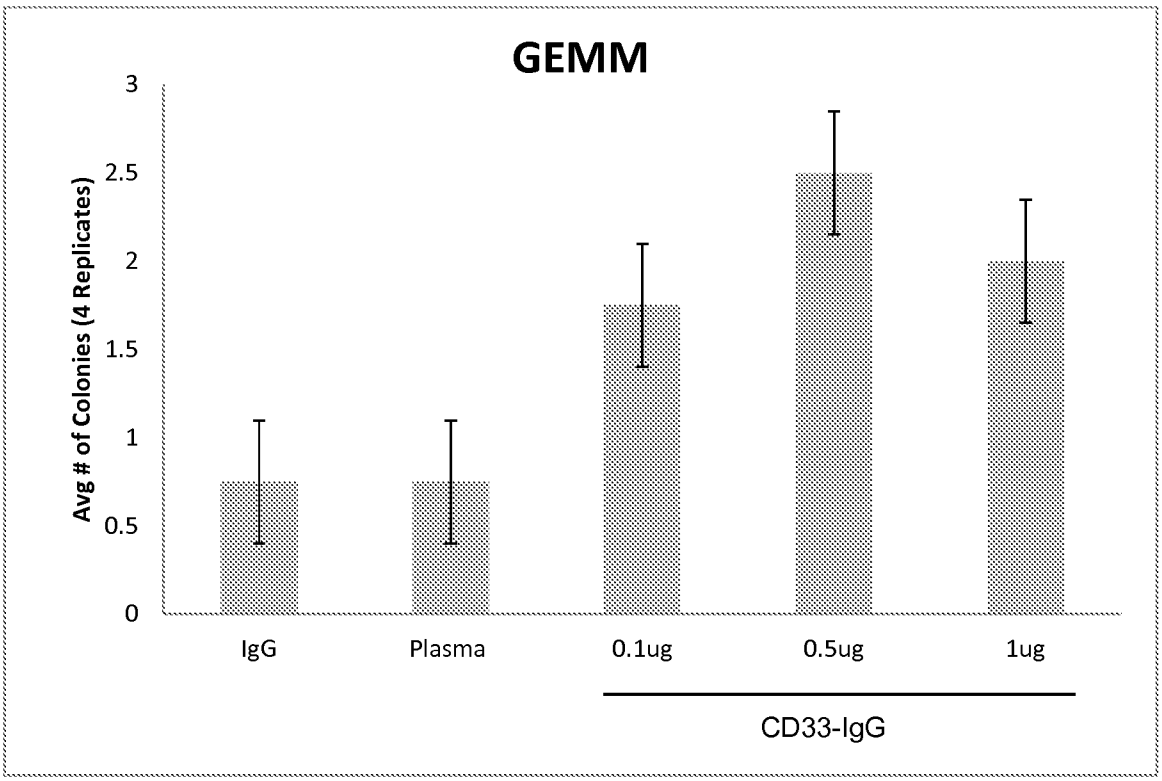

FIGURE 14A

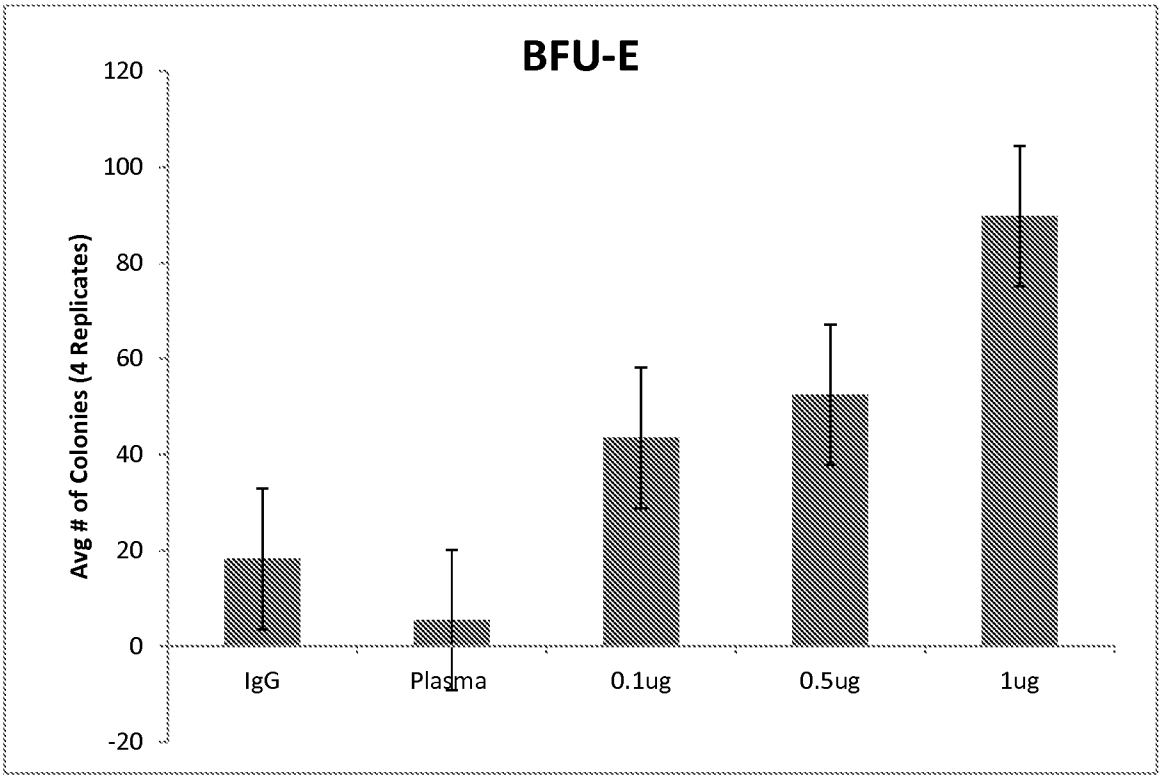

FIGURE 14B

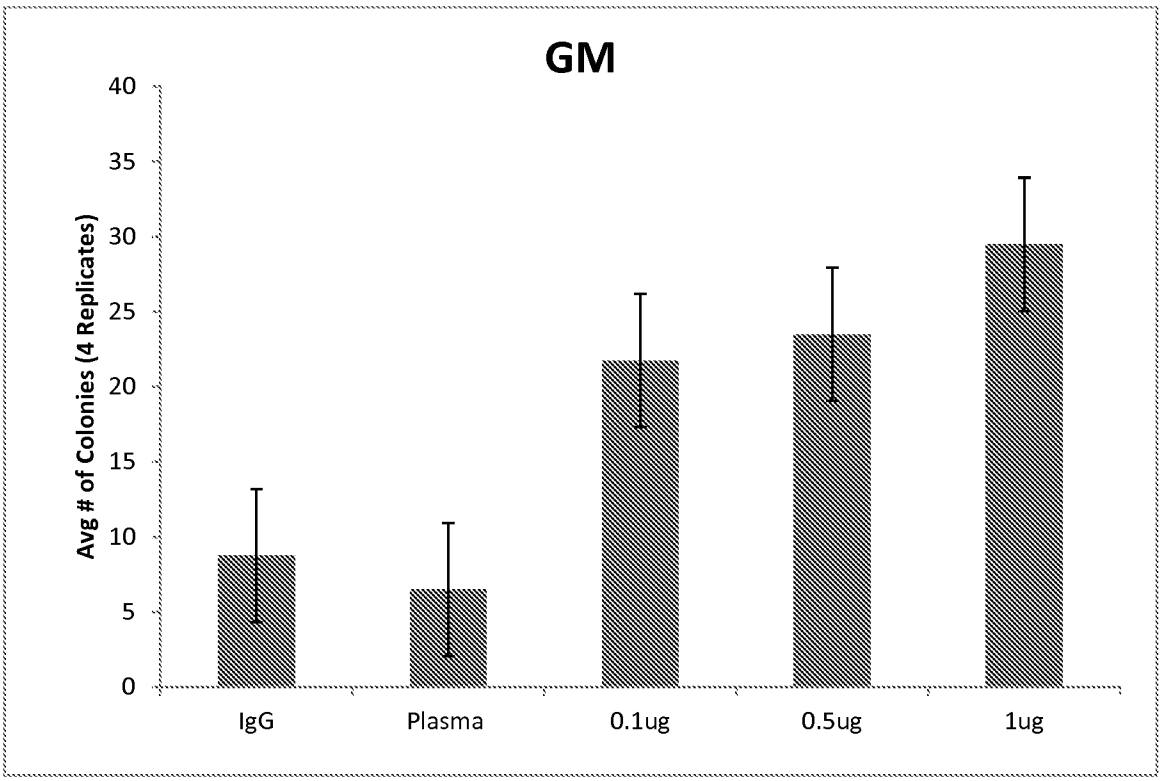

FIGURE 14C

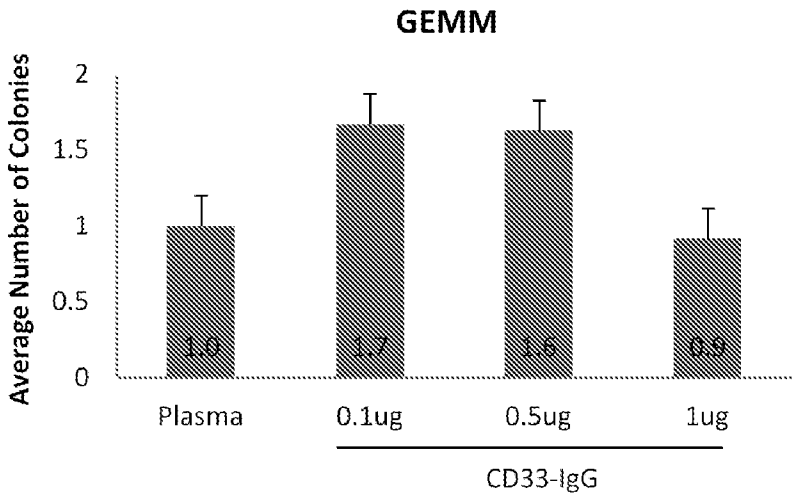

FIGURE 15A

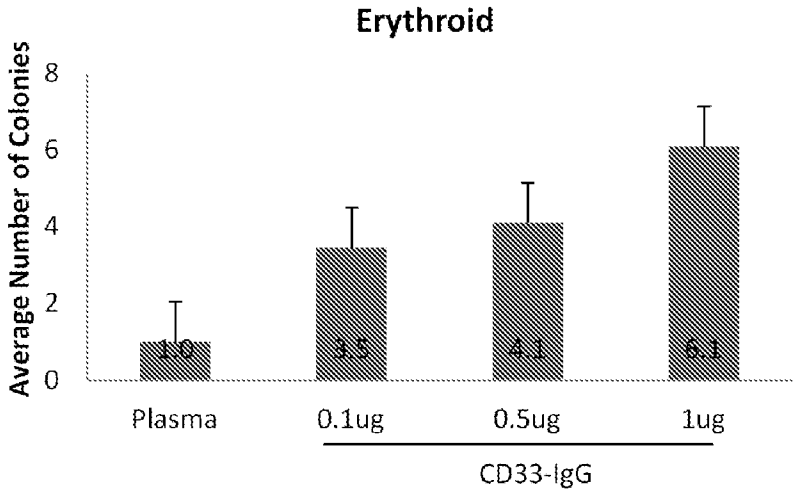

FIGURE 15B

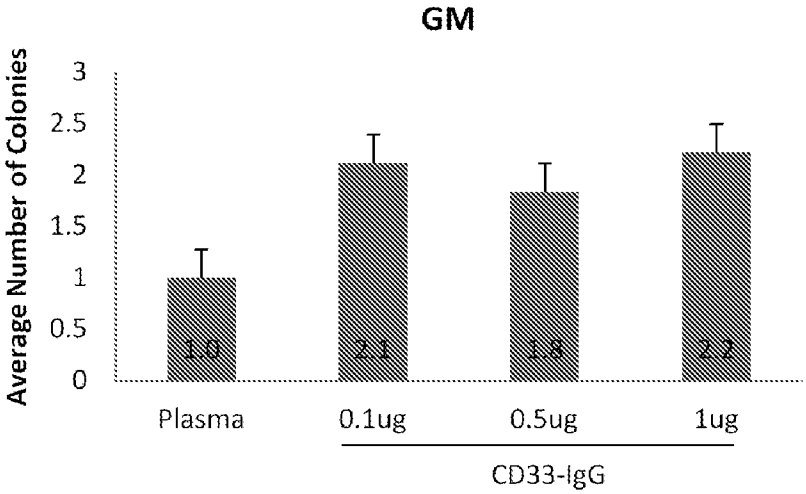

FIGURE 15C

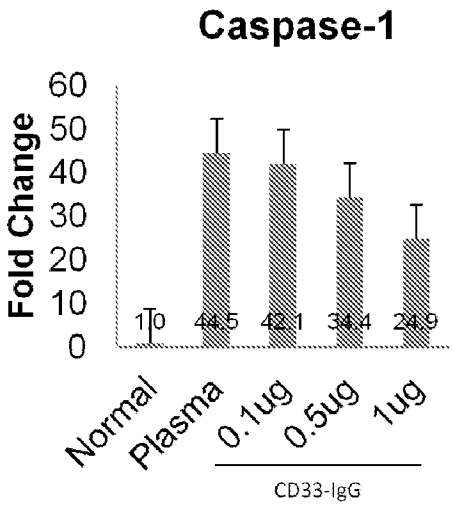

FIGURE 16A

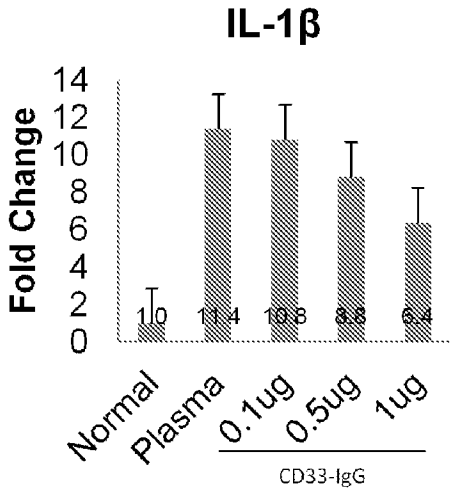

FIGURE 16B

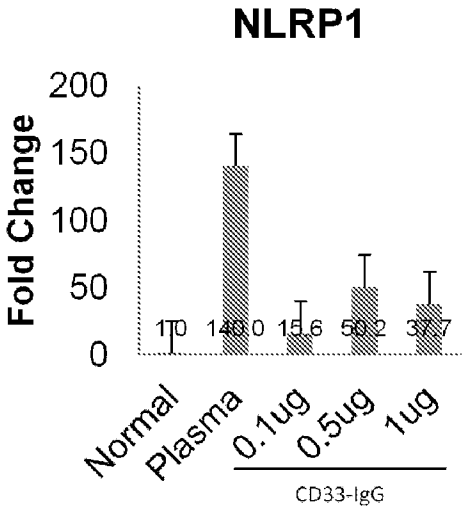

FIGURE 16C

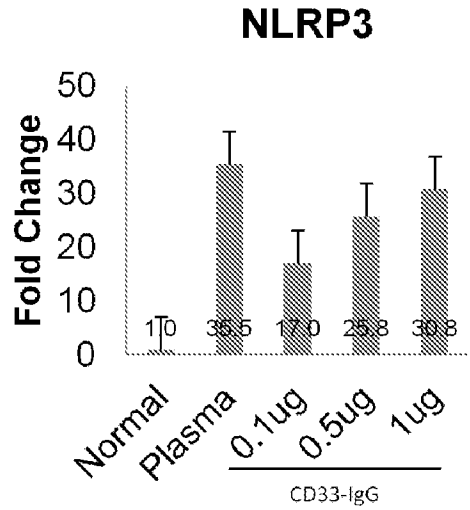

FIGURE 16D

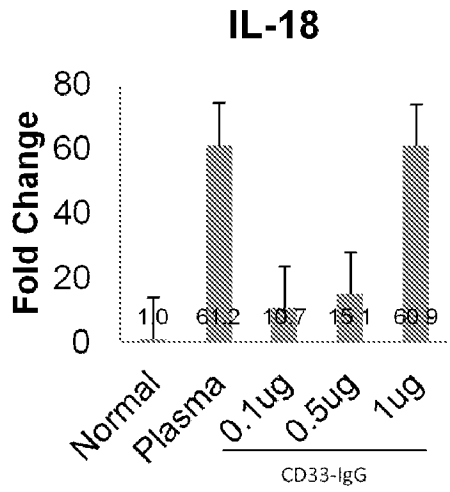

FIGURE 16E